1986

Investigation of deep hole drilling /

Chang-sheng Liu
Lehigh University

INVESTIGATION OF DEEP HOLE DRILLING

by

Chang-sheng Liu

A Thesis
Presented to the Graduate Committee
of Lehigh University
in Candidacy for the Degree of
Master of Science
in
Industrial Engineering

Lehigh University
1986

CERTIFICATE OF APPROVAL

This thesis is accepted and approved in partial fulfillment of the requirements for the degree of Master of Science.

5/26/86
Date

Nicholas C. Cheng
Professor in Charge

George E. Kane
Chairman of the Department

ACKNOWLEDGEMENTS

I wish to extend my thanks to my thesis advisor, Dr. Nicolas G. Odrey, who was helping me in all stages of preparing this thesis, especially leading me to familiarize the scientific manners in conduting a research experiment.

I also wish to extend my thanks to Professor George E. Kane for his helpful advice concerning the assymetric phenomenon of the X and Y component force.

In addition, I also wish to express my gratitude to Mr. Gilbert Zambeli, technician of the Manufacturing Technology Laboratory at Lehigh University, who helped me in preparing the needed experiment work material and equipments, and Miss Wei-Jyuan Chern who was helping me in preparing the script of this thesis.

I dedicate this thesis to Shi-Wei Liu and Yu-Hwa Yang Liu, my beloved parents. Their years' financial and moral supports during my study of master degree makes this work possible.

TABLE OF CONTENTS

FIGURES

TABLES

ABSTRACT

This thesis involves the investigation of the forces/torque relationship and their possible effects on the deep hole drilling process.

An experiment, using central composite design, was conducted and the forces/torque were recorded during the cutting period. Tool flank wear was measured after each cut. The response model was determined to use a three-variable second order equation to represent both the main effects and the interaction and quadractic effects of the machining parameters. Machining parameters included cutting speed, feed and length of cut to diameter ratio (L/d ratio). Response contour plots were drawn to aid to visualize the response pattern of each forces/torque and wear model.

The result of this investigation leads into a better understanding of the operations of the deep hole drilling. Response surface methodology was used to aid in the selection of the optimal cutting conditions in deep hole drilling.

CHAPTER ONE

INTRODUCTION AND STATEMENTS OF OBJECTIVES

1.1 Introduction

Deep hole drilling has been a special topic in drilling operations. Although the question, how deep is deep, is still an unsettled argument, the Machining Data Handbook [20] recommends to lower the speed and feedrate if the length of cut to diameter ratio is more than 2.

A manufacturing difficulty parameter was proposed by Burnham [4] to estimate the degree of difficulty for drilling and to define the limitation of length in conventional drilling. The suggested parameter, Jo, was expressed in the following form :

$$Jo = \frac{Hb \times (L/d)^2 \times f^{0.8}}{(68203) \times d^{1.2}} \qquad (1.1)$$

where, L : length of cut in inch
d : diameter of drill in inch
f : feedrate in IPR

It was suggested by Burnham that when the parameter Jo is less than or equal to one, a conventional drilling method could be employed. Otherwise, it would become mandatory to use non-traditional material removal methods such as ECM and EDM for hole-making that requires

accuracy on the hole straightness.

There have been three problem areas which frequently occur in deep hole drilling :

a. Hole surface quality

b. Path wander and tool breakage in the workpiece

c. Replacement strategy for the worn drill

Hole surface quality, typically measured as surface finish, is not an essential problem for the hole making process because one could simply bore the hole for surface finish improvement after the plain drilling operation. Naturally this would increase the manufacturing cost.

The straightness of a drill path and prevention of drill breakage in the work material are the critical problems in deep hole drilling. The tendency of a twist drill to "drift" from a straight direction is well known. A typical drill will break in the work material if one increases the feedrate and speed to shorten the drilling process time without considering the critical load on the drill. The critical load of a drill depends on the material property, the geometry of a drill and the length of the hole. Burnham [4] has inferred that the thrust force could serve as a measurable index of the critical

load for the drill.

One operating function which has yet to become totally automated economically under computer numerical control is tool wear monitoring. The decision to replace or to resharpen a worn drill is still nearly the function of an experienced operator. Yee and Blomquist [30] have developed a successful on-line method of determining tool wear and predicting drill breakage by applying time domain analysis to the accelerometer signal. One problem still needed to be solved is the determination of the threshold value of the accelerometer signal of different size drills under different cutting conditions. According to Farris and Podder [2], the end of tool life can be accurately determined for all practical purposes by monitoring the rate of change of thrust and torque. Their investigation indicated that:

> "Tool breakage occurs when the present rate of change in the thrust and torque is bigger than previous rate of change in thrust and torque plus a safty coefficient."

It is suggested from such observations that a machining condition selection strategy is needed for the deep hole drilling operation. A strategy which will compensate for the contrasts in different drilling

performance indexes can be used as a control mechanism for future investigations in developing an adaptive control system.

1.2 Objective statement and approach

The purpose of this research is to investigate the performance of deep hole drilling. The experiment is designed to investigate the optimum cutting condition by constructing empirical models for predicting the behavior of different drilling peration responses. The responses considered are tool wear, cutting time, drilling forces and the rate of change in drilling forces. After emperically determining predicting models and locating the optimum condition for deep hole twist drilling, this research will recommend a strategy for selecting machining condition for improved drilling performance.

CHAPTER TWO

LITERATURE REVIEW

Previous research in drilling has investigated the effect of the primary independent variables of cutting speed, feedrate and length of cut on the reponse variables of drill flank wear and thrust force. [1,2,3,4,7,8,10,12]

For this investigation, the literature review focuses on the following topics :

a. Hole surface quality and thrust force.

b. Path wander, drill breakage and thrust force.

c. Workpiece hardness and thrust force.

d. Drill flank wear and thrust force.

2.1 Hole surface quality and thrust force

Radhakrishnan and Wu [10] proposed an on-line hole quality evaluation method in drilling a composite material. The authors defined a lamination frequency, F, which corresponded to the rate at which the drill penetrate through the layers of the laminated composite work material. The lamination frequency was given by

$$F = \frac{\text{\# of lamination per inch for composite materail}}{\text{Time for drill to penetrate an inch of material}} \quad (2.1)$$

During the process of drilling the composite material, a low frequency, less than 1.6 Hz, was found to be dominant in both the thrust and the surface waviness data. This low frequency was the same as the calculated lamination frequency of equation (2.1). The change in standard deviation of this frequency with the thrust signal was found to be closely correlated with the change in the waviness of the hole surface under all working conditions. [10] Since the lamination frequency is a special character of composite material, the result obtained might not be applicable to other materials. In addition, the authors concluded that the standard deviation of the thrust force gave an indication of the hole waviness. Their findings indicated that the thrust force standard deviation would be an applicable response variable in investigating hole surface quality.

2.2 Path wander, drill breakage and thrust force

Several authors have investigated the mechanics of drilling and have developed theoretical models for tool path wander. [3,4,8] The following list states some of

the investigators results that will cause either drill path wander or drill breakage : [3]

1. The drill is loaded above its critical axial load. The critical load will be defined and discussed in a subsequent section.
2. The initiator of path wander is found of sufficient size to cause a tip deviation from the straight path.
3. The variance of hardness in work material is large to cause drill breakage.

2.2.1 Critical axial load of drill

When drill penetration occures, a thrust force is applied on the drill. The higher the feedrate, the greater is the thrust force. The critical axial load of a drill can be estimated by Column Analysis [1], or even more accurately be estimated by the Hole Curvature Interaction Model. [3] In Column Analysis, the drill is considered as a long slender column (Fig. 2.1) such that it is possible to calculate the critical instability or buckling load. This critical load can be expressed by the following equation : [3]

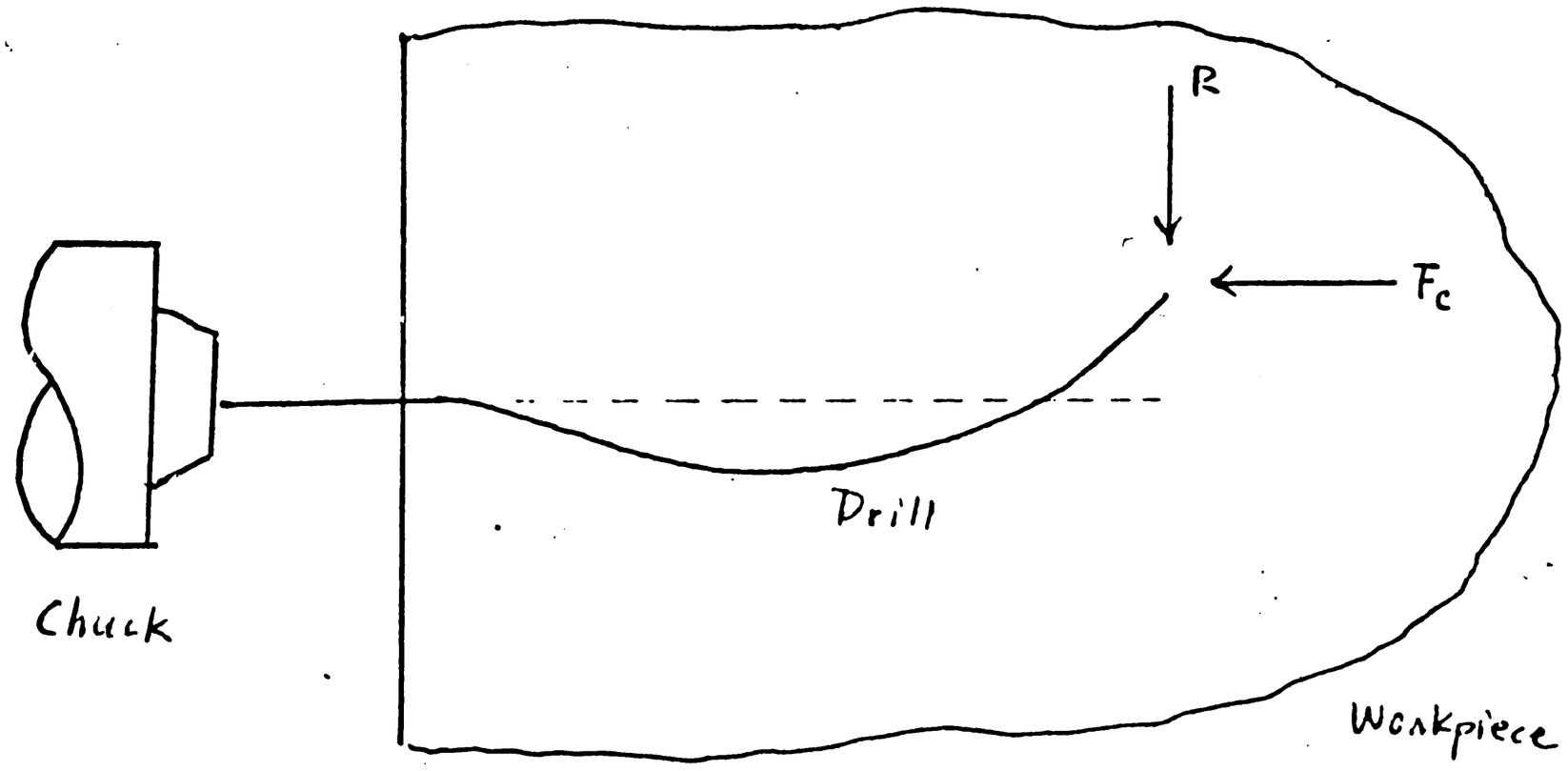

Fig. 2.1 Column Analysis Schematic : The drill in column analysis is considered as a long slender column. The chuck is to be the rigid base to support drill.

(F_c : the thrust force or axial load
R : side force)

$$F_c = 20.16 \times E \times I / l^2 \qquad (2.2)$$

where, F_c : critical load, lb-f

E : Young's modulus, lb-in^2

I : moment of inertia of the drill cross section, in^4

l : drill length in inch

A design factor which greatly limits the permissible load and lowers the critical load is the flute length of drill. (Fig 2.2) The advantage of the Hole Curvature Interaction model over the Column Analysis is in that it treats the drill not as a uniform circular cross section but, more practically, as two sections, the shank and the flute. The shank is a circular column such that its critical load may be obtained from equation (2.2). The flute may be represented as a removal of material from the drill cross section (Fig. 2.3) so that the moment of inertia of the flute is smaller than that of the shank. By numerically integrating the cross section of the flute, the moment of inertia of the flute section can be viewed as an equivalent moment of inertia of a shank with reduced diameter. Since a reduced diameter section is less stiff because of the smaller diameter, it is much easier to deflect. The Column Analysis by equation (2.2)

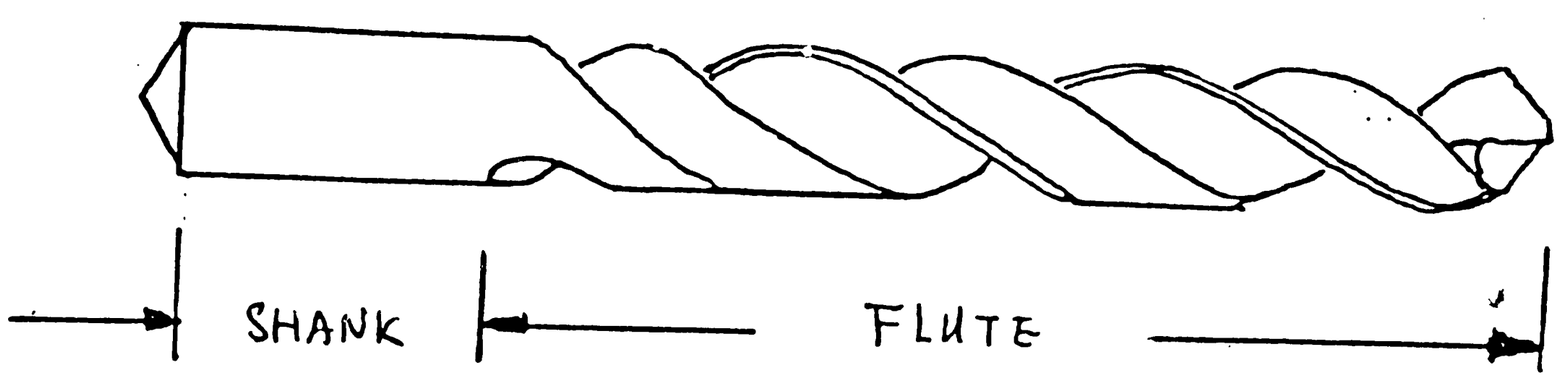

Fig. 2.2 Illustration of standard twist drill. Flute is the section that can penerate into the work material because it was designed to sweep the cutting chips out of work material.

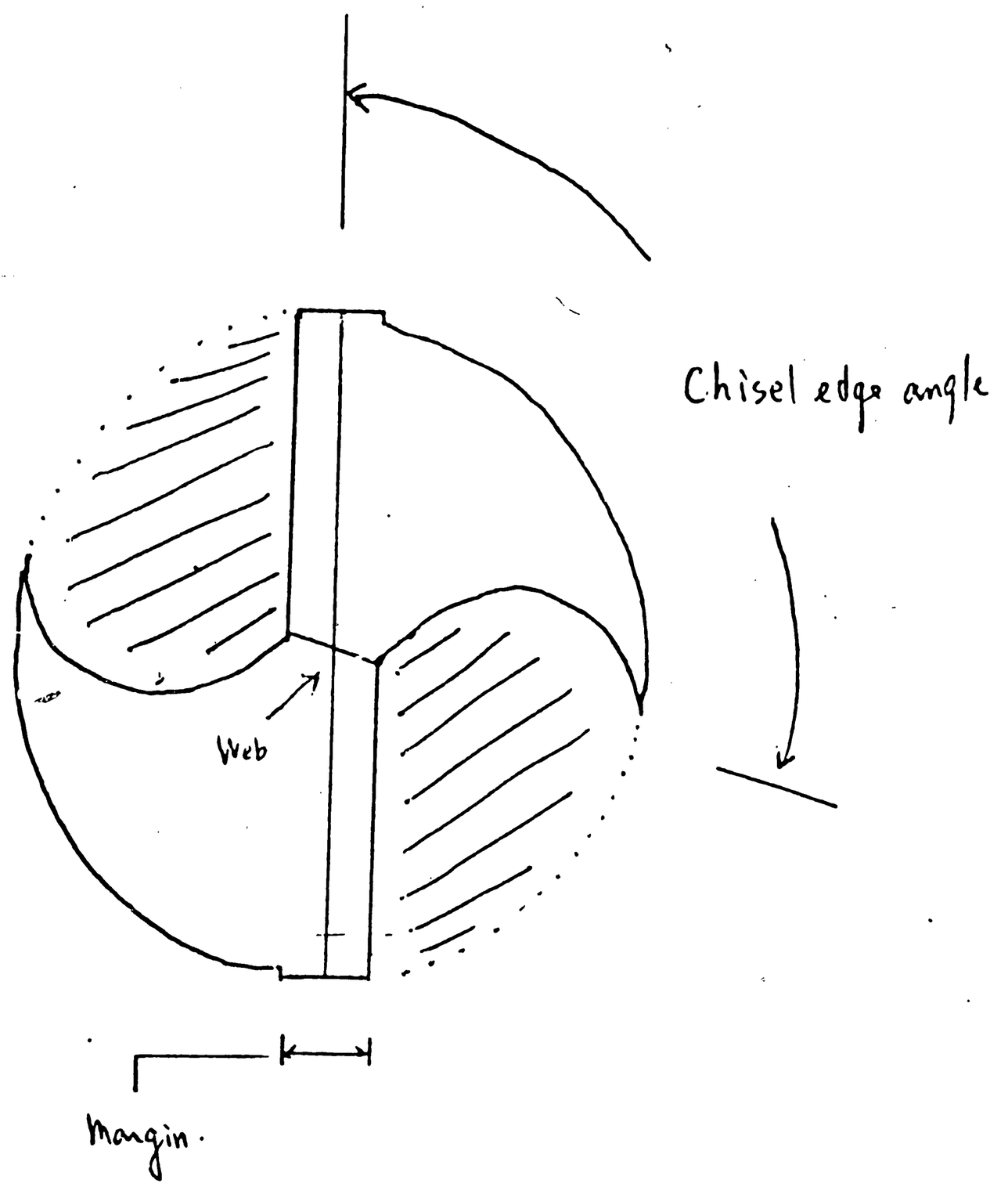

Fig. 2.3 Cross section of flute of the twist drill. The area under hatch line represents the removal of material from the cross section of a circular column.

indicated that the longer the drill length, l, the less is the permissible critical load of the drill. That implies that a short small-diameter column can be substituted by a long large diameter column as long as the moment of inertia of these two columns are equivalent. In other words, the flute section can be substituted by a larger circular column which has the same diameter as the shank. The effective total drill length, l_e, can be expressed by the following term :

$$l_e = l_s + (d_s / d_f)^2 \times l_f \qquad (2.3)$$

where, l_e : effective length of drill

l_s : shank length of drill

l_f : flute length of drill

d_s : shank diameter of drill

d_f : equivalent flute diameter of drill

The effective drill length, l_e, as calculated in equation (2.3) can be substituted for drill length, l, in equation (2.2) to estimate the critical load of drill. Knowledge of the critical load enables one to monitor the thrust force of drilling operation such that critical load of the drill is not exceeded and fracture is avoided in the drilling process.

2.2.2 Initiators of drill wander

In general there are two common causes of drill wander. [3] They are :

a. Hole side variations including score marks, and the possibility of some partially attached fragments on the hole surface or the wedged chip fragment on the drill (Build Up Edge).

b. Eccentricity of the drill cutting edge relative to the geometric center of the drill.

These two common causes can not be totally eliminated in any practical operations. A very small chip fragmant is all that is necessary to trigger drill wander. [4] Drill wander can be controlled by using brand new drills in each cutting operation and by using coolant to avoid the possible adhesion of a chip fragment to the hole surface and drill edge. Without the chip fragment and the eccentricity, even at the critical load the drill would merely whip around inside the hole and possibly only polish the hole surface.

The most effective method of reducing wander is in "reducing the axial load of the drill ". [4] One equation used to determine the deflection curve of centerline is as follow :

$$y = \frac{-e\left\{\dfrac{\left[e^{B_0 X}\,SIN\,B_1(l-X) - SIN\,B_1 l\right]}{\cos(B_1 l + \tau_0)} + K\cdot X\right\}}{\left[\,Kl - \dfrac{SIN\,B_1 \cdot l}{\cos(B_1 l + \tau_0)}\,\right]} \qquad (2.4)$$

where, y : deflection in inch

X : distance from the base of tool holder to the selected deflection measuring point

$B_0 = K \times \sin \tau_0$

$B_1 = K \times \cos \tau_0$

$K^2 = F_z / (E \times I) = B_0^2 + B_1^2$

F_z : thrust force (axial load) in lbf

E : Young's modulus
I : moment of inertia
l : length of drill in inch, from the base of tool holder to drill tip
e : eccentricity
τ_0 : parameter

Equation (2.6) illustrates the interaction between thrust force and eccentricity of the cutting edge relative to a drill's geometric center and the maximum distance, y, of deflection from the center line of the drill. Young's modulus and moment of inertia can be looked upon as constants if the same sized drill and work material is used. Assuming that the eccentricity of every drill is the same, the thrust force and length of

drill outside the tool holder will then be the control variables that can be used to limit the path wander during a drilling operation.

2.2.3 Hardness variation of work material

A report by Subramanian & Cook [12] commented that the hardness of the work material plays a dominant role in the cutting and extrusion forces in drilling. It was determined that the harder the material, a lower feedrate should be used to maintain the same thrust force. The effects of workpiece hardness on drilling may be given by the following statements :

a. For a constant thrust force drilling, when the drill enters from hard region to softer region, feedrate would increase and might exceed the allowable torque on the drill and then causes drill fracture.

b. For constant feedrate drilling, the harder the work material, the higher is the thrust force. When the thrust force is to the critical load, a defective path wander will then be generated.

The following equations have been used to interpret

the relationship between the material hardness and the thrust force:

a. Shaw & Oxford equation : [16]

$$Fz = [\ 0.195 \times BHN \times 1420 \times f^{0.8} \times d^{0.8}\ ] + [\ 0.0022 \times (\ BHN \times 1420\ ) \times d^2\ ] \qquad (2.5)$$

b. Cook's equation : [12]

$$Fz = Ko\ [(\ f^{0.8} \times d^{0.8} \times B\ ) + (\ d^2 \times E\ )] \times 2.86 \qquad (2.6)$$

where, BHN : Brinnel Hardness Number
f : feedrate, IPR
d : diameter, inch
B = 1.36
E = 0.032, for standard twist drill with point angle 118 dg.

$$Ko = -0.2 \times BHN^2 + 170 \times BHN - 2000$$

Though these equations are empirically derived and are not equal to the thrust force that are measured by a dynamometer for different cutting conditions and different materials, they may be used as a reference magnitude to check the drilling operation and obtain a possible range of thrust force.

2.3 Tool wear and thrust force

An investigation by Subramanian & Cook noted that

the growth pattern of tool flank wear and thrust force are correlated. [12] The conclusion they made was that if the variation in thrust force with change in flank wear is to be siginificant, the variation in workpiece hardness has to be held within 5% of the mean workpiece hardness value. Such a condition is very difficult to meet in practice.

Farris and Podder [2] investigated the effect of cutting conditions on tool flank wear and concluded :

> "The magnitude of thrust force is not an indicator of tool life; however, the rate of increase of either thrust force or cutting torque is a good indicator of the rate of wearland."

They recommended that the end of tool life can be accurately determined by monitoring the rate of change in thrust force or torque and that the end of tool life will occur when the following condition exists :

$$dF / dt > [dF \text{ (previous)} / dt] + s \times F \text{ (previous)} \qquad (2.7)$$

where, F : thrust force or torque
s : safty coefficient, suggested 0.15. Maximum scatter value of the force at any point.

The value, dF/dt, may be obtained by calculating the rate of change or the slope of force, and could serve as one of the response variables of a drilling operation.

By analyzing the relationship between this value with control variables, such as speed, feedrate and length of cut, some important characters may be obtained in governing the tool wear behavior in deep hole drilling.

2.4 Summary of literature review

The literature review enables one to conclude that the thrust force may be the key factor for constructing a control algorithm for optimum performance of a deep hole drilling operation. Beside the axial thrust force, there also exist side force components in drilling (forces in the X and Y directions) (Fig. 2.4). Currently, minimal investigations have been conducted to define the role of these forces. The X and Y forces can be attributed to hard spots or hardness variance in the workpiece, the curved chips on the drill, or the tool wear. Relationship between these side forces and the tool path deflection would be an interesting aspect to investigate.

In summary, the literature review served to focus the current research investigation on the following topics :

a. The standard deviation of forces versus hole surface finish.

b. The critical thrust force on a drill.

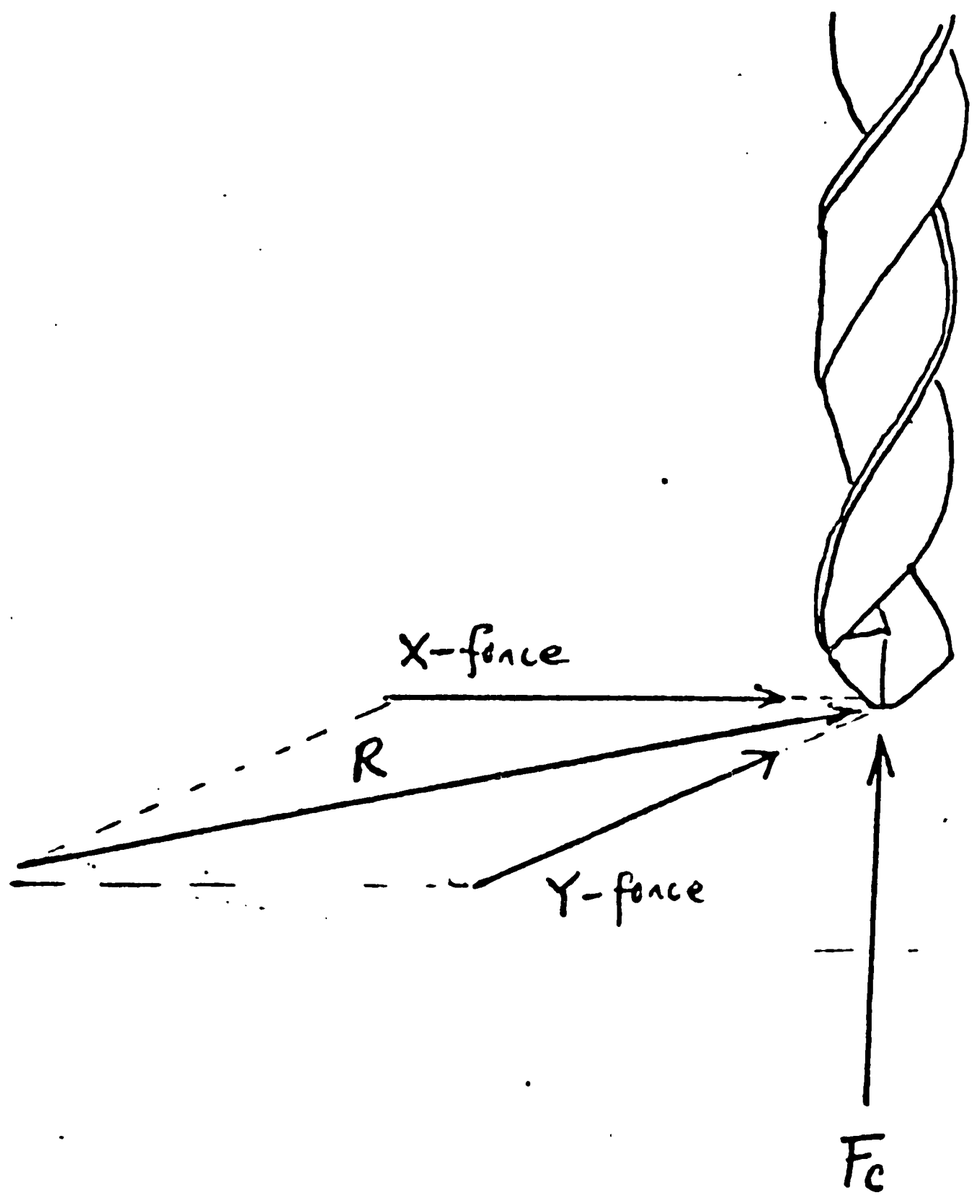

Fig. 2.4 Side forces in drilling.

c. The interaction of thrust force, drill length and their influence on path deflection.

d. The relationships between work material hardness, feedrate, drill diameter and the thrust force.

c. The relations between rate of change in thrust force and tool life.

e. The influence of X and Y side forces on drilling operation.

CHAPTER THREE

EXPERIMENT DESIGN, PREPARATIONS AND PROCEDURES

This chapter is devoted to the description of the experimental design and the preparations and procedures used in the deep hole drilling investigation. First, the experiment is discussed and the experimental design is selected to serve the purpose of this investigation. After the structure of the experimental design is determined, the proper choice of cutting conditions is made to include the experimental region within the constraints of the tool bits and the available machinery. The preparation of work material and experimental equipment are stated to define the experimental working environment. The measurement methods for the responses, such as the measure of force and tool flank wear, were also documented for reference.

3.1 Experimental design considerations

The responses of this experiment consist of torque, thrust force, X-force and Y-force components and flank wear readings which includes average flank wear, inside flank wear and outside flank wear. Machining parameters of the experiment include cutting speed, feedrate and the ratio of length of cut to diameter. It was the intent of

this investigation to choose an experimental design which would generate a response surface. Such designs typically incorporate main effects and interaction effects. Main effects indicate the first order linear relationship between machining conditions and system responses. The interaction terms and quadratic terms in the experimental design model define the curvature of the system's responses. The combination of both main and interaction effects results in a second order three-variable linear equation of the type :

$$Y = B_0 + B_1X_1 + B_2X_2 + B_3X_3 + B_{12}X_1X_2 + B_{23}X_2X_3 + B_{13}X_1X_3 + B_{11}X_1^2 + B_{22}X_2^2 + B_{33}X_3^2 + B_{123}X_1X_2X_3 \qquad (3.1)$$

where, Y : response measurement

X_1 : cutting speed

X_2 : feedrate

X_3 : ratio of length of cut to dia.

B_i : coefficients of the model

The model given by equation (3.1) is one such model that may be employed in modeling the response of the system.

An orthogonal design is the second consideration of

an experimental design. An important characteristic of an orthogonal design is that one can obtain the uncorrelated estimates of the model coefficients. [23] The third consideration of the experimental design is the property of rotatability. An experimental design with this latter characteristic can be rotated with its design center without losing the accuracy of the system. To be rotatable, the experiment is to be constructed in such a way that the variance of the estimated response is a function only to the distance from the design center and not the direction to the point. A rotatable design is constructed to be unbiased in selecting the experiment conditions.

From these three considerations, an experimental design was chosen (the central composite design) which can explore second order interaction effect, and which exhibited orthogonality and rotatability.

3.2 Central composite design

Figure 3.1 illustrates the arrangement of the experimental design for a central composite design having three factors. The structure of a central composite design is a conventional 2^3 factorial design with added center points and six outer axial points. The distance

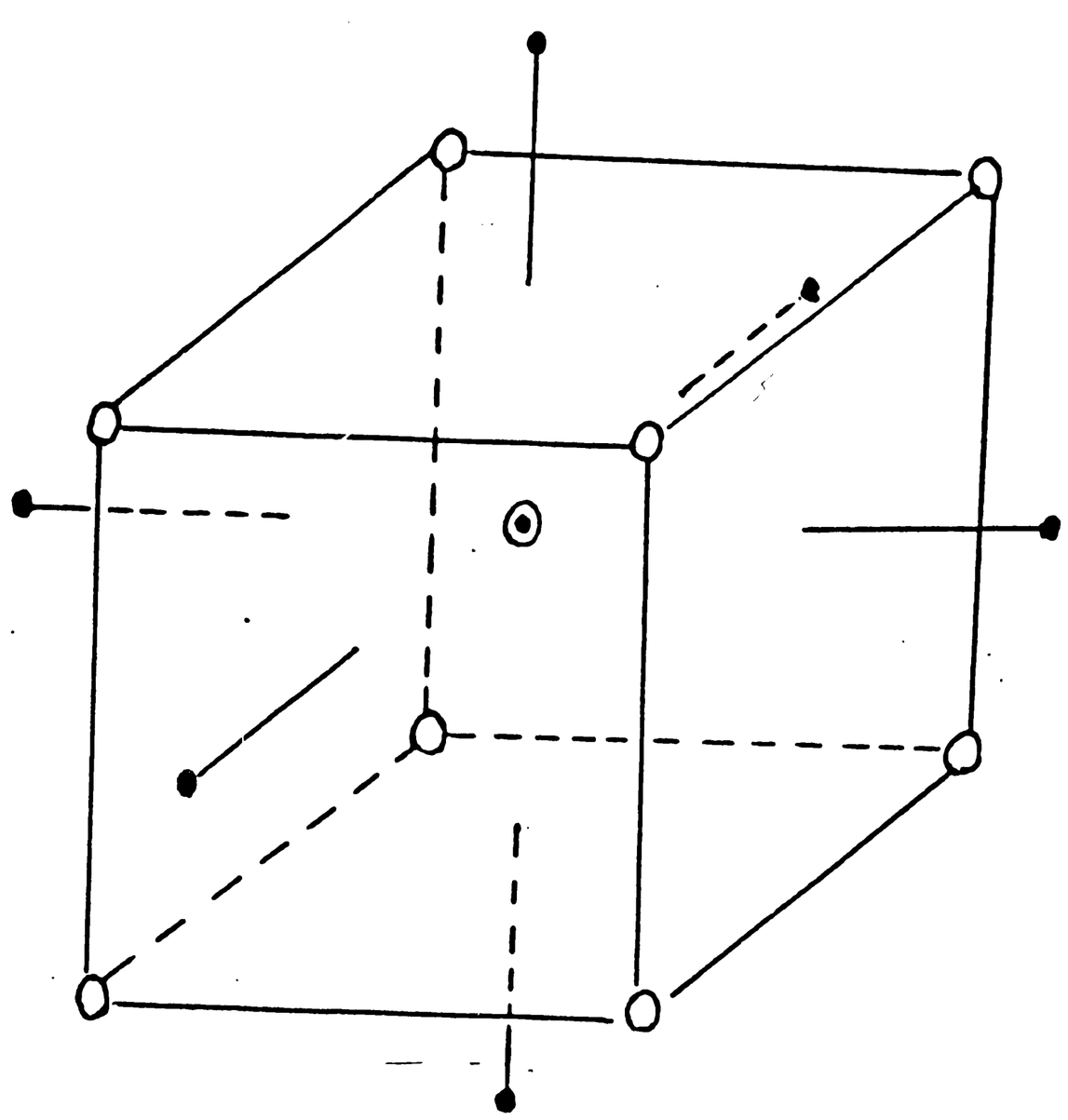

Fig. 3.1 Structure of central composite design.

between each point and the center point is 1.682 times the unit distance. The unit distance is defined to be half of the distance between two factorial experimental points. Because the experimental conditions are chosen and located at the same distance from the center point to all surrounding points, the bias in selecting experimental conditions is eliminated. The distance from the center point to all the surrounding points indicates that all the surrounding points are on the surface of the sphere and that the center point of the sphere is the experimental design center. The central composite design exhibits both the properties of orthogonality and rotatablity. More over, the central composite design, with the 2^3 factorial design embedded with in, is also a design that can explore second order interaction effect among factors. In conclusion, the central composite design matches all the properties desired for this investigation and was chosen to be the experimental design for this research.

3.3 Choice of cutting condition

The choice of cutting conditions was made by taking into account the type of work material, tool material, flute length of the drill and the capability of the

the machinery. The cutting tools (drill bits) used in this experiment were CLE-LINE high speed steel, straight shank, jobber length twist drills which were supplied by Kennemetal Co. Two different diameters of drills were used for comparison (1/8" drill and 19/64" drill). The reasoning to support the selection of these two diameters was :

a. Drills with diameters ranging between 1/8" and 1/2", are the most common used drills. [29]

b. The machining data handbook [20] recommends to lower the cutting speed and feedrate if the ratio of length of cut to diameter is greater than 2. Many engineers categorize any hole length more than six diameters as deep hole drilling. [28] The flute length of the 19/64" drill is 3 1/4 inches (11 diameters) and the flute length for 1/8" drill is 1 11/16 inches (13.5 diameters). The flute lengths of both size of drills are adequate to serve the purpose of studying deep hole drilling.

The Machining Data Handbook [20] recommends the drilling conditions according to criteria of workpiece hardness, size of drill, and type of drill. For HSS twist drills, 1/8" and 19/64" in diameter, and an alloy

steel work material with hardness between 225 BHN and 275 BHN, the recommended cutting conditions are :

19/64"drill ==> 0.0046 ipr and 55 sfpm(707 RPM)
1/8" drill ==> 0.003 ipr and 55 sfpm (1680 RPM)

Cutting conditions for the center points of the central composite experimental design were chosen on the Bridgeport CNC machine to be as close as possible to the recommended feed and speed. The following center point conditions were thus chosen :

	feedrate (ipr)	cutting speed (RPM)	Length of cut over diameter
19/64"	0.0046	700	6
1/8 "	0.003	1700	7

The experimental points, corresponding to the constraints of machine tool, drills, and the requirement of the central composite design, were selected and are listed in Table 3.1. For convenience, these experimental points have been coded such that the lower level corresponds to -1, the higher level to 1, and the center point to the origin, 0. The transforming equations to relate each cutting conditions to the coded values are as follows:

$$HV == 2 \times (V - 700) / (900 - 500) \quad (3.2)$$

$$HF == 2 \times (F - 0.0046) / (0.0066 - 0.0026) \quad (3.3)$$

$$HR == 2 \times (R - 6) / (8 - 4) \quad (3.4)$$

TABLE 3.1 Selected cutting conditions for experiment

Coded value			1/8" drill			19/64" drill		
V	F	D	V(RPM)	F(IPR)	D(IN.)	V(RPM)	F(IPR)	D(IN.)
1	1	1	2400	.0066	1.125	900	.004	2.375
1	1	-1	2400	.0066	0.625	900	.004	1.1875
1	-1	1	2400	.0026	1.125	900	.002	2.375
1	-1	-1	2400	.0026	0.625	900	.002	1.1875
-1	1	1	1000	.0066	1.125	700	.004	2.375
-1	1	-1	1000	.0066	0.625	700	.004	1.1875
-1	-1	1	1000	.0026	1.125	700	.002	2.375
-1	-1	-1	1000	.0026	0.625	700	.002	1.1875
1.682	0	0	2877.4	.0046	0.875	1036.4	.003	1.7813
-1.682	0	0	522.6	.0046	0.875	363.4	.003	1.7813
0	0	1.682	1700	.0046	1.2953	700	.003	2.7799
0	0	-1.682	1700	.0046	0.4545	700	.003	0.7826
0	1.682	0	1700	.0079	0.875	700	.0048	1.7813
0	-1.682	0	1700	.0012	0.875	700	.0013	1.7813
0	0	0	1700	.0046	0.875	700	.003	1.7813
0	0	0	1700	.0046	0.875	700	.003	1.7813

$$LV = 2 \times (V - 1700) / (2400 - 1000) \quad (3.5)$$

$$LF = 2 \times (F - 0.003) / (0.004 - 0.002) \quad (3.6)$$

$$LR = 2 \times (R - 7) / (9 - 5) \quad (3.7)$$

where, H : 19/64" drills
L : 1/8" drills.
V : cutting speed in RPM
F : feedrate in IPR
R : length of cut to diameter ratio.

3.4 Preparation of work material

The work material chosen in the investgation was AISI 4145 heat treated alloy steel with a hardness average of 247 BHN and variance 11.85. (Appendix I) The alloy steel was obtained as round stock, 3 inches in diameter and 24 inches in length. The steel was cut into cylindrical specimens with a height of 4 inches.

The dimensions of the work specimen were chosen for the following reasons :

a. The effect of drilling breakthrough phenomenon on tool wear is more severe than continuous drilling. [8] Four inches in height can offer enough space for the selected length of cut and avoid the effect of breakthrough phenomenon.

b. Because of the restriction of the dynamometer

used, it was necessary to measure the forces within the range of the dynamometer's sensitivity region (3 inches by 3 inches measuring table). A three inches diameter for the workpiece specimens was within the dynamometer's range.

3.5 Equipment

A BRIDGEPORT CNC series 1 milling machine located in the Manufacturing Technology Laboratory at Lehigh University was selected to perform the experiment. Three control variables (length of cut, feedrate, and cutting speed), were programmed into the CNC controller to assure the accuracy and repeatability of these control variables and to avoid potential human error.

The data acquisition system of this experiment consisted of a Kistler four-component dynamometer, four Kistler dual mode amplifiers, four Analog to Digit (A/D) converters and the PDP 11/34 computer system. Through the amplifiers, the four-component dynamometer was linked to the PDP 11/34 computer system to record all force components generated during each drilling test. Torque,

thrust, X-force, and Y-force signals read by the dynamometer were first amplified and then were converted from an analog signal to a digital signal by the A/D converters. The digitized signals were recorded through each channel by executing a FORTRAN-based data acquisition program [Appendix II] developed as part of this research.

After each cut, the tool flank wear was examined with a " ToolMakers " microscope. Corresponding cutting time for each cut was measured by the built-in timer on the PDP 11/34 minicomputer. A block diagram of the experimental equipment is shown in Fig. 3.2.

3.6 Procedures for Data acquisition

The measurements of the experimental responses of the study consist of force measurements and flank wear measurements. Force measurements were obtained by the data acquisition system described in the previous section. Flank wear measurements were standardized and obtained with the Toolmakers' microscope.

3.6.1 Forces measurement

Forces were measured by a piezo-electric Kistler

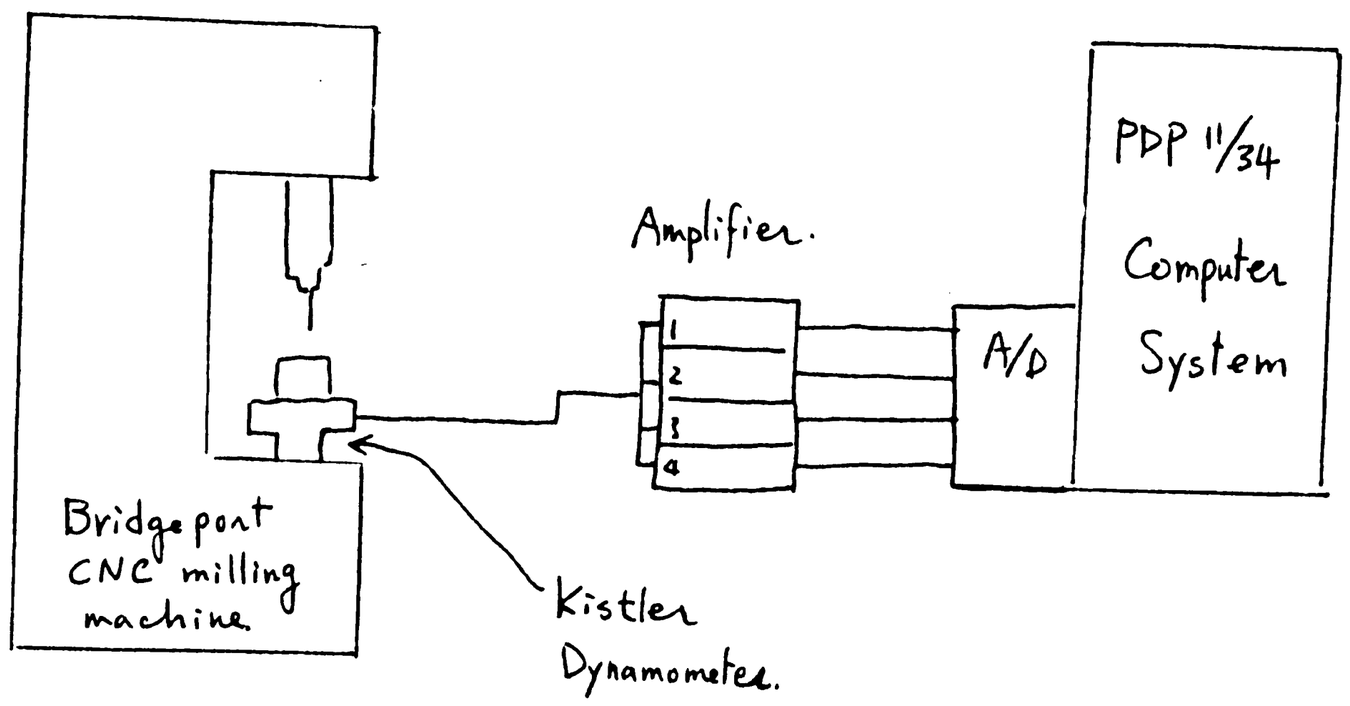

Fig. 3.2 Block diagram of experiment equipment setup

four-component dynamometer. Each output force channel of dynamometer was connected to a different amplifier. The set-up of each amplifier is different due to different sensitivity levels of the dynamometer for each force/torque component to be measured. The basic procedure for the setup of the dynamometer and the amplifiers was as follows :

1. The possible range of thrust force and torque for specific cutting condition was conducted by either (1) consulting the Machining Data Handbook [20], or (2) calculating the estimated forces from Cook's equation. (equation 2.6)

2. The sensitivity levels of the dynamometer for force/torque were set according to the operating manual i.e. 219.63 pC /ft-lb (Pico Columb per foot-pound) for torque, - 8.674 pC/lb for thrust, and 8.86 pC/lb for X- and Y-force.

3. The setup of each amplifier for proper sensitivity and range calculated [Table 3.2] were calculated using the following equations :

   a. $[\text{Sensi.}]_{\text{dynam}} = [\text{Sensi.}]_{\text{amplr}} \times [\text{Range}] \times [\text{Factor}]$

   b. $[\text{Range}] == [\text{Scale}]_{\text{amplr}} \times 10$

TABLE 3.2. Setup of amplifiers

	Torque	Thrust	X-force	Y-force
1. Desired range	0 - 1000 ft-lb	0 - 2500 lbf	0 - 100 lbf	0 - 100 lbf
:= (4)(9)*				
2. Dynamo. Sensit.	219.64 pC/volt	8.674 pC/volt	16.68 pC/volt	16.68 pC/volt
3. Dynamo. output	0 - 219640 pC	0 - 21685 pC	0 - 1668 pC	0 - 1668 pC
4. A/D converter range	0 - 10 volt	0 - 10 volt	0 - 10 volt	0 - 10 volt
5. Ampli. sensit.	0 - 21964 pC/volt	0 - 2168.5 pC/volt	0 - 166.8 pC/volt	0 - 166.8 pC/volt
:= (1)/(2)*				
:= (6)(7)(8)*				
6. Amplifier sensitivity setting	2.19	2.17	1.67	1.67
	(adjustable setting, from 0 - 9.99)			
7. Amplifier sensitivity range	100 - 1k	10 - 100	1 - 10	1 - 10
	(adjustable range, from 0.1 to 10k)			
8. Amplifier sensitivity scale	100	100	100	100
9. Aquisition program factor	100	250	10	10

* the numbers in parantheses is the row number.
For example : The desired range of torque at row 1 is equal to the multiplication of the corresponding column element in row 4 and row 9.

After the force data was collected, the average, slope, standard deviation, and 95% confidence interval for the various regression models were obtained by executing an analysis program [Appendix II], developed for this research.

3.6.2 Flank Wear Measurement

The measurement of drill flank wear was carried out by a Toolmakers' microscope after each cut. The wear data was measured and recorded according to the following procedures :

1. The measurements were taken at four points. Two points located at a distance 1/8th of the total diameter of a drill bit from each cutting margin defined the outside flank measurement points. The other two points were located at a distance 3/8ths of the total diameter from the cutting margin and were used to define the inside flank wear. Figure 3.3 exhibits the location of the four measuring points.

2. The average of the above four wear readings were taken to represent the average flank wear. The average of the two inside flank readings was

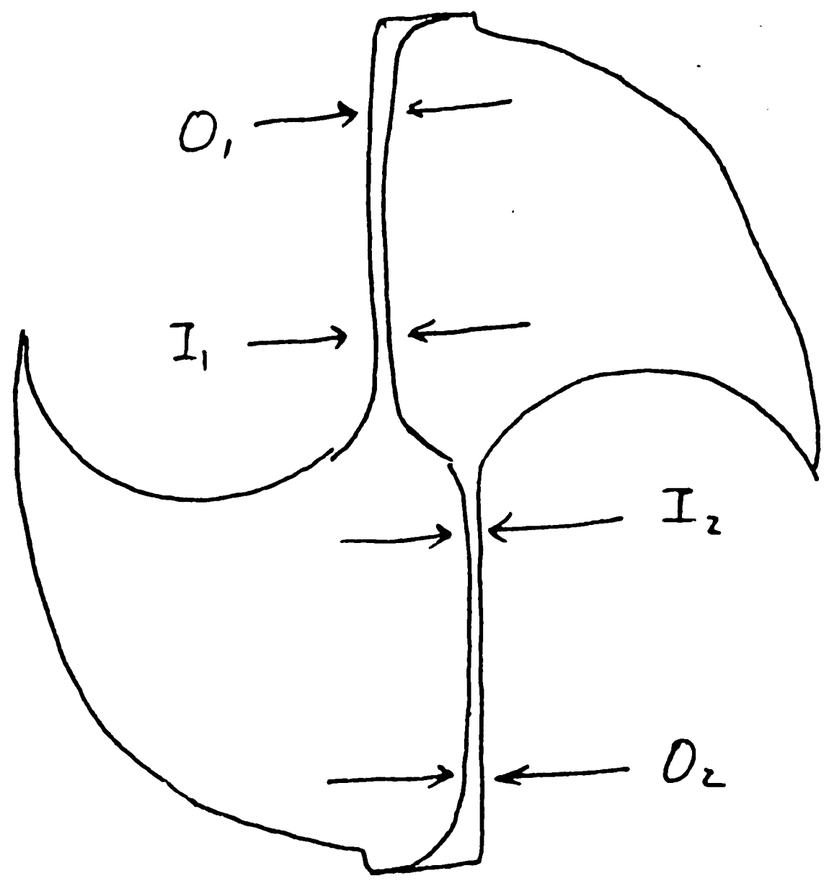

Fig. 3.3 Flank wear measurement layout

[O : outside flank wear measurement point;

I : inside flank wear measurement point]

defined as the inside flank wear. The outside flank wear was defined as the average of the two outside flank readings.

CHAPTER FOUR

EXPERIMENT RESULTS AND ANALYSIS

Following the preparations, setups, and procedures discussed in chapter three, the experiment using the Central Composite Design was conducted. The recorded measurements of response variables are tabulated in Appendix III. The experimental cutting conditions of both sizes for the drills used in this investigation were replicated four times. The response measurements can be categorized into two parts: direct measurements and derived measurements. In direct measurements, responses consisted of total average flank wear, inside flank wear and outside flank wear. Derived measurements consisted of the average rate of flank wear, the mean value of all forces and torque, the slope of forces and torque, and their standard deviations.

4.1. Estimation of Fitted Model Coefficients

The estimations of coefficients for the regression models generated in this research were obtained by a Fortran-based program. [Appendix II] In this program, a three-variable second order model (equation 3.1) is employed in modeling the response systems. Using the

technique of multivariate linear regression, the coefficients, B_i, of the model for each responses were obtained from the following matrix operation :

$$B = (X' \ X)^{-1} \ X' \ Y \qquad (4.1)$$

where, B : coefficient matrix
X : coded experiment conditions
X': transpose matrix of the X matrix
Y : response matrix

$(X' \ X)^{-1}$: inverse matrix of the product matrix

The coefficient matrix B of both the direct and derived measured responses for the 19/64" drill and the 1/8" drill are tabulated in Appendix VI.

An F-test of each of the response models was performed to identify the significance of each of the main effects and interaction effects for each response model. The selected results of the F-tests are tabulated in Appendix V. The coefficient of multiple determination, R^2, is appended to the tables in Appendix VII for judging the adequacy of the regression model. R^2 values were obtained by use of the following equation :

$$R^2 = \frac{SSR}{SST} \times 100\% \qquad (4.2)$$

where, SSR : Sum of the squares due to the regression model
SST : Sum of the squares about mean responses

R^2 is a measure of the proportion of total variation of the response about the mean of the responses explained by the fitted regression equation. For instance, a R^2 value equal to 97% means that 97% of the total variation of the response about the mean of the responses can be explained by the fitted equation. A lack-of-fit test was also employed to examine whether a regression model was adquate to fit the data or not. Hypotheses for the lack-of-fit test were :

Ho : The model adequately fits the data.

Hl : The model does not fit the data.

The null hypothesis, Ho, will be rejected if the lack-of-fit F-test value exceeds the value of F(5, 48, .01) = 2.00 with an α = 0.01 significant level. The value of F(5, 48, .01) was the value obtained for the upper one percent of the F distribution with 5 and 48 degrees of freedom. The degrees of freedom for the multiple regression model corresponding to the central composite design used in the research were obtained as follow :

a. The degrees of freedom associated with the system are the number of the total observations in the

experiment. A three factors central composite design contains 15 observations. They are a 2^3 factorial design with 8 observations, six axial points and one conter pointer point. In this experiment, An extra center point was performed for all the replications of the design. The total number of experimental conditions was thus 16. Each experimental condition was replicated four times. Total observations for the experiment are thus equal to four times sixteen (4 x 16 = 64).

b. Each coefficient in the regression model contains one degree of freedom. There are ten coefficients in the model (excluding the constant) which account for 10 degree of freedom.

c. The degrees of freedom associated with the error term of the regression model was obtained by calculating the difference between the total degrees of freedom for the system and the degrees of freedom for the regression model. The degrees of freedom of the error term then become 53, which is obtained by substracting 10 (model) and 1 (constant) from 64 (total observations).

d. The regression model can be partioned into the

following effects; main effects, interaction effects, quadratic effects and the mixed effect (tri-factor effect). The interaction effect contains three coefficients, X_{12}, X_{13}, and X_{23}, and accounts for three degrees of freedom. The quadratic effects have three coefficients, X_{11}, X_{22}, X_{33} which therefore contribute three degrees of freedom. Each of the main effects of the system has only one degree of freedom. The mixed effect term has one degree of freedom.

Pure error and lack-of-fit terms are obtained from the consideration of the partition of the error term. The degrees of freedom associated with the pure error and lack of fit terms are 48 degrees of freedom and 5 degree of freedom, respectively. If Ho is not rejected, then there is no statistically based apparent reason to doubt the adequacy of the model. Hypothesis testing for each of the coefficients in the model corresponding to a response variable were also conducted. Dependent on the degrees of freedom for each term, the F-test values for rejecting the null hypothesis were chosen at an α = 0.01 confidence level such that F(1,48, .01) = 2.82 for one degree of freedom and F(3,48, 0.01) = 2.21 for three degree of freedom. If the null hypothesis is

rejected, it can be concluded, with 99% confidence, that the coefficient terms are not equal zero. By deleting the coefficients that were not significant determined by an F-test for the individual coefficient, the final fitted models were refined for each response.

4.2 Response Contour Plots

It is difficult to visualize the response surface of any of the variables investigated in this research by presenting only the coefficients of the models. As an aid to visualize the behavior of each response variables as a function of the main effects (cutting speed, feed, and length of cut to diameter ratio), a computer program [Appendix II] which uses the TEMPLT graphic package, was written to generate the contour plots for each model. Because the response models are in the form of three-variable second order equations, the contour plots are made possible by surpressing one parameter at a time as a constant. The constant is initially set at the level zero for each experimental conditions. The following subsections discuss the response surfaces generated as a result of the tests conducted.

4.2.1 Response Surface Plots of the Flank Wear

Table 4.1 lists the flank wear models (average wear, outside wear and inside wear) for the 1/8" diameter drill and the results of their associated statistical tests (significant F test for and the R^2 values for the complete model). All of the wear models were found to be significant at a 99% level. Each of the terms of these three models were also statistically significant at the 99% confident level. Figure 4.1 illustrates the response surface plot of the average flank wear for the 1/8" diameter drill with a constant length of cut to diameter ratio (L/d) of 7. A minimum flank wear value (0.0291 in.) was detected (Fig. 4.1) under the following cutting conditions: feedrate 0.0016 IPR, cutting speed 1500 RPM. Figure 4.2 exhibits the interaction effects of feedrate and length of cut to diameter ratio. The length of cut to diameter ratio was found to be a dominant factor on the growth of the flank wear when the feedrate was higher than 0.002 IPR.

Comparing the response plots of the average wear (Figs. 4.1 and 4.2) and the outside wear (Figs. 4.3 and 4.4), the responses of the outside flank wear was found to be highly correlated with the response of the average

TABLE 4.1 Flank wear model for 1/8"diameter HSS drill

Model**	Main effect*	Interaction*	Quadratic*	Mixed*	Significance	R^2
Average flank wear	0.0351+0.00325X1 +0.00758X2 +0.0146 X3	+0.00248X1X2 +0.00519X1X3 +0.0128 X2X3	+0.00516$X1^2$ +0.00264$X2^2$ +0.0007 $X3^2$	+0.00319 X1X2X3	99%	0.736
Outside	0.0461+0.00886X1 +0.0125 X2 +0.0183 X3	+0.0027X1X2 +0.00783X1X3 +0.0146 X2X3	+0.00684$X1^2$ +0.00504$X2^2$ -0.00342$X3^2$	+0.00273 X1X2X3	99%	0.667
Inside	0.0241-0.00197X1 +0.00117X2 +0.00883X3	+0.00256X1X2 +0.00225X1X3 +0.011 X2X3	+0.00352$X1^2$ +0.00269$X2^2$ +0.00227$X3^2$	+0.0303 X1X2X3	99%	0.546

97

* : F-test significant level for each effect is 99%

** : Coefficients for model may be obtained from Appendix iv, TABLE A4.2

X1 : Coded cutting speed, using transformation equation 3.5.

X2 : Coded feedrate, using transformation equation 3.6

X3 : Coded length of cut to diameter ratio, using transformation equation 3.7

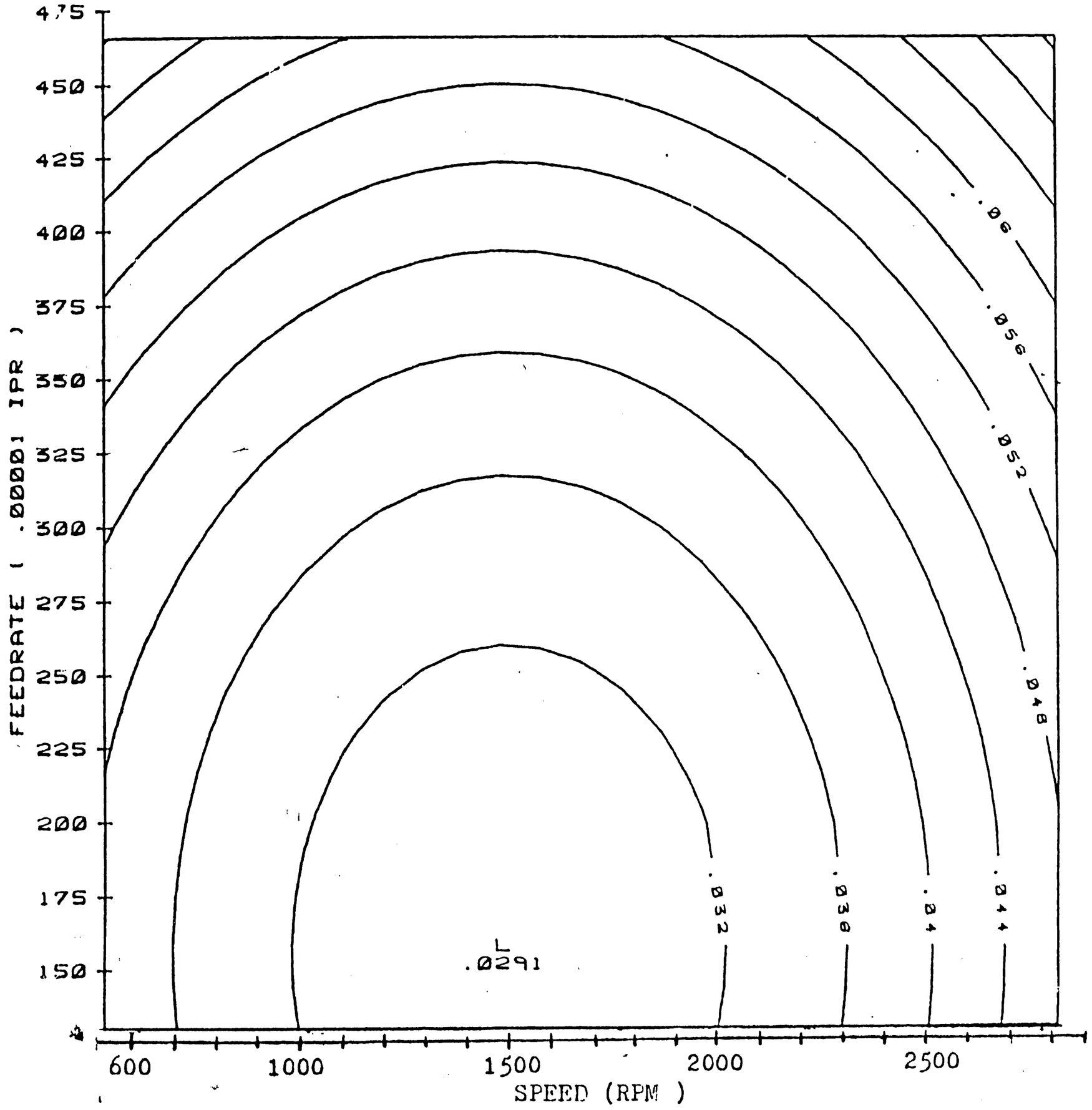

Figure 4.1 Response plot of the average wear for a 1/8" HSS drill with a constant length of cut to diameter ratio equal to 7. Contours represent equal average wear in inches. (work material : AISI 4145 HOT ROLLED alloy steel)

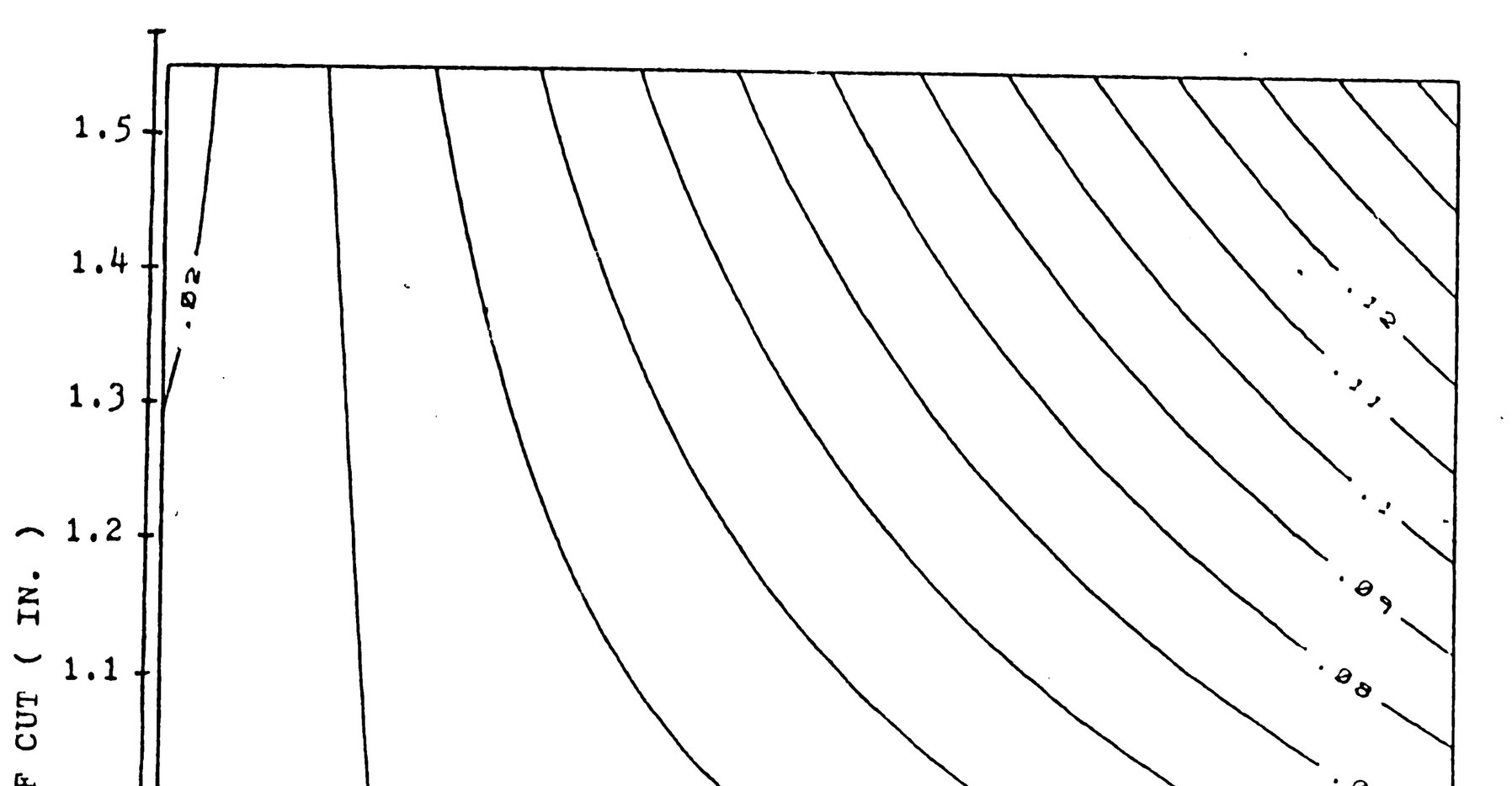

Figure 4.2 **Response surface plot of the average wear for a 1/8" HSS HSS drill at a constant cutting speed of 1700 RPM. Contours represent equal average wear in inches. (work material : AISI 4145 HOT ROLLED alloy steel)**

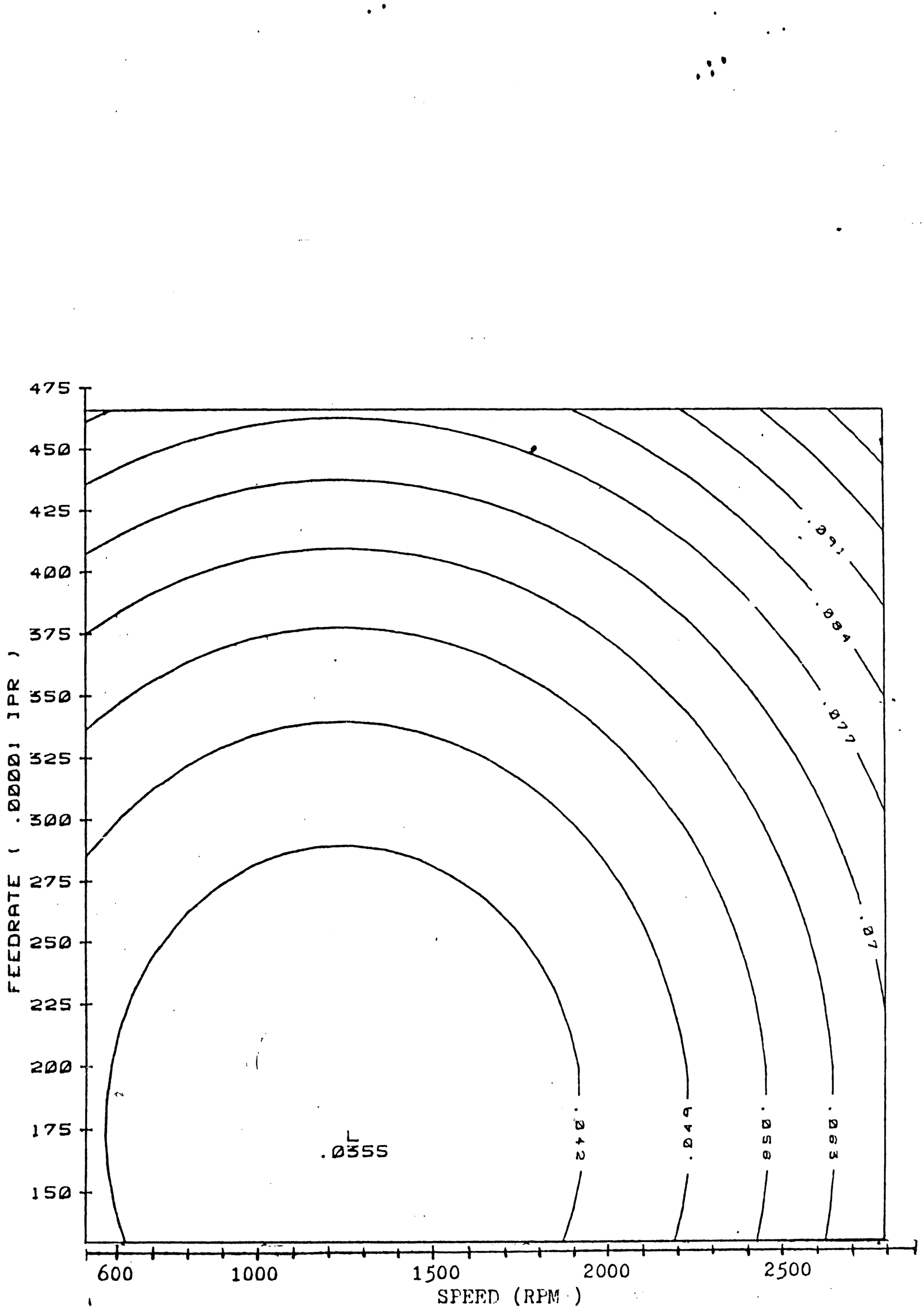

Figure 4.3 Response surface plot of the outside wear for a 1/8" HSS drill with a constant length of cut to diameter ratio equal to 7. Contours represent equal outside wear in inches. (work material : AISI 4145 HOT ROLLED alloy steel)

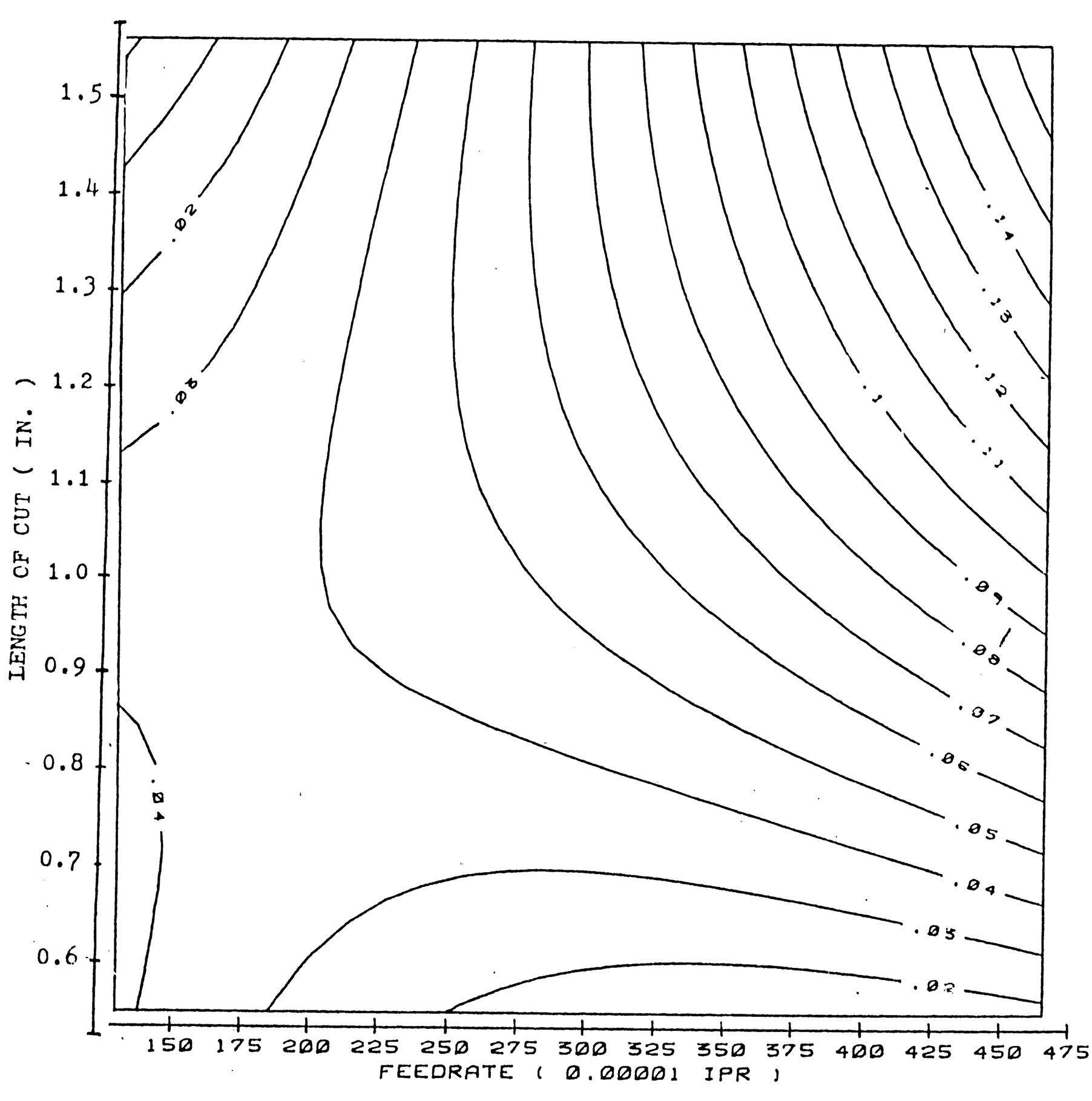

Figure 4.4 Response surface plot of the outside wear for a 1/8" HSS drill at a constant cutting speed of 1700 RPM. Contours represent equal outside wear in inches. (work material : AISI 4145 HOT ROLLED alloy steel)

flank wear. Table 4.2 summarizes the correlation analysis between each of the response variables of the investigation. The correlation coefficient between the average wear and the outside wear for the 1/8" diameter drill is 0.978. The cutting conditions for minimum outside wear was 0.0355 inches and is found from figure 4.3 to be at a cutting speed of 1300 RPM and a feedrate of 0.0017 IPR for a 1/8" diameter drill. The cutting conditions for the minimum average flank wear and the minimum outside wear were thus almost identical.

The response plot for the inside wear were different when comparing the results for the 1/8" diameter drill and the 19/64" drill. For a drill size equal to 1/8", the response pattern of the inside flank wear (Fig. 4.5) was similar to the average wear and outside wear as given in figures 4.1 and 4.3. The inside flank wear for the larger size drill (19/64" diameter) with a constant length of cut to diameter ratio equal to 6, (Fig. 4.6) is mainly influenced by cutting speed rather than influenced by the combined effect of feedrate and cutting speed as for the 1/8" drill. In general, length of cut to diameter ratio and cutting speed were found to be the dominant factors in generating the average and outside flank wear.

TAPLE 4.2 Correlation analysis of the response variables for 1/8" diameter drills

	Rate		Mean					Slope				Standard dev.			
Rate of wear	OW	IW	TM	Mz	Fz	Fx	Fy	Mz	Fz	Fx	Fy	Mz	Fz	Fx	Fy
Average	.978	.89	-.55	-.018	.50	-.13	-.17	.37	.853	-.07	-.01	.41	.77	.07	.32
Inside		.80	-.54	-.032	.48	-.16	-.10	.39	.820	-.07	-.01	.42	.75	.06	.04
Outside			-.52	-.035	.45	-.10	-.30	.25	.805	-.09	-.01	.23	.68	.02	.11
Mean															
Time				.462	.02	-.18	.35	-.22	-.31	.26	.24	.11	-.1	.22	.06
Torque					.44	.21	.44	.50	.17	.18	.18	.58	.32	.40	.26
Thrust						.14	.01	.31	.64	.04	.06	.60	.73	.35	.52
X force							.17	.40	-.06	-.07	-.10	-.1	-.1	.14	.14
Y force								.17	-.13	.11	.05	.25	-.0	.02	.36
Slope															
Torque									.42	.01	.02	.49	.40	.15	.21
Thrust										-.01	.07	.45	.87	.11	.32
X force											.97	-.1	.09	.03	.10
Y force												.10	.15	-.0	.11
Standard dev.															
Torque													.63	.53	.65
Thrust														.22	.48
X force															.26
Y force															

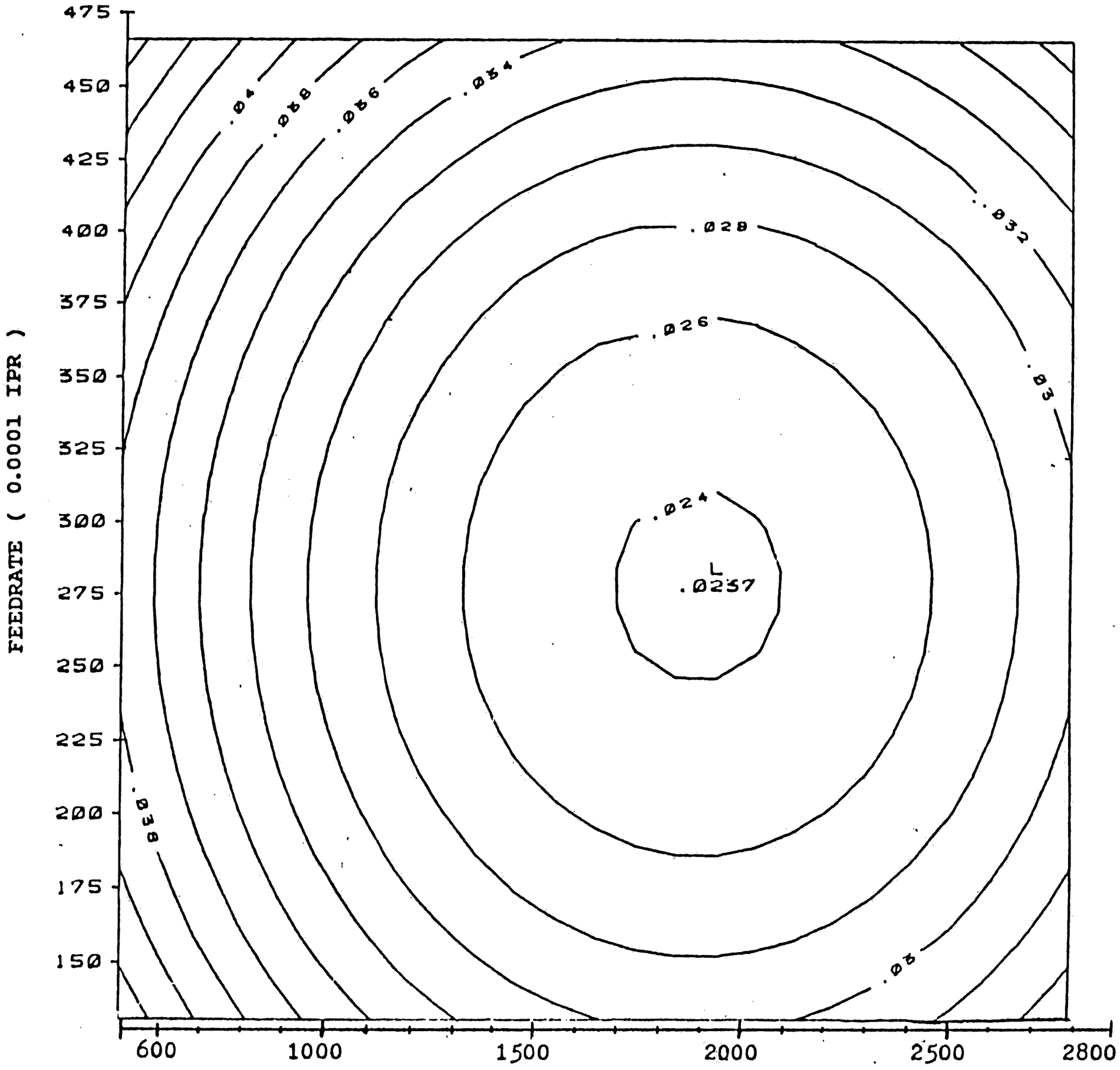

Figure 4.5 Response surface plot of the inside wear for a 1/8" HSS drill with a constant length of cut to diameter ratio equal to 7. Contours represent equal inside wear in inches. (work material : AISI 4145 HOT ROLLED alloy steel)

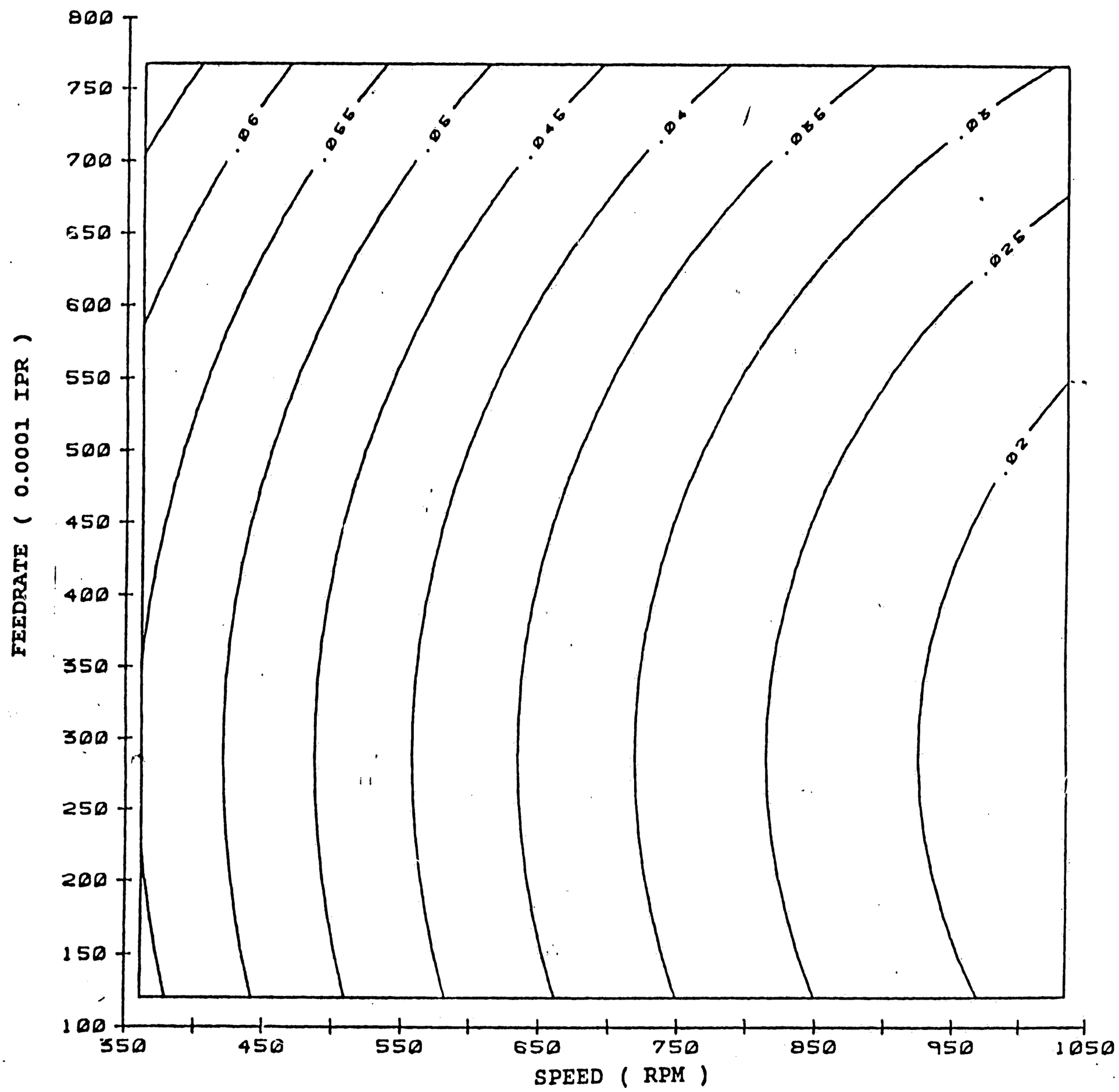

Figure 4.6 Response surface plot of the inside wear for a 19/64" HSS drill with a constant length of cut to diameter ratio equal to 6. Contours represent equal inside wear in inches. (work material : AISI 4145 HOT ROLLED alloy steel)

4.2.2 Response Surface Plots of the Flank Wear Rate

Flank wear rate in this investigation is defined by the following expression :

$$\text{Flank wear rate} = \frac{\text{Flank wear}}{\text{Cutting time}} \qquad (4.3)$$

The flank wear rate represents the average wear rate rather thanthe instaneous wear rate. Figure 4.7 illustrates the average wear rate with respect to a flank wear curve. Average wear rate is obtained by dividing the flank wear by the total cutting time. The angle (α) between the horizontal time line axis and to a line generated from the origin to any flank wear point on the curve can be viewed as the average wear rate for the tool for a specific time period. Flank wear progression is characterized by three representative sections which can be identified on a typical flank wear curve. A sharp increase of the flank wear will be experienced in section I which is the initial cut (break-in region) of a new (sharp) tool. Section III represents the growth of flank wear after thermal instability. Section II corresponds to the gradual flank wear growth that occurs when the number of the holes or cutting time increaser. Gradual flank wear progression (section II) is the region

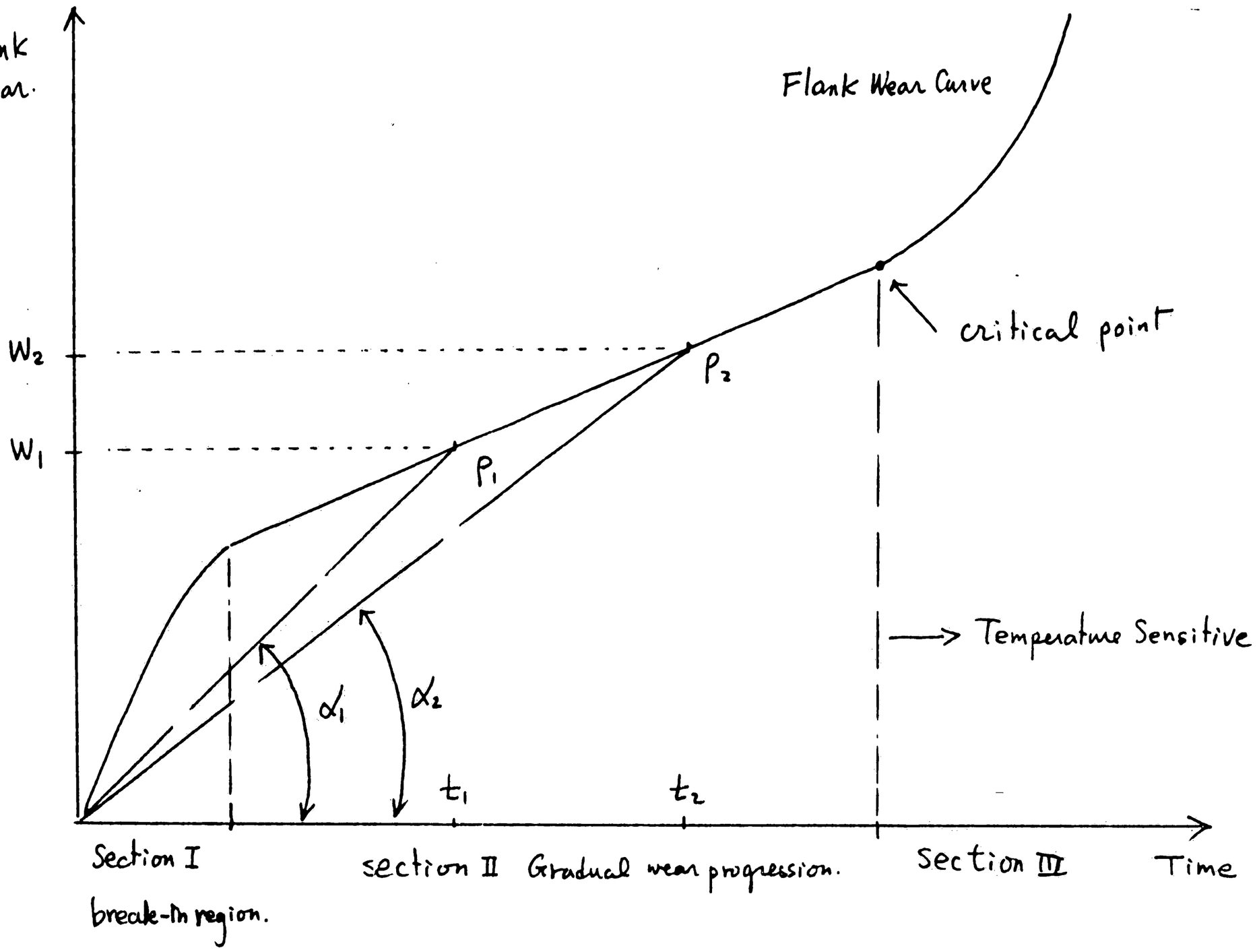

P_1, P_2 : Wear measurement on the flank wear curve.

α_1, α_2 : Angles between horizontal line and the line between origin and the wear point P_1 or P_2.

W_1, W_2 : The corresponding flank wear on the drill bit with respect to P_1, P_2.

Instaneous rate of wear : $\dfrac{W_2 - W_1}{t_2 - t_1}$

Figure 4.7 Illustration of the definition of the average wear rate with respect to a typical flank wear progression.

of concern in this thesis. As is apparent for section II of the flank wear curve, the smaller the angle between the horizontal line and the line between the origin point and the wear point, the larger the tool flank wear and the smaller the average wear rate. The instaneous wear rate can be represented by the slope of the flank wear curve to a particular point as indicated in Fig. 4.7.

The flank wear rate model and the slope of the thrust force model for both sizes of drill are given in Table 4.3. The F-test results for all of the models in Table 4.3 indicated significance at the 99% level. Figure 4.8 illustrates the response surface plot of the average flank wear rate for the 1/8" diameter drill with a constant cutting speed of 1700 RPM. A ridge exists in the low feedrate, low length of cut area of the experimental region. As expected, the wear rate increases with an increase in feedrate. In the low length of cut to diameter ratio area, where the length of cut is less than 0.9 inch, the effect of length of cut on the wear rate is found to exceed the effect of the feedrate. The response surface plot of the slope of thrust force for the 1/8" diameter drill (Fig. 4.9) exhibits a similar response pattern. The slope of the thrust force was mainly dependent on the feedrate when the length of cut was

TABLE 4.3 Flank wear rate and the slope of thrust model for 1/8" and 19/64" diameter HSS drills

Model**	Main effect*	Interaction*	Quadratic*	Mixed*	Significance	R^2
1/8"						
Wear rate	0.000139+.00009X1 +.0000779X2 +.0000226X3	+.0000355X1X2 +.0000349X1X3 +.0000571X2X3	+.0000296X1^2 +.0000143X2^2 -.00000111X3^2	+.000038 X1X2X3	99%	0.851
Slope of thrust	.179 +0.146X1 +0.180X2 +0.111X3		+0.0771X1^2 +0.0291X2^2 -0.00885X3^2	+0.158 X1X2X3	99%	0.828
19/64"						
Wear rate	0.0000373+.00000228X1 +.0000147X2 -.00000836X3	-.00000697X1X2 +.0000216X1X3 -.00000406X2X3	-.00000218X1^2 -.00000147X2^2 +.00000441X3^2	+.00000356 X1X2X3	99%	0.644
Slope of thrust	.151 +0.0264X1 +0.0934X2 -0.0442X3			-0.00936 X1X2X3	99%	0.608

* : F-test signifi-cant level for each effect is 99%

** : Coefficients for the models may be obtained from Appendix IV.

NOTE: The results generateed from wear rate modelare in (in./ 1/30ths sec.), the results from slope of thrust are in (lbf/ 1/30ths sec.).

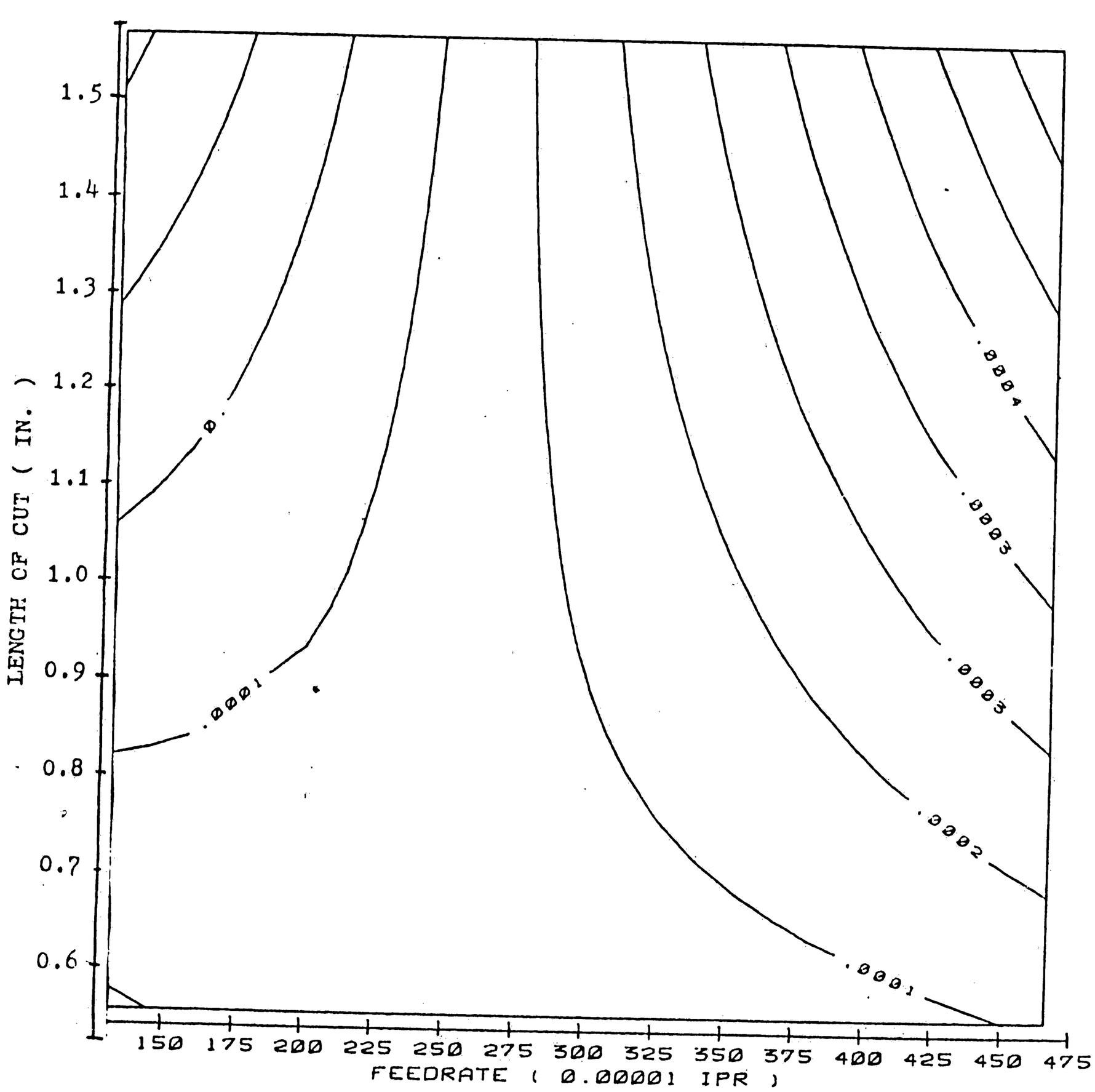

Figure 4.8 Response surface plot of average wear rate for a 1/8" HSS drill at a constant cutting speed of 1700 RPM. Contours represent equal average wear rate in inch / 1/30ths sec. (work material : AISI 4145 HOT ROLLED alloy steel)

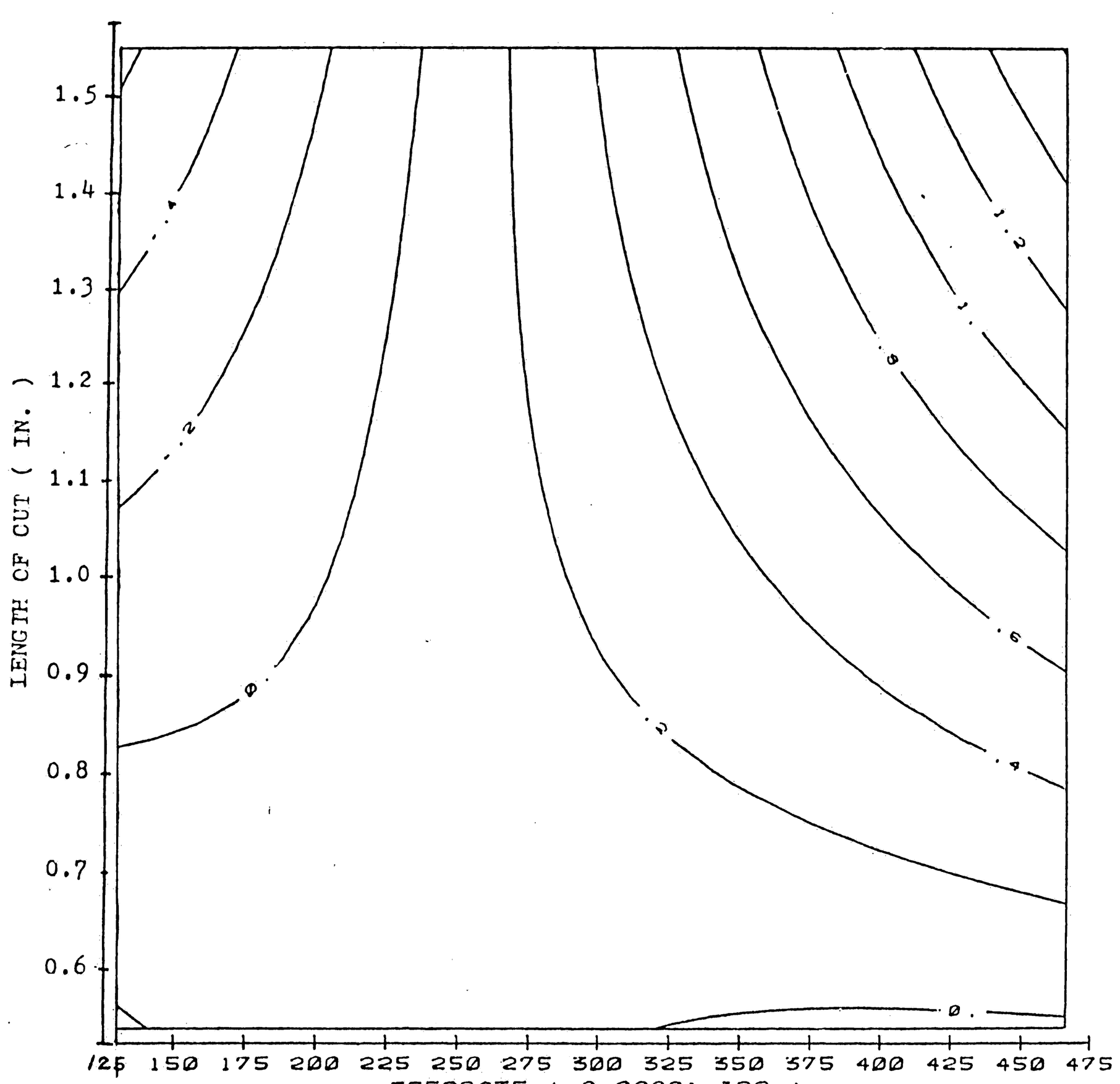

Figure 4.9 Response surface plot of the slope of thrust force for a 1/8" HSS drill at a constant cutting speed of 1700 RPM. Contours represent equal slope of thrust force in lbf / 1/30ths sec. (work material : AISI 4145 HOT ROLLED alloy steel)

greater than 0.9 inches. The result of the correlation analysis [Table 4.2] supports this finding. A correlation coefficient of 0.853 was obtained between the average flank wear rate and the slope of the thrust force. The response plot of average wear rate and the slope of thrust force (Figs. 4.10 and 4.11) at a constant cutting speed of 700 RPM, has the same tendency in their respective response models. Correlation between these two models was obtained as 0.658 [Table 4.4]. These results indicate that the slope of the thrust force may be considered as a good indicator of the flank wear rate.

4.2.3 Response Surface Plots of the Y Component Force and Torque

The models of the Y component force and the torque for the 19/64" diameter drills are listed in Table 4.5. The models for both the mean value and the standard deviation of the Y component force and torque responses was found to be statistical significant at a 99% level. Each of the terms in the models were also significant at this level.

Figures 4.12 through 4.14 exhibit the response surface plots of the standard deviation of the Y component force for the 19/64" diameter drills. The

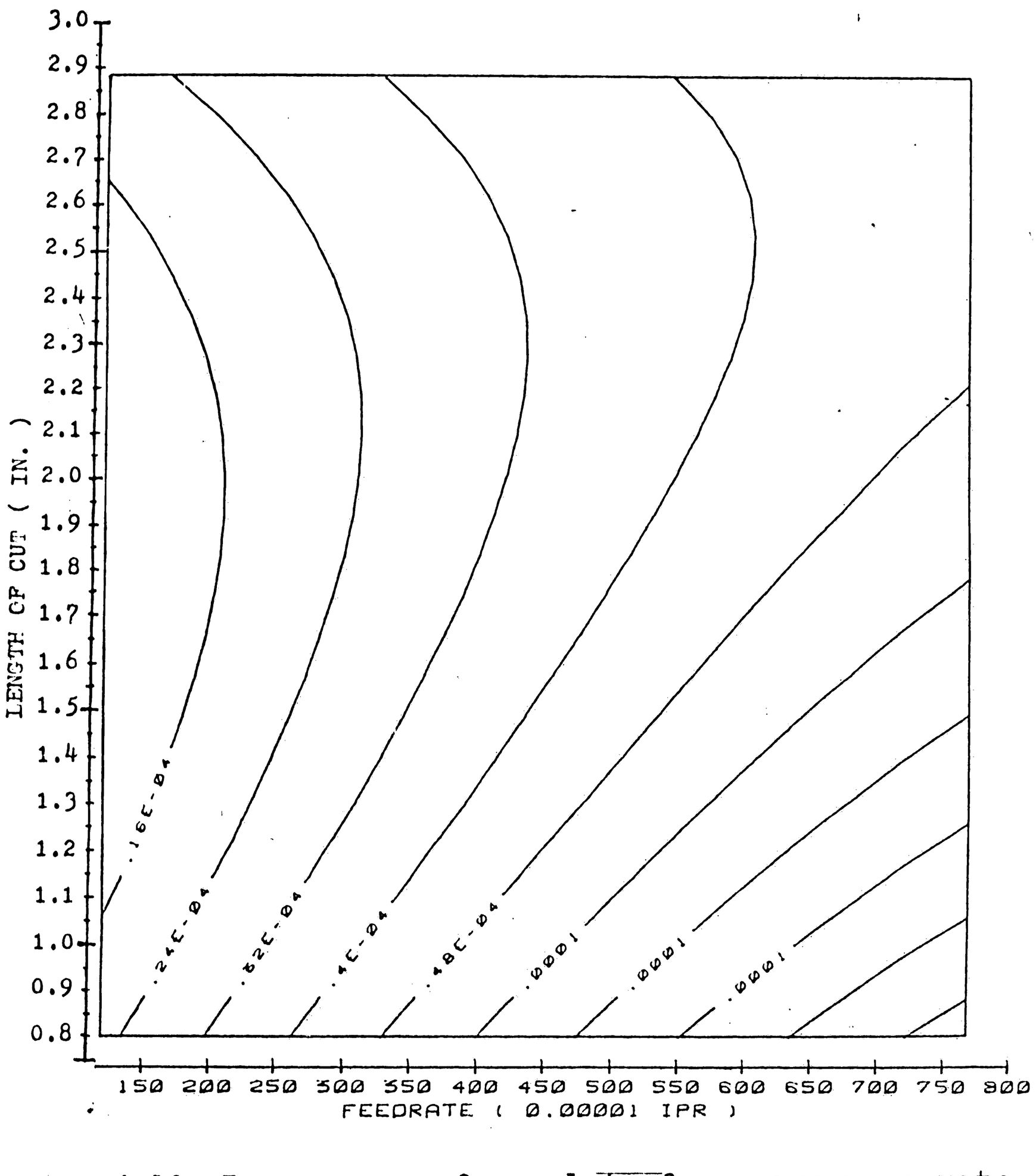

Figure 4.10 Response surface plot of average wear rate for a 19/64" HSS drill at a a constant cutting speed of 700 RPM. Contours represent equal average wear rate in inch / 1/30ths sec. (work material : AISI 4145 HOT ROLLED alloy steel)

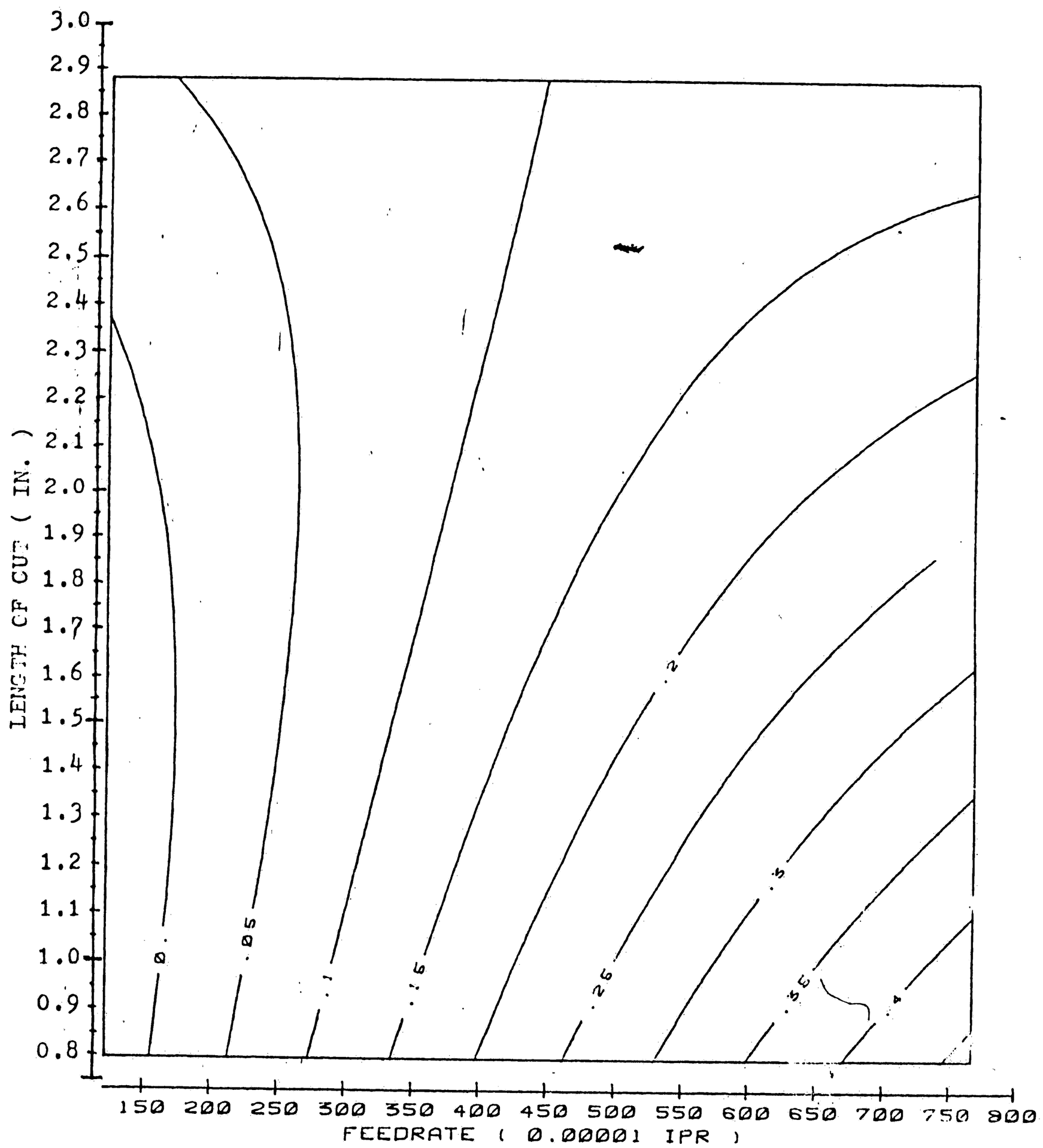

Figure 4.11 Response surface plot of the slope of thrust force for a 19/64" HSS drill at a constant cutting speed of 700 RPM. Contours represent equal slope of thrust force in lbf/ 1/30ths sec. (work material : AISI 4145 HOT ROLLED alloy steel)

TABLE 4.4 Correlation analysis of the response variables for 19/64" diameter drills

<u>Rate of wear</u>														
Average	.951	.36	-.67	.37	.50	.34	-.06	.26	.658	.14	.23	.12	.52	-.13	-.09
Outside		.24	-.63	.34	.46	.28	-.03	.24	.653	.10	.29	.08	.46	-.14	-.105
Inside			-.21	.11	.14	.21	-.09	.51	.147	.04	.11	.03	.15	-.09	-.108
<u>Mean</u>															
Time				-.42	-.5	-.4	.25	-.3	-.61	-.3	-.3	-.1	-.3	.14	.077
Torque					.77	.36	-.19	.60	.411	.13	.07	.56	.47	.34	.265
Thrust					.31	-.19	.32	.636	.11	.07	.48	.76	.34	.214	
X force						.18	.27	.242	.22	-.3	-.1	-.2	-.06	.316	
Y force							.02	-.27	-.2	-.3	-.1	-.2	.03	.445	
<u>Slope</u>															
Torque								.322	.05	-.1	.12	.09	.09	.083	
Thrust									.23	.11	.20	.57	-.08	-.092	
X force										.14	.02	.05	-.21	-.046	
Y force											.09	.11	-.23	-.312	
<u>Standard deviation</u>															
Torque												.51	.47	.647	
Thrust													.13	.145	
X force														.232	
Y force															

TABLE 4.5 Mean and standard deviation of the torque and Y component force model for 19/64" HSS drills

Model**		Main effect*	Interaction*	Quadratic*	Mixed*	Significance	R^2
Mean							
Torque	3.27	-0.152X1 +0.854X2 +0.417X3	-0.0386X1X2 -0.0106X1X3 +0.0762X2X3	$-0.0577X1^2$ $-0.193X2^2$ $-0.101X3^2$	+0.134 X1X2X3	99%	0.821
Y force	5.26	-0.138X1 -0.458X2 -0.0203X3	-1.53X1X2 -0.0443X1X3 +0.0743X2X3	$+0.0929X1^2$ $-0.124X2^2$ $-1.1\ X3^2$	+0.0908 X1X2X3	99%	0.760
Standard deviation							
Torque	0.616	-0.0525X1 +0.0986X2 +0.0978X3	+0.0153X1X2 -0.0674X1X3 -0.0551X2X3	$-0.0468X1^2$ $-0.0697X2^2$ $-0.0422x3^2$	+0.0221 X1X2X3	99%	0.454
Y force	2.41	-0.134X1 +0.155X2 +0.370X3	-0.640 X1x2 -0.0447X1X3 -0.0418X2X3	$-0.340X1^2$ $-0.124X2^2$ $-0.57X3^2$	-0.37 X1X2X3	99%	0.701

* : F-test significant level for each effect is 99%

** : Coefficients for models may be obtained from Appendix IV.

X1 : coded cutting speed, using equation 3.5

X2 : coded feedrate, using equation 3.6

X3 : coded length of cut to diameter, using equation 3.7

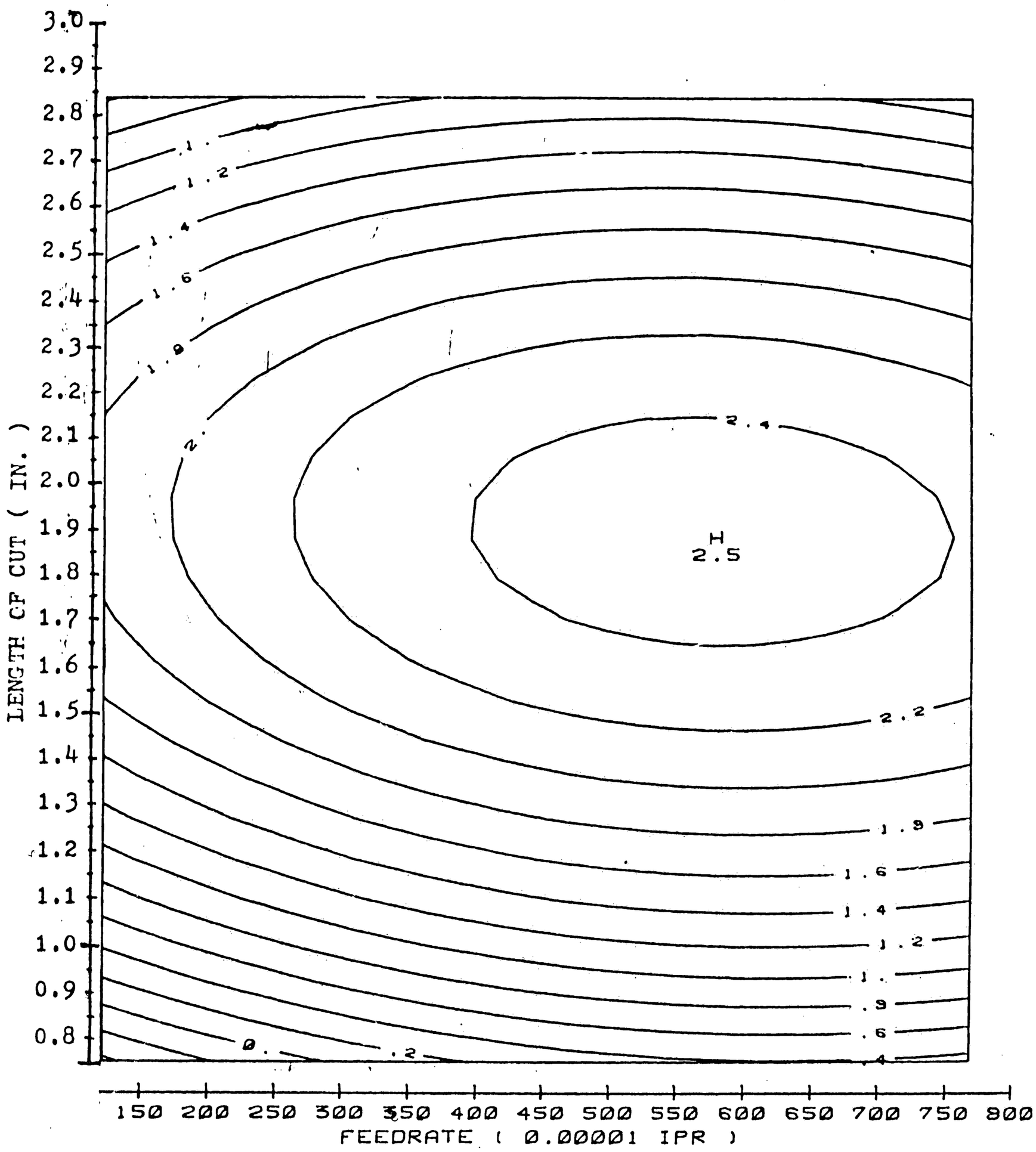

Figure 4.12 Response surface plot of the standard deviation of Y component force for a 19/64" HSS drill at a constant cutting speed of 700 RPM. Contours represent equal standard deviation of Y component force in lbf. (work material : AISI 4145 HOT ROLLED alloy steel)

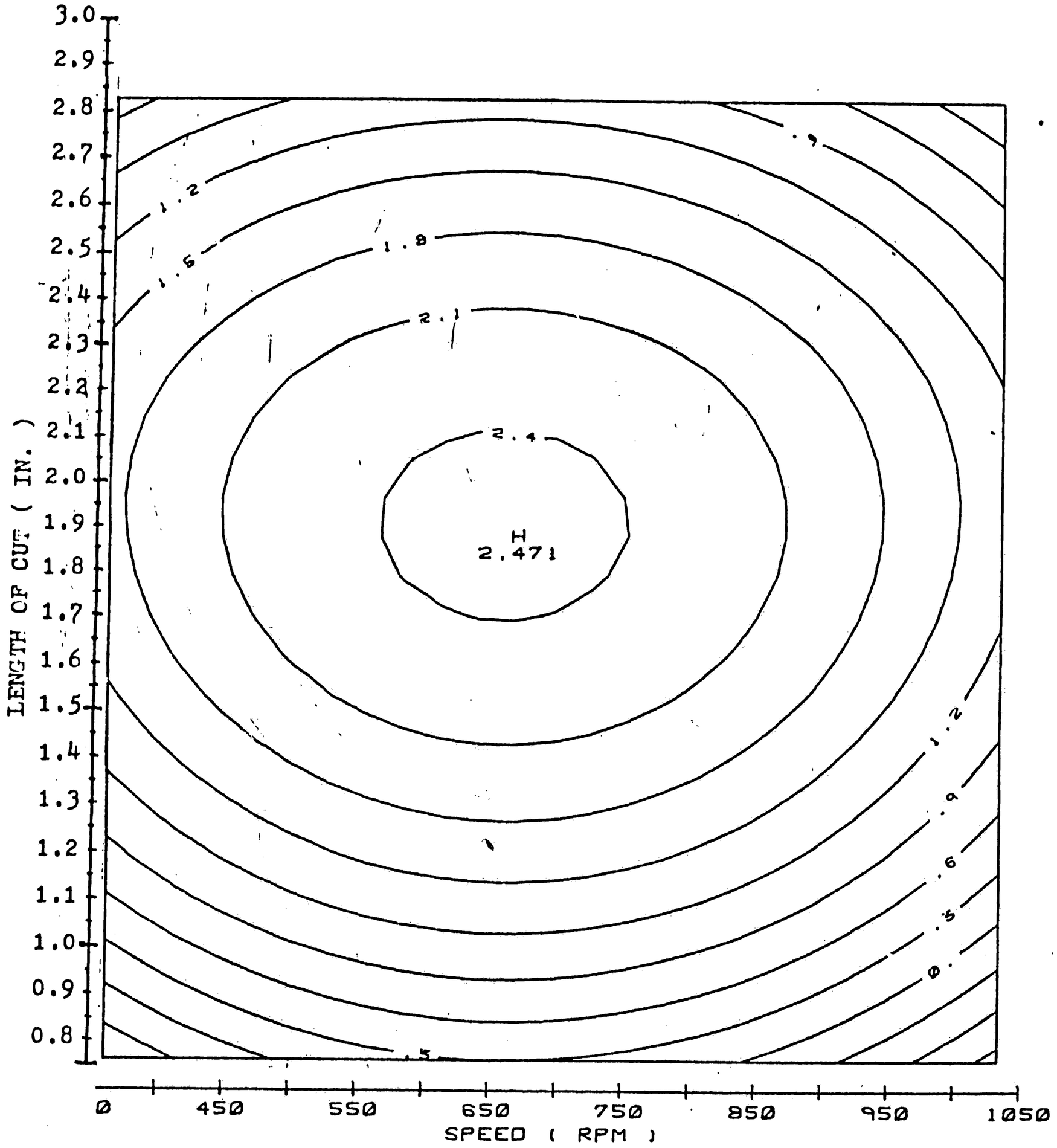

Figure 4.13 Response surface plot of the standard deviation of Y component force for a 19/64" HSS drill at a constant feedrate 0.0046 IPR. Contours represent equal standard deviation of Y component force in lbf. (work material : AISI 4145 HOT ROLLED alloy steel)

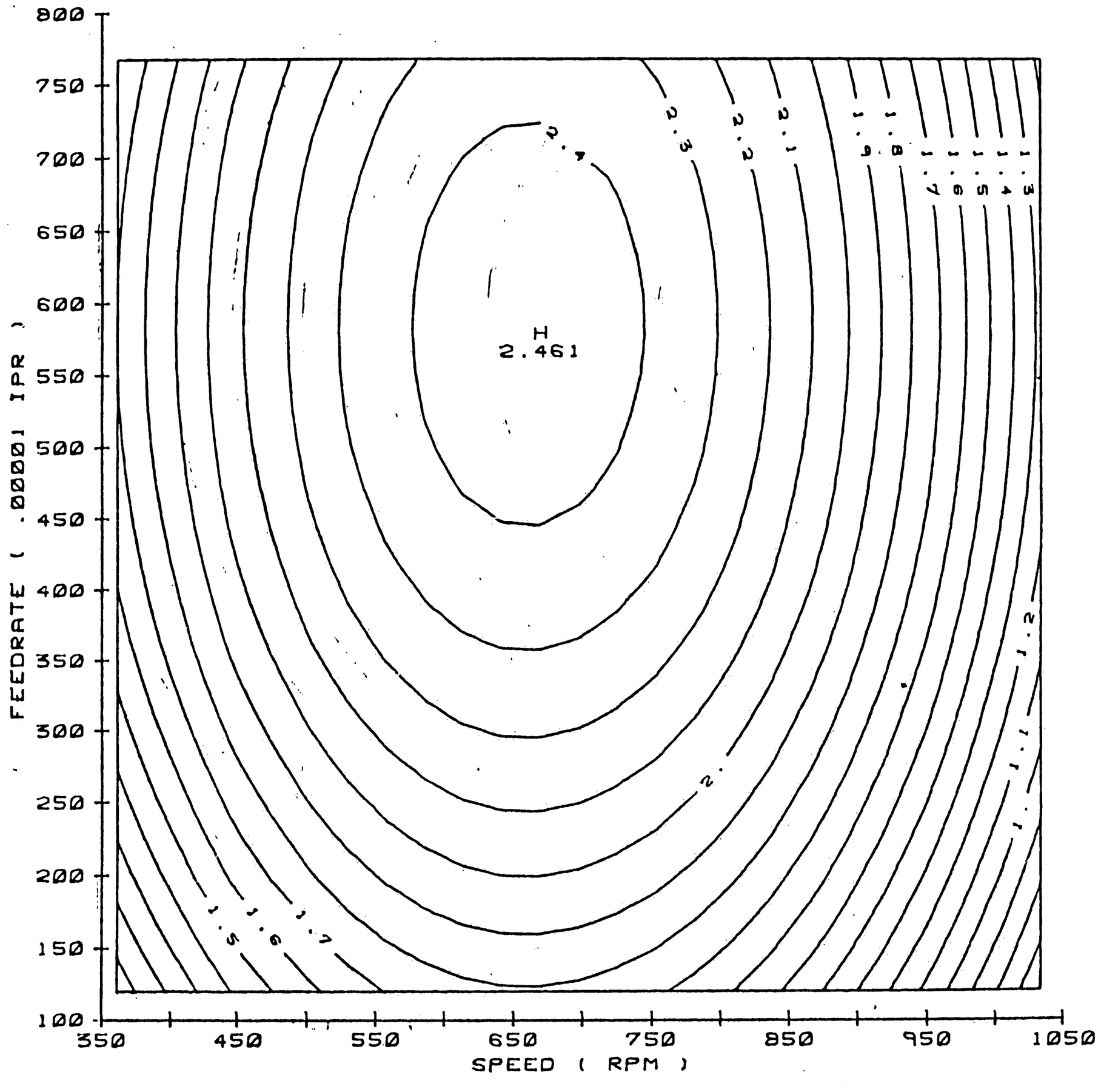

Figure 4.14 Response surface plot of the standard deviation of Y component force for a 19/64" HSS drill with a constant length of cut to diameter ratio equal to 6. Contours represent equal standard deviation of Y component force in lbf. (work material : AISI 4145 HOT ROLLED alloy steel)

maximum standard deviation of Y component force from these three figures is located at the following cutting conditions: 0.00575 IPR feedrate, a spindle speed of 700 RPM, and 1.95 inches in length of cut (6.6 diameters). The response surface plot of the standard deviation of the Y component force (Fig. 4.15) and the standard deviation of the torque (Fig. 4.16) for the 1/8" diameter drill indicate a common feature i.e. the standard deviation of the responses for both the Y component force and the torque increases when the length of cut to diameter ratio increases. Given the same feedrate (0.003 IPR) the standard deviation of the Y component force and the standard deviation of the torque at a cutting speed of 1700 RPM were found to be always higher than the forces/torque values at the cutting speeds lower or higher than 1700 RPM. The analysis of the experimental data indicates that the responses for both sizes of drills had a similar response pattern. From Tables 4.2 and 4.4, the correlation coefficients between the standard deviation of the Y component force and the torque were 0.652 and 0.647, respectively for the 1/8" drill and 19/64" drill. The standard deviation of the forces/torque represents the stability of the forces/torque responses during the drilling operation. The term stability is used to represent the magnitude of

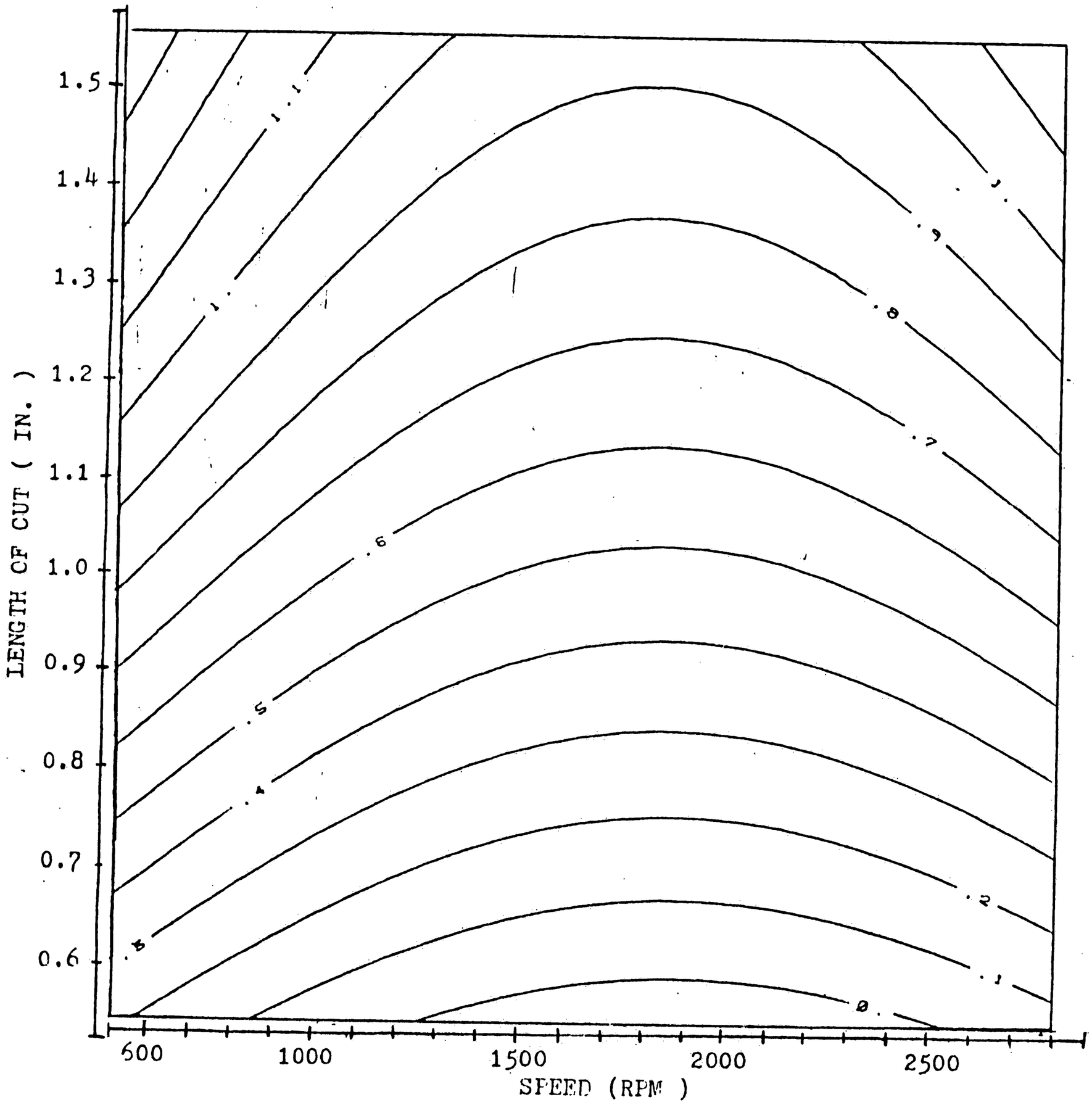

Figure 4.15 Response surface plot of the standard deviation of the Y component force for a 1/8" HSS drill at a constant feedrate 0.003 IPR. Contours represent equal standard deviation of Y component force in lbf. (work material : AISI 4145 HOT ROLLED alloy steel)

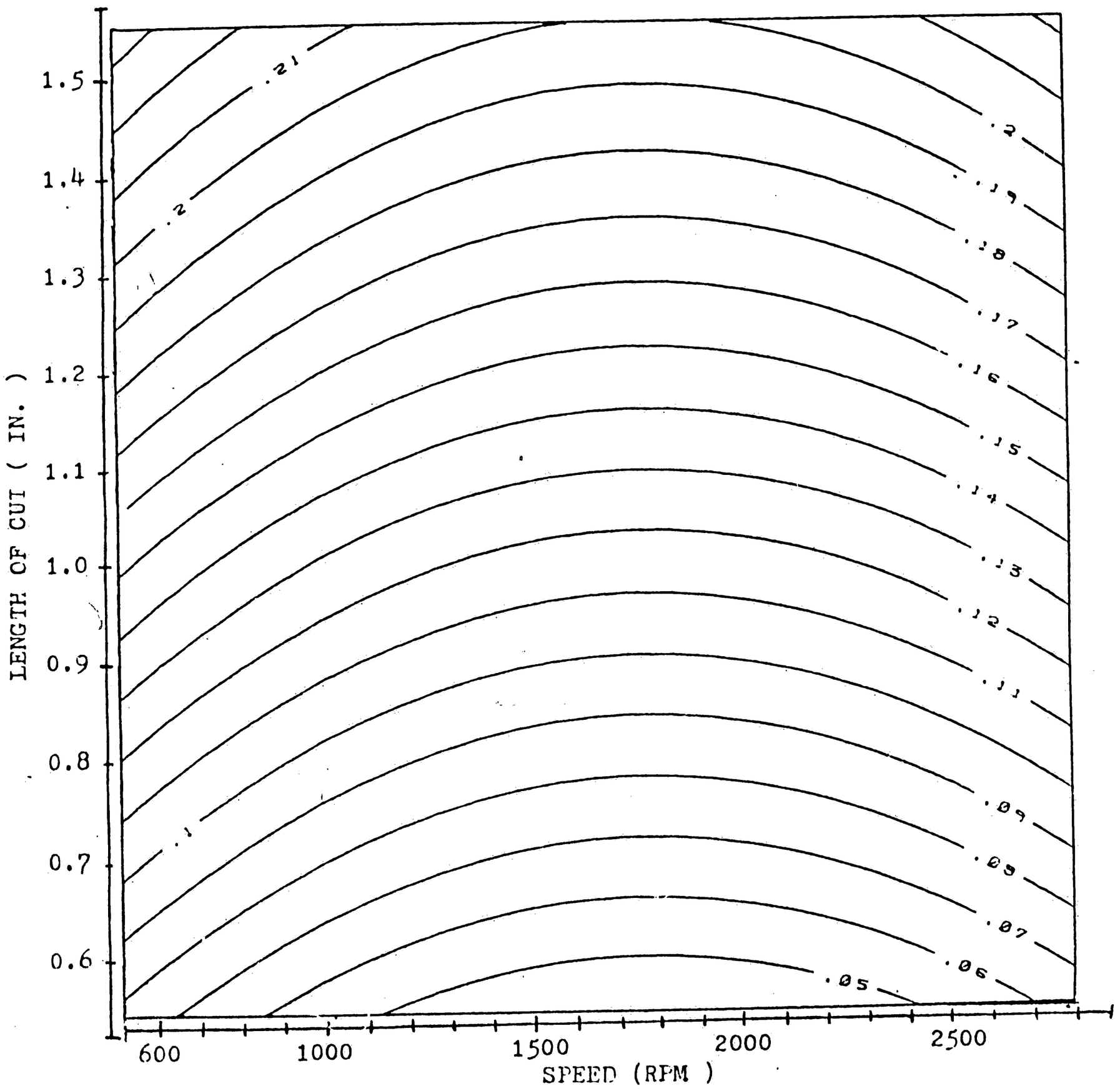

Figure 4.16 Response surface plot of the standard deviation of torque for a 1/8" HSS drill at a a constant feedrate 0.003 IPR. Contours represent equal standard deviation of thrust force in lbf. (work material : AISI 4145 HOT ROLLED alloy steel)

the standard deviation associated with the tests. A large standard deviation is considered to be more unstable than a small standard deviation. The similar response pattern of the stability of the Y component force and the torque indicates that the responses of the Y component force and the torque were influenced by the same machining parameters of the drilling operation. Thus, change in one machining parameter indicates an effect on the stability of the torque and the Y component force. For example, a reduction in the length of cut to diameter ratio would cause both the standard deviation of the torque and the Y component force become smaller. Therefore, the torque and Y component force to readings would be more stable than the data measurements taken at the higher length of cut to diameter ratios.

The response plot of the slope of the torque and the slope of the Y component force exhibits an inverse relationship if compared with the responses of the standard deviation of the torque and the Y component force. A minimum value for the slope of the Y component force was detected while a maximum response was found for the slope. A minimum value of the slope of the Y component force was found for both sizes of drills. The cutting conditions for the minimum value of the slope of

the Y component force (Fig. 4.17) for the 19/64" diameter drill were found to be : cutting speed = 600 RPM, a constant feedrate of 0.0046 IPR, and a length of cut of 1.95 inches (6.6 diameters). Conversely, there existed maximum values of the slope of the torque for both sizes of drills. The cutting conditions for the maximum slope of the torque for the 19/64" drill were: cutting speed = 700 RPM, a constant feedrate of 0.0046 IPR and the length of cut of 2.025 inches (6.8 diameters). (Fig. 4.18) The optimal (maximal versus minimal) cutting conditions for both responses occur at the identical fedrate but different cutting speeds and slightly different length of cut to diameter ratio. Response surface plots of the slope of the Y component force (Fig. 4.17) and the torque (Fig. 4.18) for the 19/64" drill were then compared with the response surface plots of the 1/8" diameter drill(Figs.4.19, 4.20). The cutting conditions for the minimum slope of the Y component force of the 1/8" diameter drill occured at a cutting speed of 2100 RPM, a feedrate of 0.00375 IPR, and a constant length of cut to diameter ratio of 7 (0.875 inches). A cutting speed of 2100 RPM, a constant feedrate of 0.003 IPR, and a length of cut of 0.975 inches (7.8 diameters) were found to give the maximum slope of the torque. The cutting conditions for the

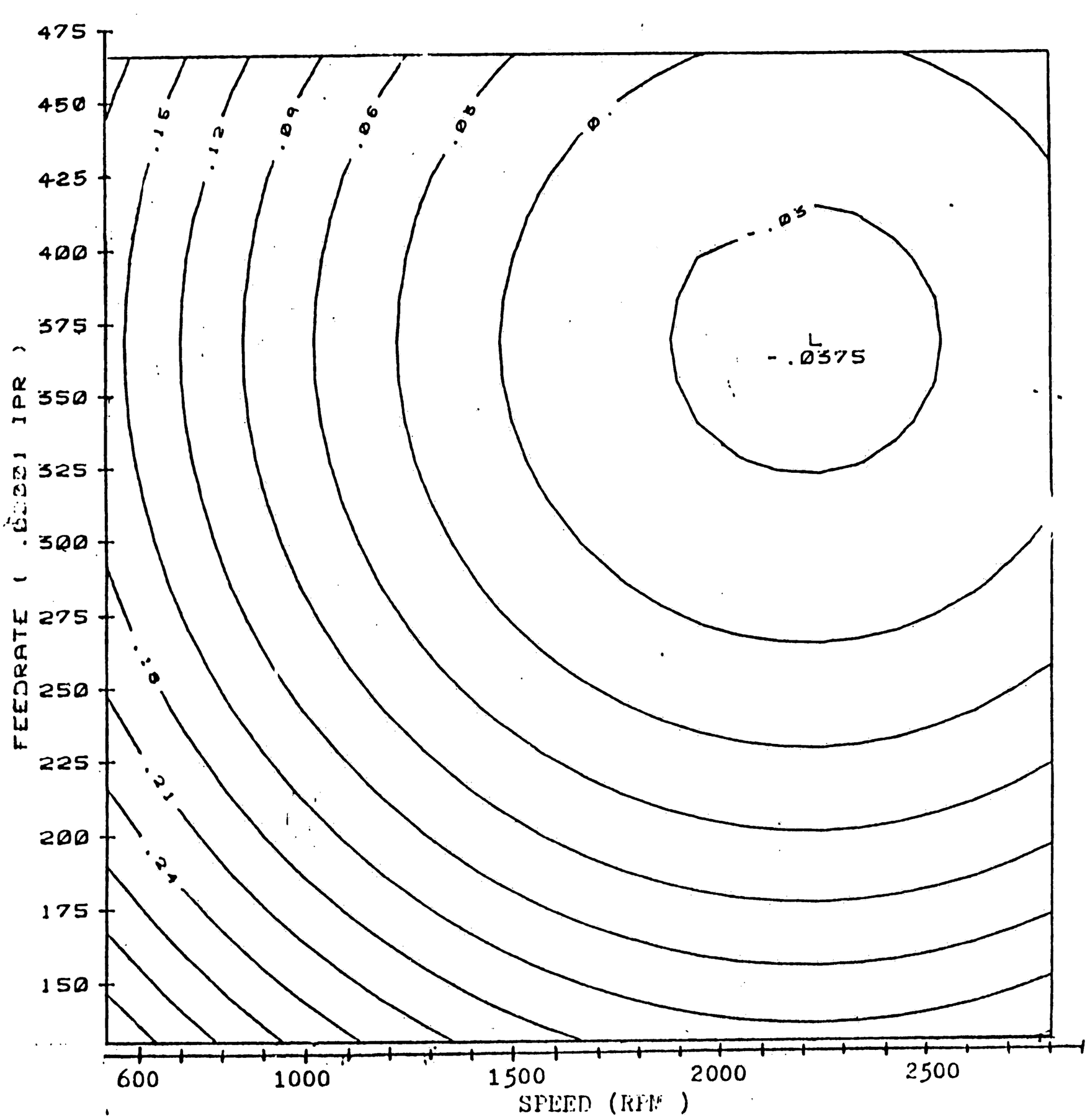

Figure 4.17 Response surface plot of the slope of Y component force for a 1/8" HSS drill with a constant length of cut to diameter ratio equal to 7. Contours represent equal Y component force slope in lbf / 1/30ths sec.. (work material : AISI 4145 HOT ROLLED alloy steel)

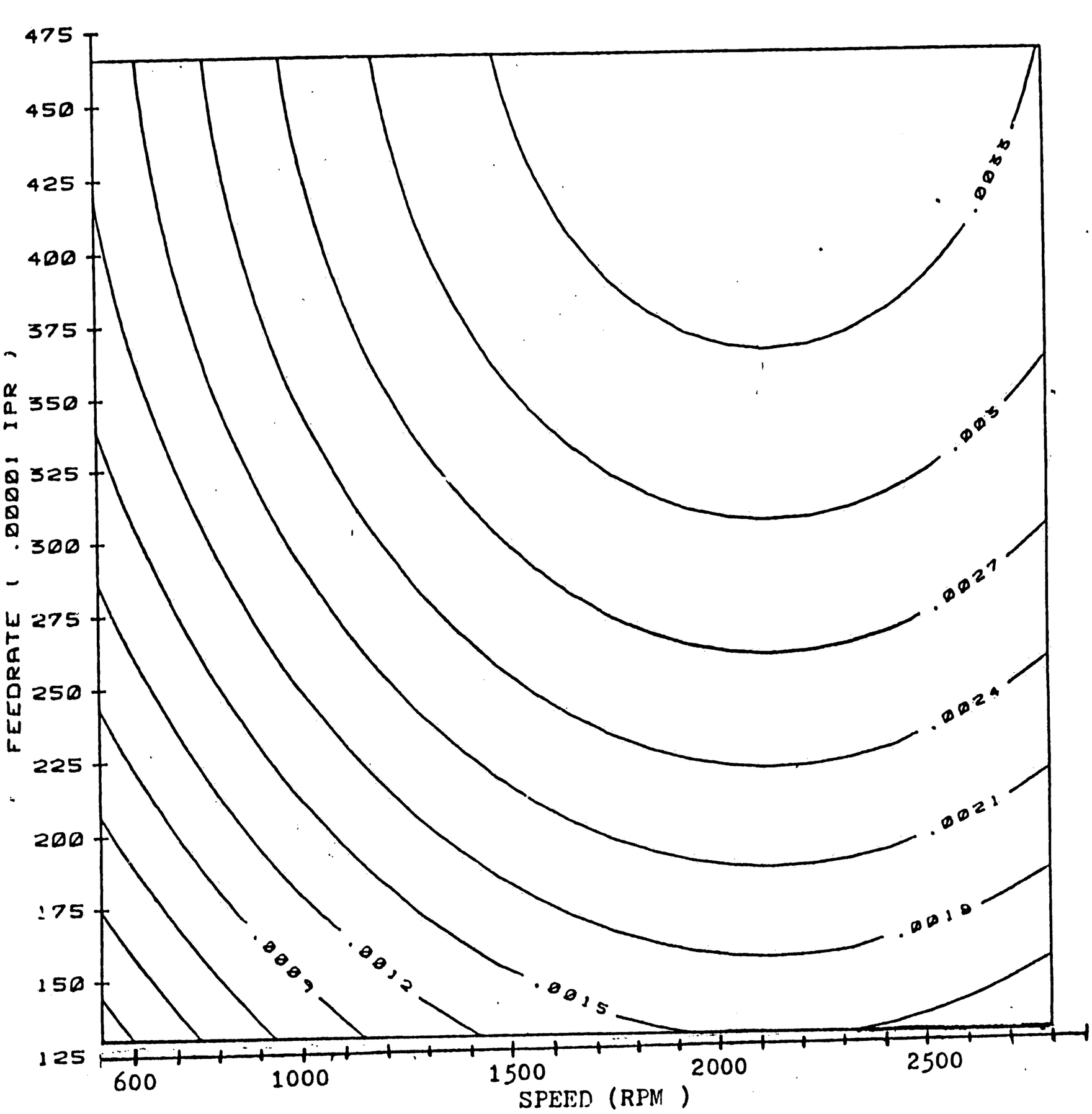

Figure 4.18 Response surface plot of the slope of torque for a 1/8" HSS drill with a constant length of cut to diameter ratio equal to 7. Contours represent equal torque slope in ft-lb / 1/30ths sec.. (work material : AISI 4145 HOT ROLLED alloy steel)

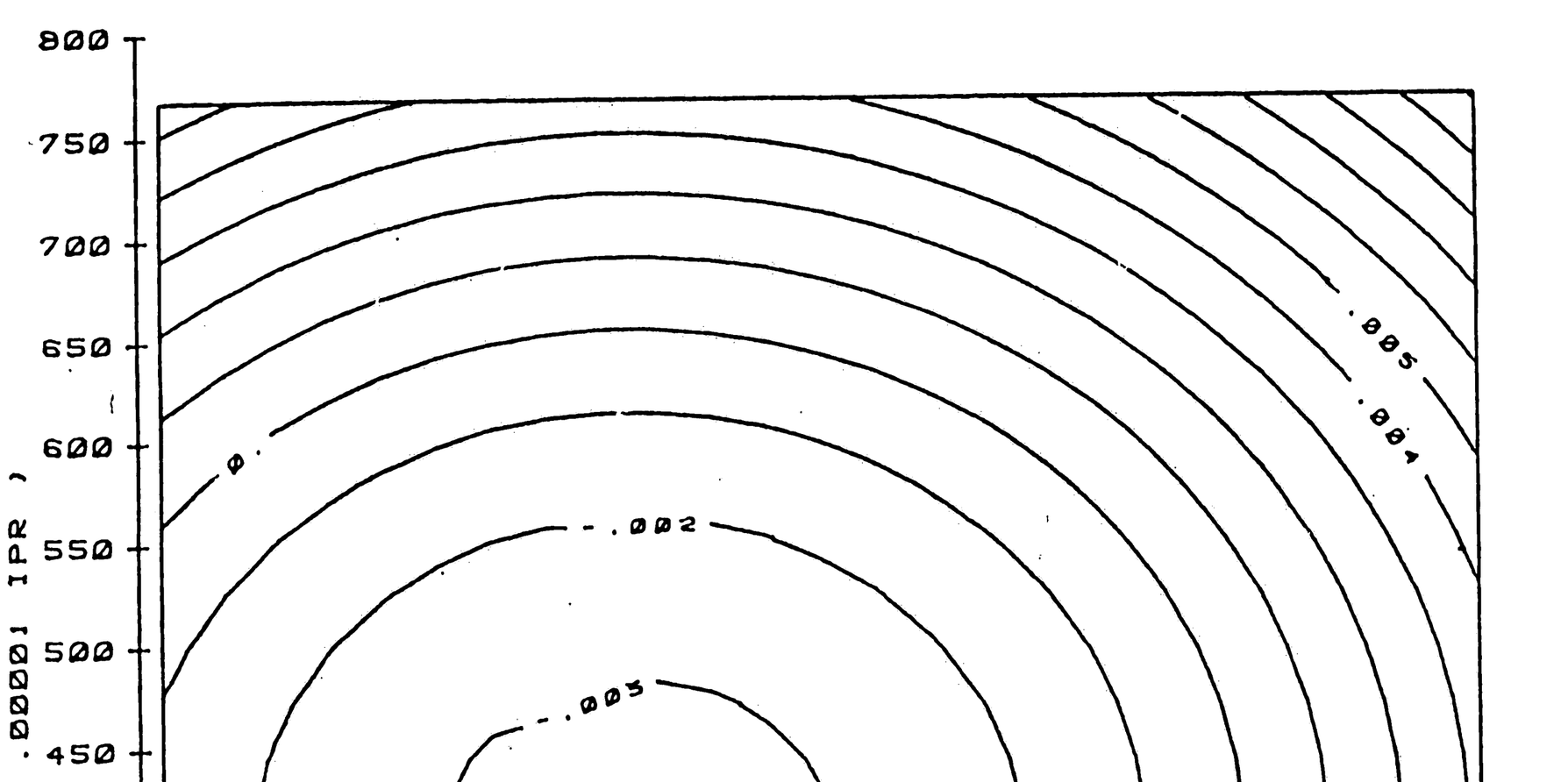

Figure 4.19 Response surface plot of the slope of Y component force for a 19/64" HSS drill with a constant length of cut to diameter ratio equal to 6. Contours represent equal Y component force slope in lbf / 1/30ths sec.. (work material : AISI 4145 HOT ROLLED alloy steel)

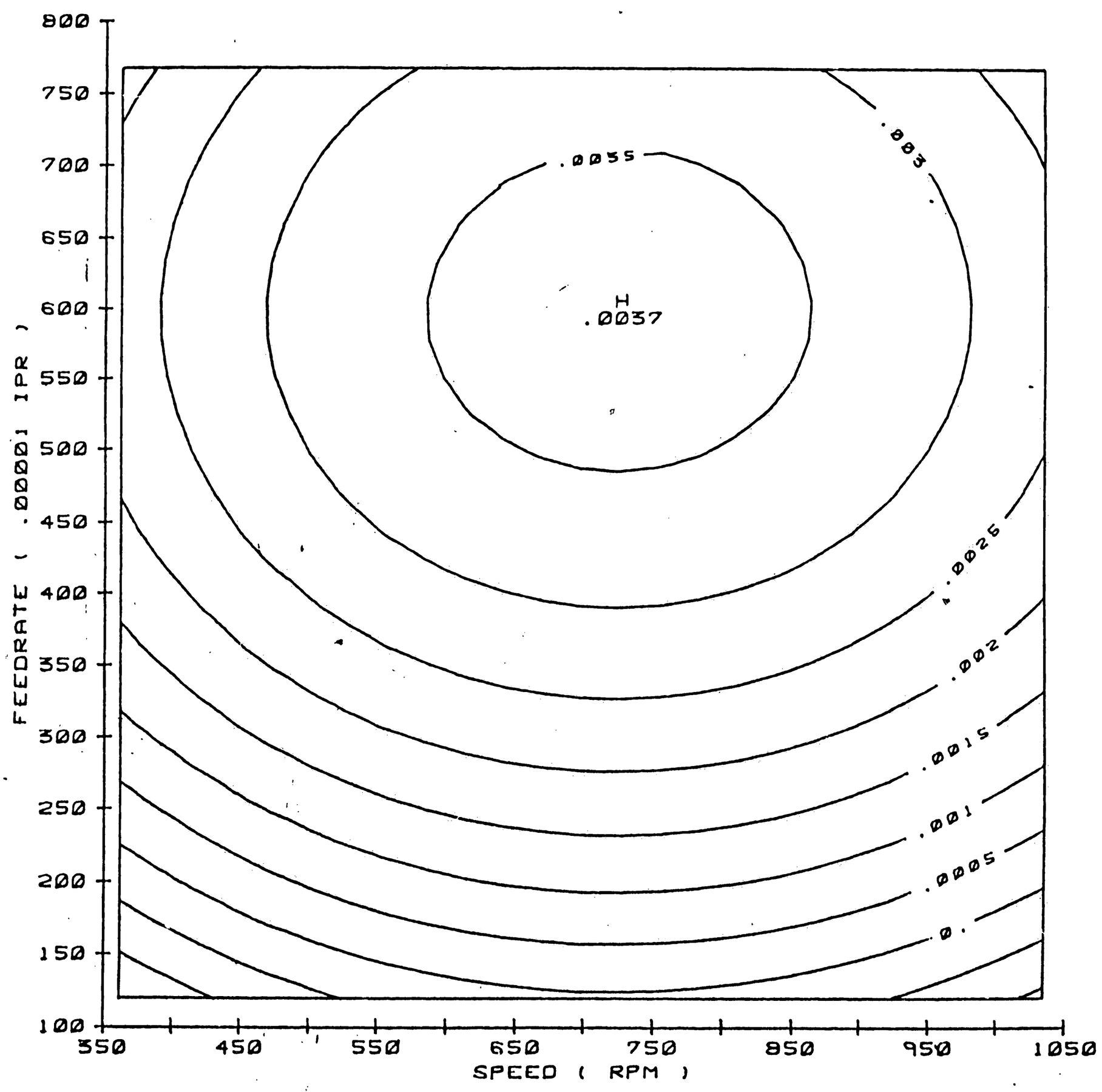

Figure 4.20 Response surface plot of the slope of the torque for a 19/64" HSS drill with a constant length of cut to diameter ratio equal to 6. Contours represent equal torque slope in ft-lb / 1/30ths sec.. (work material : AISI 4145 HOT ROLLED alloy steel)

minimum/maximum response for the slope of Y component and the slope of the torque may be summarized as follows :

TABLE 4.6 : Comparison of the Optimal Cutting Condition for Torque and Y Component Force Rates in Machining AISI 4145 Hot Rolled Alloy steel

	1/8" twist drill		19/64" twist drill	
	slope of torque	slope of Y-force	slope of torque	slope of Y-force
speed (RPM)	2100	2100	700	600
feed (IPR)	0.003	0.00375	0.0046	0.0046
ratio	7.8	7	6.8	6
length of cut	0.975"	0.875"	2.025"	1.95"
X-force slpoe (lbf/sec)	-0.0375		-0.0033	
Torque slope (ft-lb/sec)	0.0031		0.0035	

As may be observed from the responses in the preceeding table and the corresponding response surface plots (Figures 4.17 through 4.20), the torque and force slope were inversely related i.e. maximum torque slope is closely associated with minimum force slope. Also of note is that for each drill size, the optimum cutting

conditions (for maximum torque slope or minmum force slope) were nearly identical.

In general, the following summary statements on the relationship between the torque and the Y component force may be said :

a. The response patterns of the standard deviation of the Y component force and the standard deviation of the torque are the same. The stability of the torque and the Y component force is affected by the same machining parameters, i.e. the length of cut and the speed-feed interaction.
b. The responses of the slope of the Y component force and the torque are inversely related with similar cutting values at the optimal conditions. This indicates that while the rate of change of the torque is decreasing, the rate of change of the Y component force with respect to the same changes of machining variables (cutting speed, feed, and length of cut) is increasing.

4.2.4 Response Surface Plots of the X Component Force

Due to the rotating drilling action, the X and Y force components would be expected to be of the same

magnitude but mutually perpendicular. The perpendicular force component parallel to the table of the machine tool is defined as the X component force. Due to the setup of the dynamometer, the Y component force is thus in a direction perpendicular to the mill table. Figures 4.21 and 4.22 illustrate the response surface for the X and Y component forces obtained with the dynamometer. Due to the symmetry of the drilling operation, it was expected that the X and Y force components would have similar response plots. The data and analysis does not support such a similarity. To investigate this finding, the initial setup (Fig. 4.23) position of the vise was rotated 90 degrees while maintaining tha same dynamometer orientation. The center point condition in the experimental design was then used as the cutting condition to test the effect of vise replacement on the X and Y component forces readings. Each drill size was replicated four times and the force and torque data collected for the switched vise setup. The X and Y component force for each test cutting were plotted against time to compare with the plots of the previously recorded X and Y component force. No differences in the values of the forces were detected between the original position and the test position from the force curves. Regardless of the position of the vise, the X and Y

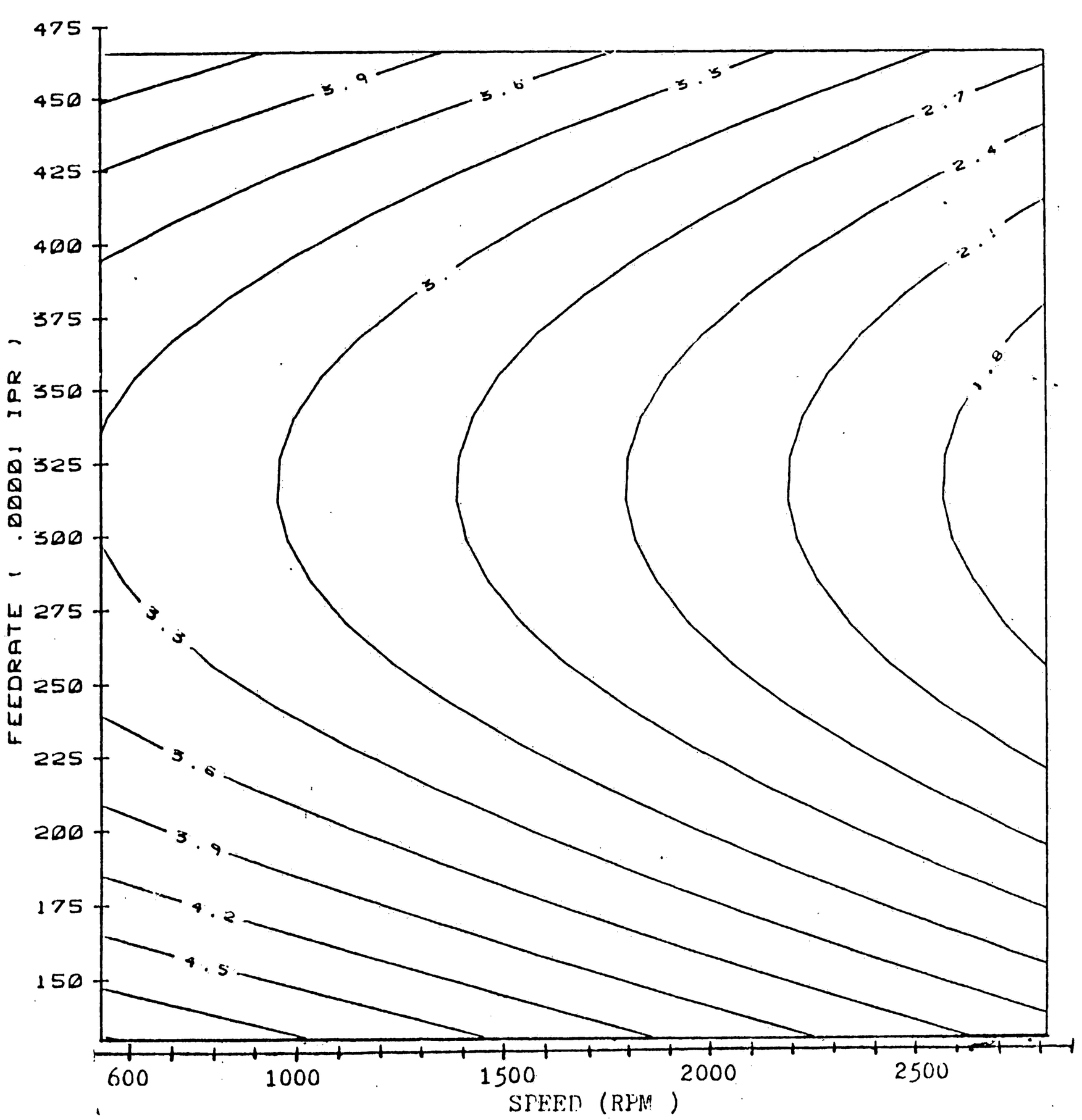

Figure 4.21 Response surface plot of the X component force for a 1/8" HSS drill with a constant length of cut to diameter ratio equal to 7. Contours represent equal X component force in lbf. (work material : AISI 4145 HOT ROLLED alloy steel)

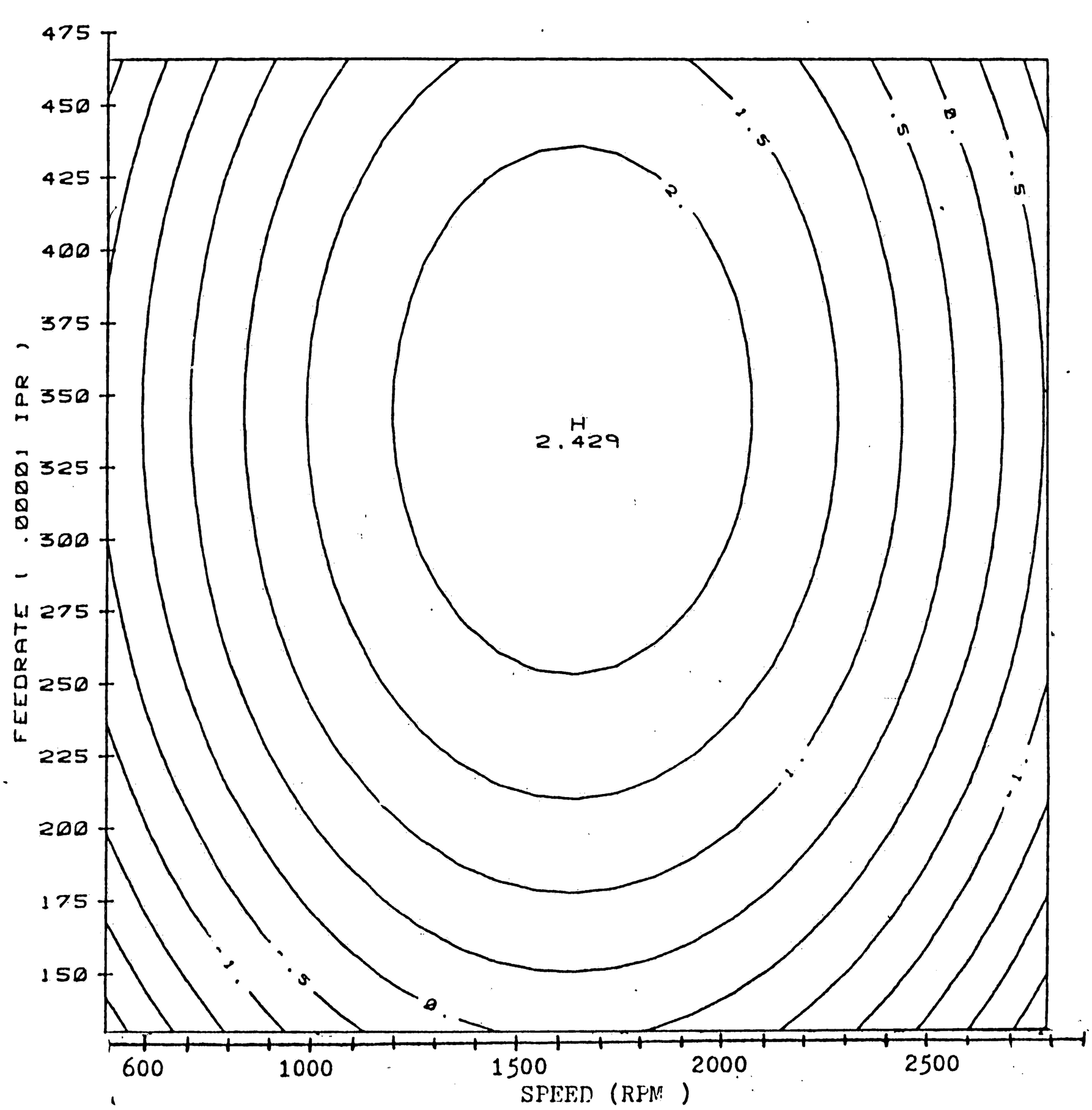

Figure 4.22 Response surface plot of the Y component force for a 1/8" HSS drill with a constant length of cut to diameter ratio equal to 7. Contours represent equal Y component force in lbf. (work material : AISI 4145 HOT ROLLED alloy steel)

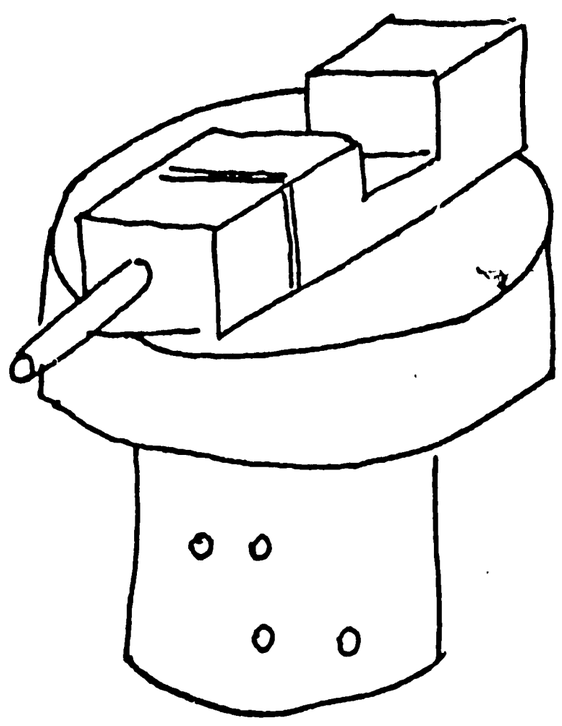

Experimental set-up

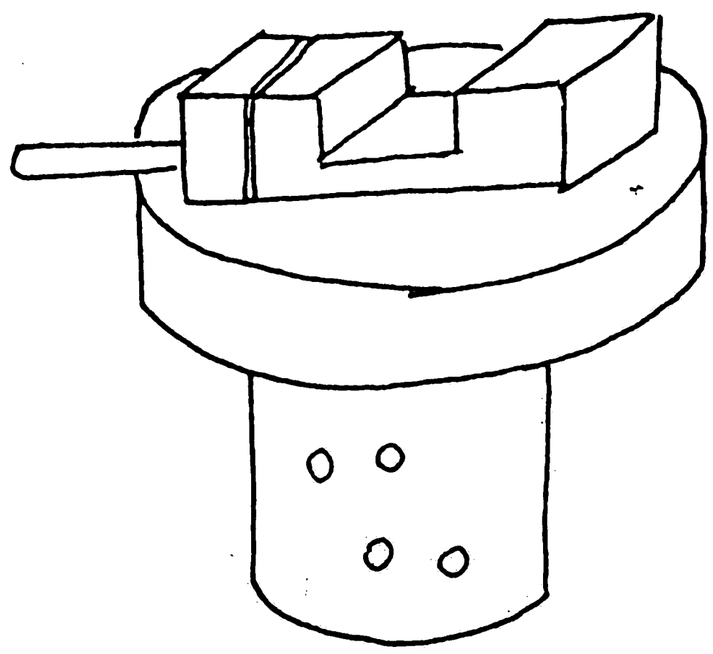

Test set-up.

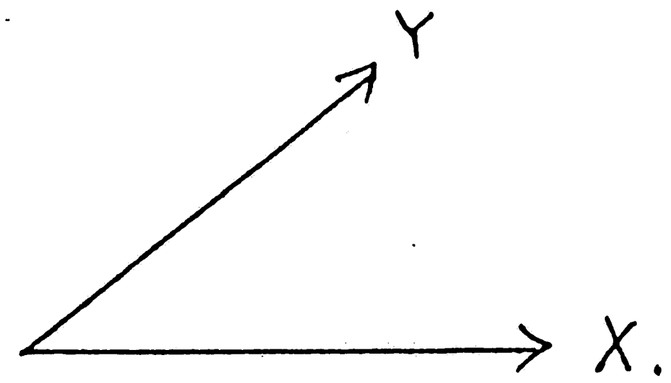

Figure 4.23 The setup of the holding vise for the drilling force dynamometer to investigate the effect of vise direction on force and torque data acquisition.

component force readings were still found to be assymmetric. The drill rotational frequency may be an explanation of this phenomenon since the plot of the recorded responses of the X component and Y component forces (Fig. 4.24) indicated a sinuioidal behavior. Another possible explanation may be the machine tool table's structural flexibility and/or gearing.

4.2.5 Response Surface Plots of Thrust Force

In general, under a constant cutting speed, the results of the analyses indicated that the effect of feedrate and the length of cut were equally important in the thrust force model. Figure 4.25 is the response surface plot indicating the contour of thrust force for length of cut and feedrate interaction. In the low length of cut region, feedrate is the dominant factor for the thrust force. The length of cut effect on the thrust force may be attributed to the tool wear. A worn drill bit would adversely affect the thrust force in the high feedrate, high length of cut region. The slope of the thrust has been discussed in section 4.2.2. It was found to be highly correlated to the average flank wear rate. The correlation coefficient (Table 4.2) between the average flank wear wear rate and the slope of the thrust

Length of cut : 0.875 in.
Cutting speed : 1700 RPM
Feedrate : 0.003 IPR
Work material : AISI 4145 alloy steel

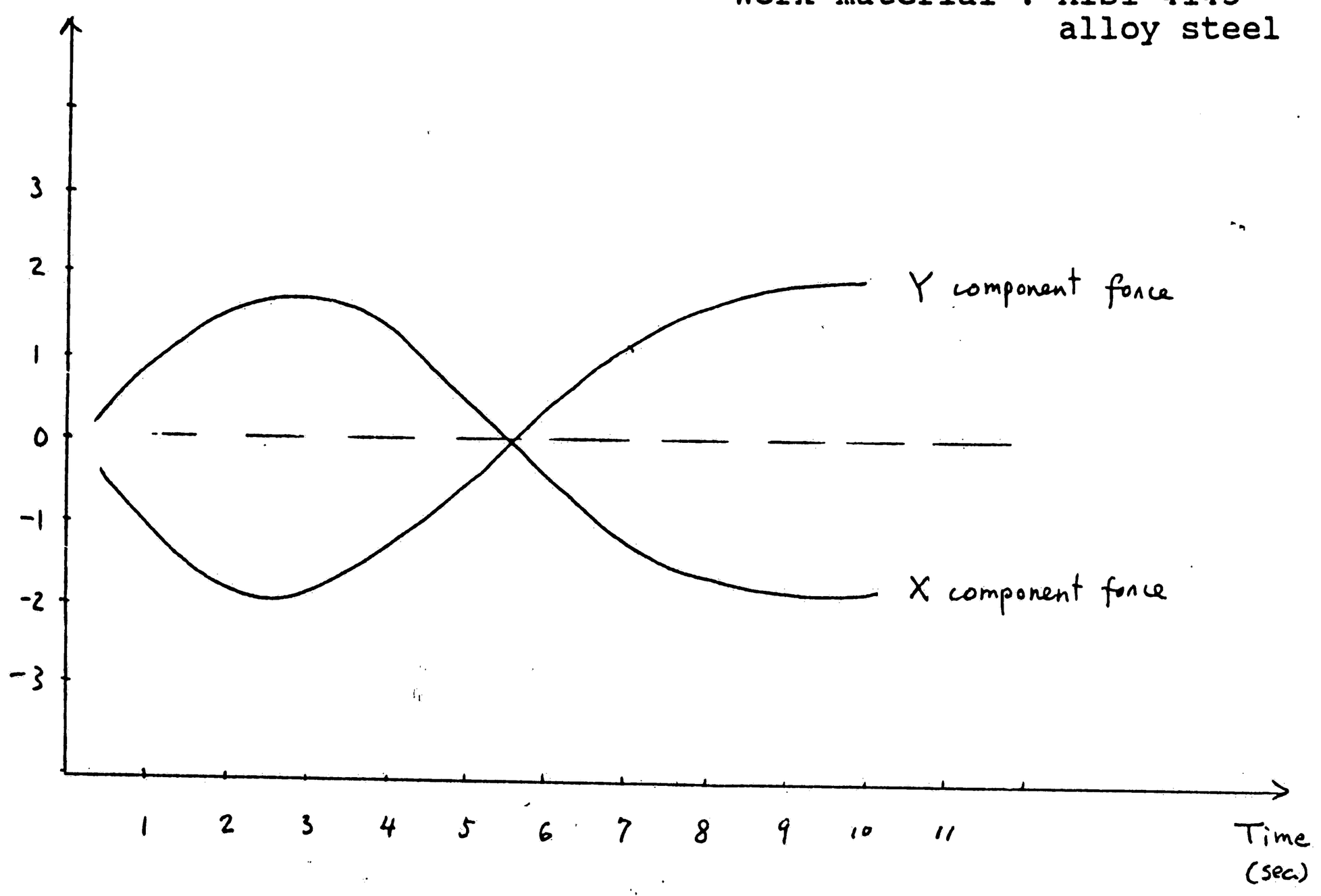

Figure 4.24 Typical plot of the X and Y component force readings for 1/8" diameter drill in lbf. Minus force reading represents in the inverse driection.

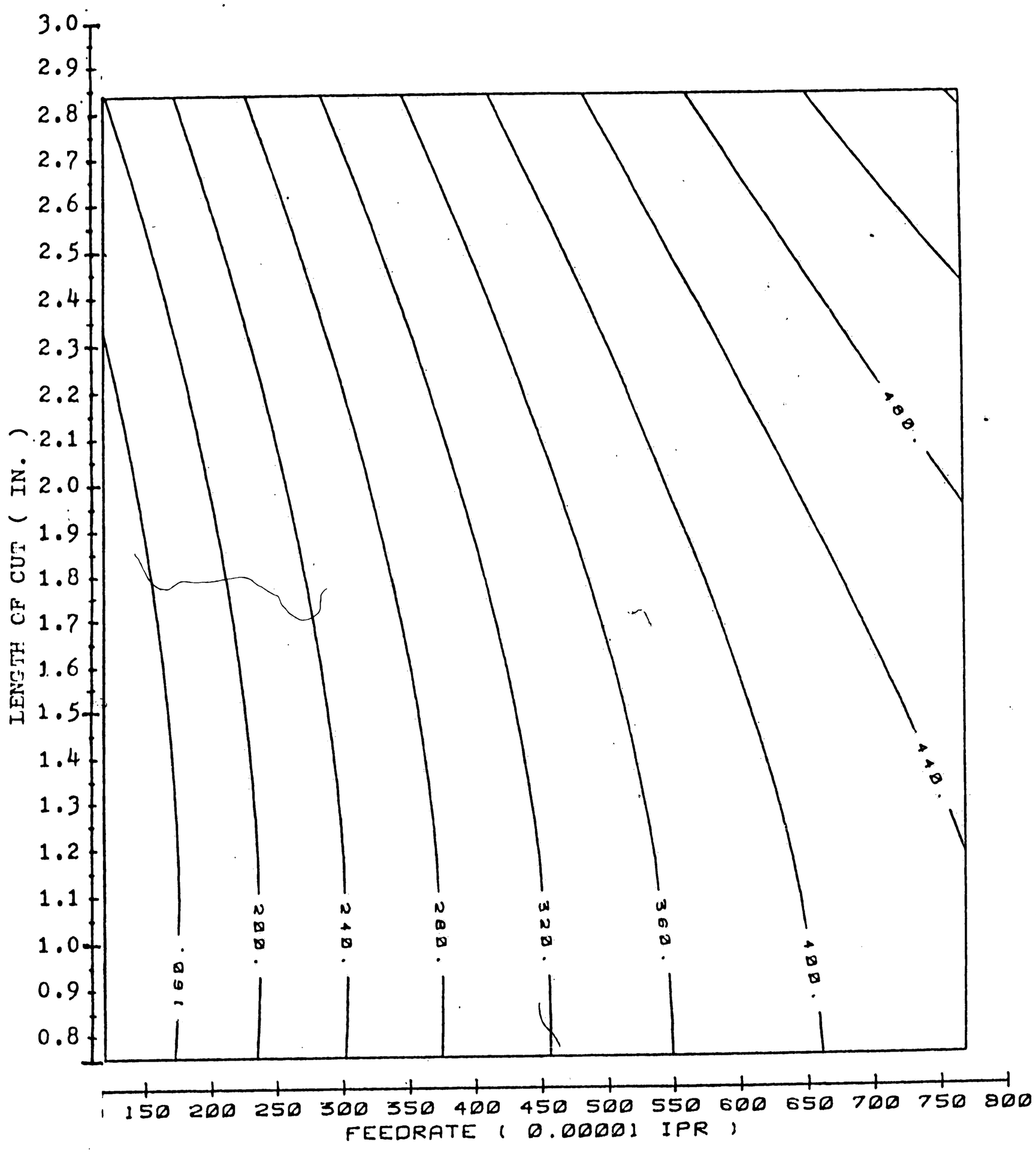

Figure 4.25 Response surface plot of the mean thrust force for 19/64" HSS drill at a constant speed of 700 RPM. Contours represent equal mean thrust force in lbf. (work material : AISI 4145 HOT ROLLED alloy steel)

force was 0.853. Figure 4.26 and Figure 4.27 exhibit the response surface plots of the standard deviation of the thrust force for the 19/64" and 1/8" drills, respectively. The following conclusions may be drawn from these two figures :

a. Feedrate is the major factor for the standard deviation of the thrust force on both sizes of drill. The higher the feedrate, the higher the standard deviation of the thrust.
b. For the 1/8" drill, at both high and low cutting speed, the cutting speed has less effect on the standard deviation of the thrust force.

4.3 A Methodology for Optimal Deep-Hole Drilling

The response surface plots generated in the previous sections served to locate the optimal cutting conditions for the deep hole drilling operation for various individual response of interest within the range of the experiment. Relationships between the performance indexes, such as tool path deflection, hole surface quality, and tool flank wear, and the on-line measureable responses, i.e. forces , torque, slope of forces and torque, and their standard deviations were reviewed in

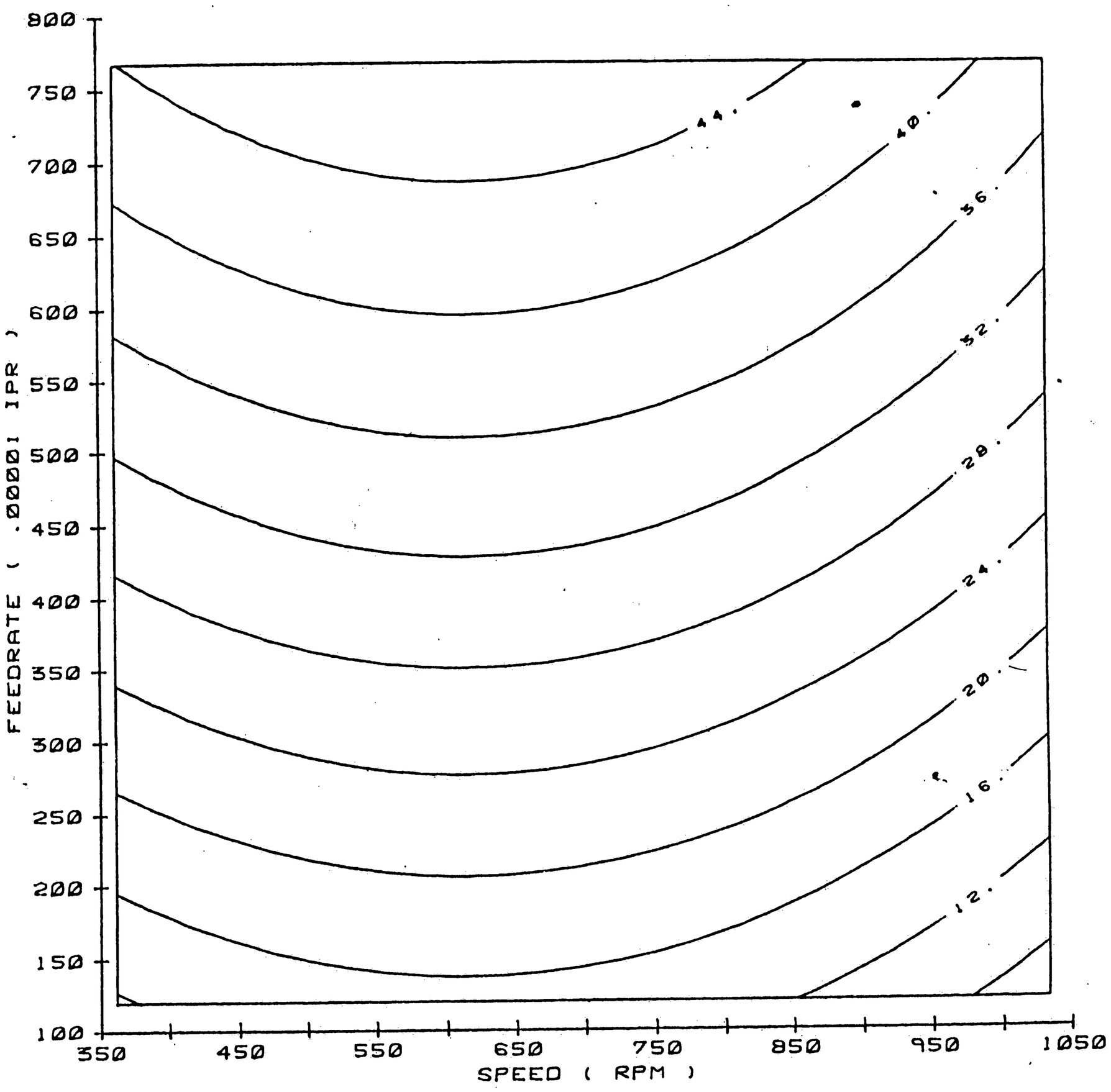

Figure 4.26 Response surface plot of the standard deviation of thrust force for 19/64" HSS drill with a constant length of cut to diameter ratio equal to 6. Contours represent equal standard deviation of thrust force in lbf. (work material : AISI 4145 HOT ROLLED alloy steel)

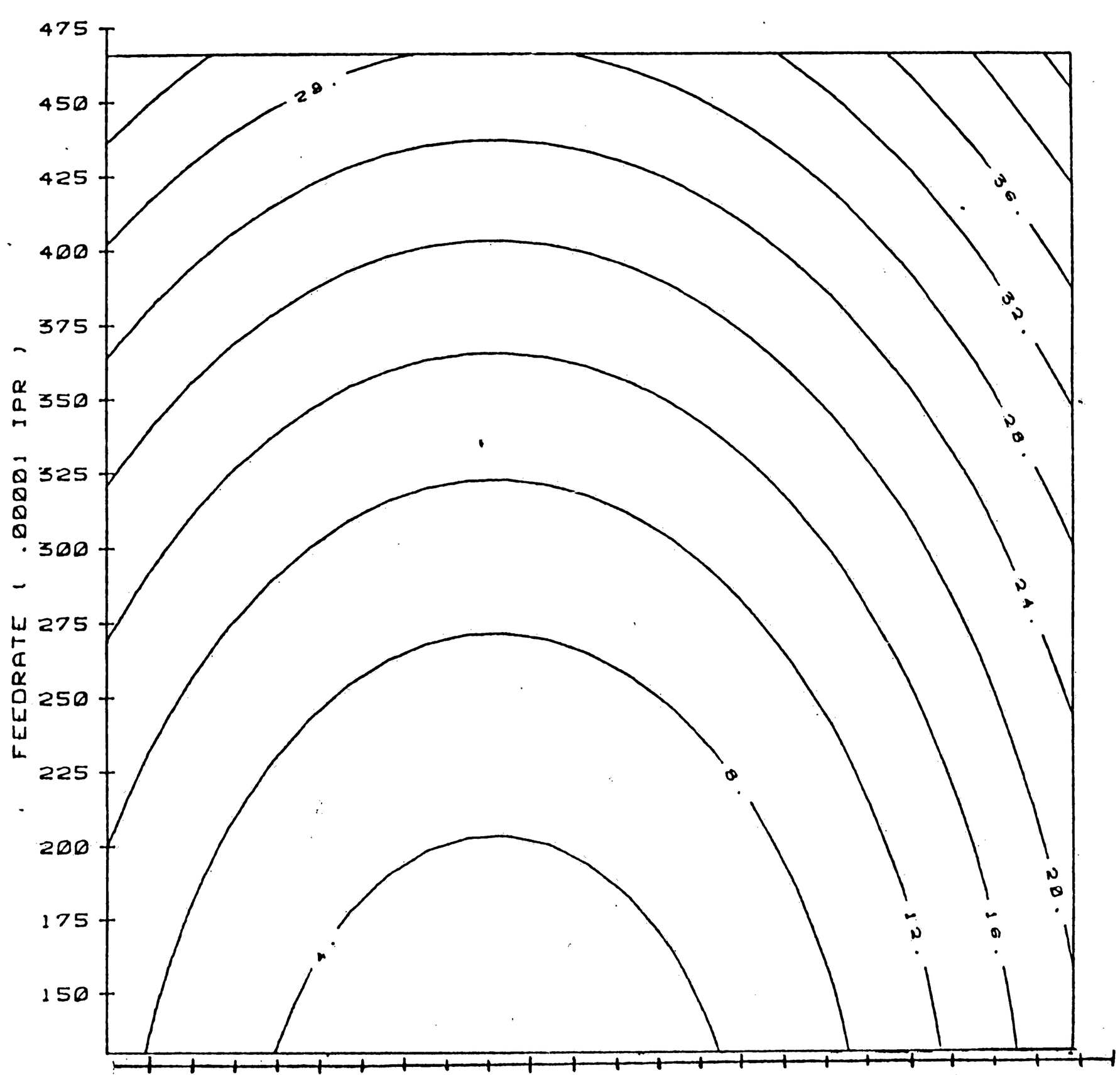

Figure 4.27 Response surface plot of the standard deviation of thrust force for a 1/8" HSS drill with a constant length of cut to diameter ratio equal to 7. Contours represent equal standard deviation of thrust force in lbf. (work material : AISI 4145 HOT ROLLED alloy steel)

chapter two. The following subsections are to demonstrate an approach to locate the overall optimal performance cutting conditions for this experiment. The status of the average flank wear for the drill can also be simulated by the slope of the thrust force.

4.3.1 Selection of Optimal Performance Cutting Conditions in Deep Hole Drilling

The criteria used in the selection of the cutting conditions for overall performance considers the following objectives :

a. Minimun flank wear to minimize the tool cost, and the setup cost.
b. Minimum cutting time to get better metal removel rate.
c. Improved hole surface quality.
d. Minimization of the thrust force to avoid tool path wander.

Radhakrishnan and Wu [10] pointed out that the standard deviation of the thrust force could be used as a good indicator of the hole surface quality. In their discussion, the response of the standard deviation of the thrust force was used to represent the standard deviation of the hole surface quality. In order to get better hole surface quality, the standard deviation of the thrust force is needed to be minimized. Even though hole surface quality was considered in this thesis, the surface

quality that was measured during this research (using a SURFTEST III stylus profilometer) resulted in high variability for the surface roughness such that no statestical significance could be detected. The surface qualitty measurements could only be taken on the 19/64 inch drill diameter holes.

In order to demonstrate the approach to locate the optimal cutting condition, Radhakrishnan and Wu's results were employed, and the standard deviation of the thrust force was used to indicate the surface quality. An illustration of the procedure to locate the optimal cutting cinditions for a 1/8" twist drill is given by the following example :

Problem specification :

The hole to be drilled is a 1/8" diameter hole. The length of the hole is 7/8" (0.875 inches). Cutting time requirement for this hole making process is set at no more than 10 seconds. No path deflection or tool bit breakage is expected to occur during drilling. The work material is an AISI 4145 alloy steel bar.

Approach to select the optimal cutting conditions :

1. Figure 4.28 illustrates the response plot of the mean flank wear for the 1/8" diameter drill with the length of cut to diameter ratio equal to 7. (length of cut equal to 7/8")

2. The time of cut, Tc, is defined by the ratio of length of cut over feedrate multiplied by spindle speed, N.

3. Figure 4.29 exhibits the response plot of the

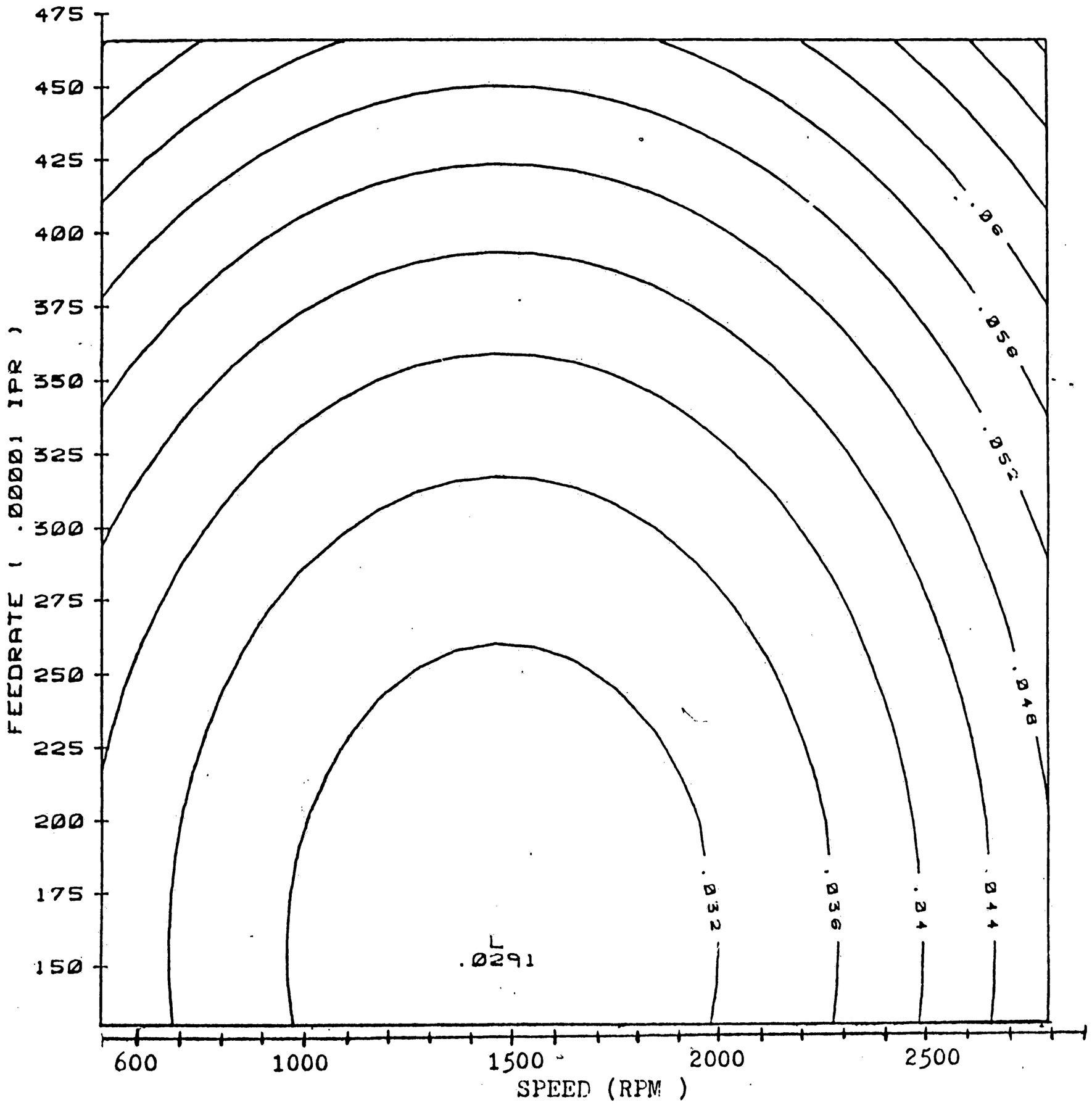

Figure 4.28 Response surface plot of the average flank wear for a 1/8" HSS drill with a constant length of cut to diameter ratio equal to 7. Contours represent equal average wear in inches. (work material : AISI 4145 HOT ROLLED alloy steel)

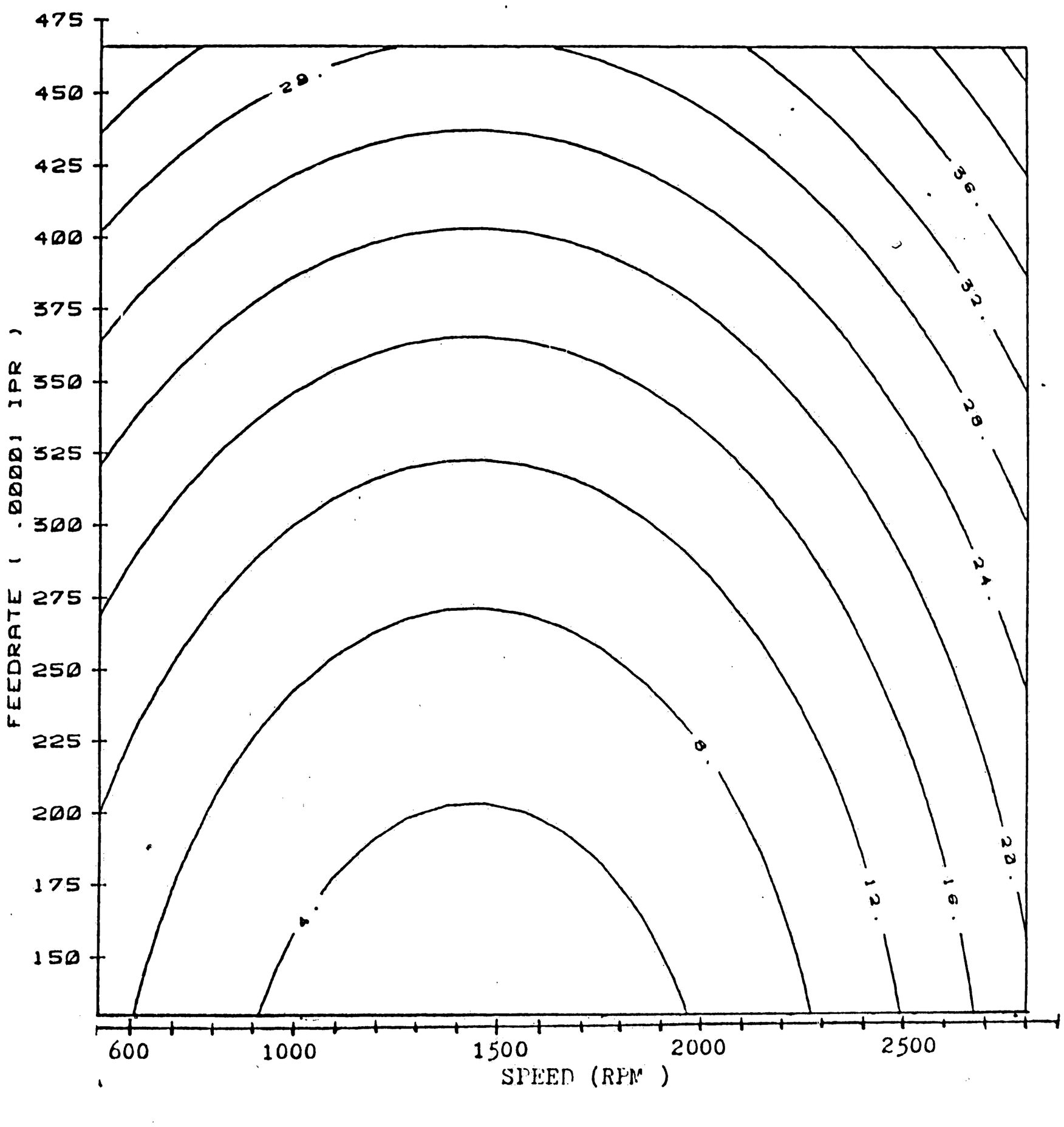

Figure 4.29 Response surface plot of the standard deviation of thrust force for a 1/8" HSS drill with a constant length of cut to diameter ratio equal to 7. Contours represent equal standard deviation of thrust force in lbf. (work material : AISI 4145 HOT ROLLED alloy steel)

standard deviation of the thrust force for the 1/8" diameter drill with the length of cut to diameter ratio equal to 7. (length of cut equal to 7/8")

4. Figure 4.30 gives the response plot of the mean thrust force for the 1/8" diameter drill with the length of cut to diameter ratio equal to 7. (length of cut equal to 7/8")

5. Mapping these three figures together and applying the constraints specified for the working environment, (i.e. the maximum cutting time for each hole is 10 seconds), the calculated critical load using equation 2.3 for a 1/8" diameter drill is 140 lbf.

6. The hatched line area in figure 4.31 represents the optimal performance working zone for the 1/8" drill. Chosing the criteria that the optimal point is located at the intersection of the minimum flank wear and minimum standard deviation of thrust force, the optimal point may be located on the combined plot (Fig. 4.31). For this example, the optimal cutting conditions resultes in a flank wear of 0.033 inches and a standard deviation of thrust force equal to 8. The optimal cutting conditions are within both the time and thrust force constraints. (time = 10 sec., thrust force = 110 lbf).

4.3.2 A Possible Approach to Monitor the Status of the Drill Flank Wear

The flank wear curve generally can be divided into three sections as indicated previously in Figure 4.7. Figure 4.32 exhibits the representatative pattern of the flank wear curve and the corresponding average wear rate curve. The average wear rate, as defined to be the wear reading divided by the total cutting time (equation 4.3),

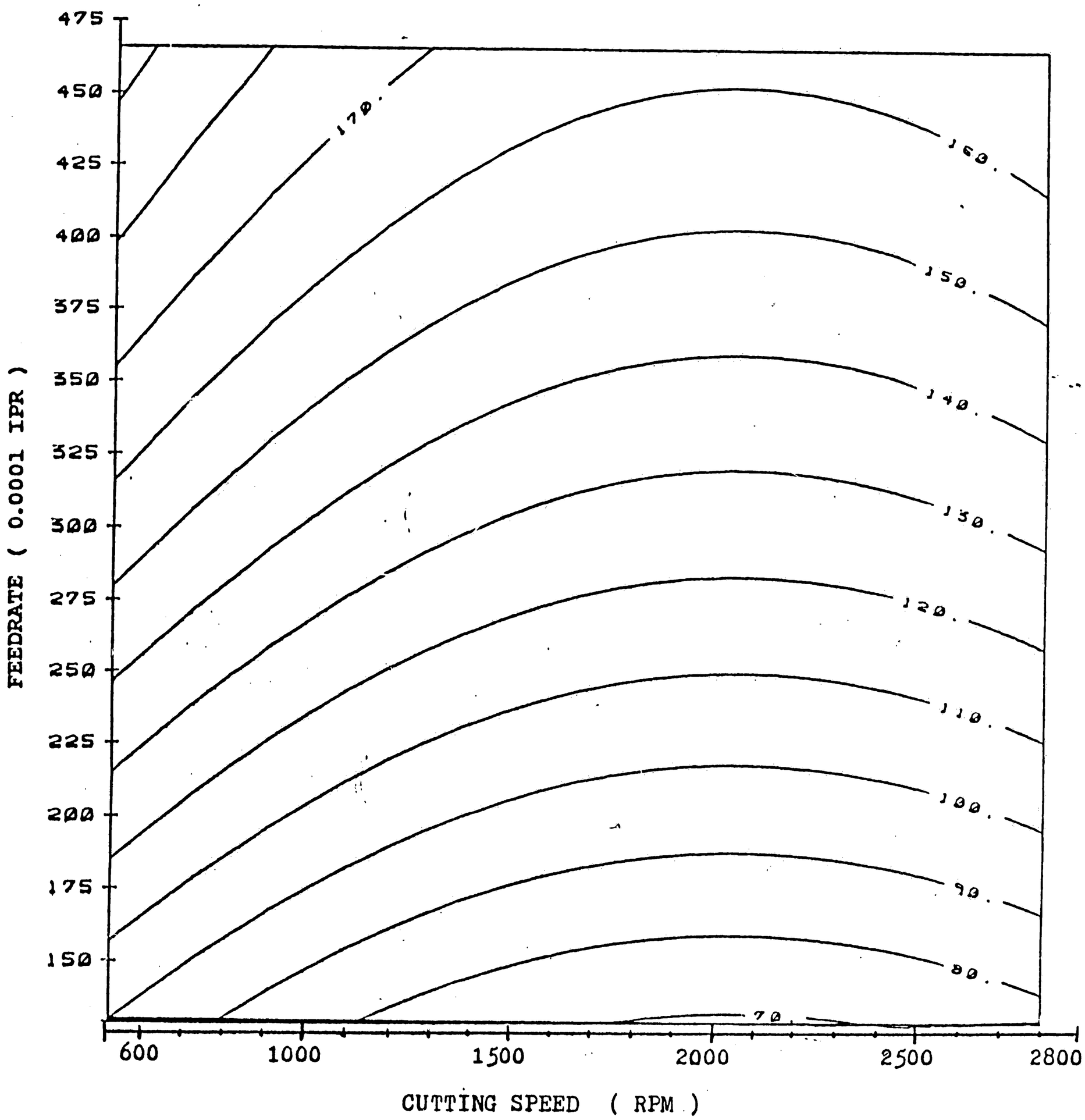

Figure 4.30 Response surface plot of the thrust force for a 1/8" HSS drill with a constant length of cut to diameter ratio equal to 7. Contours represent equal thrust force in lbf. (work material : AISI 4145 HOT ROLLED alloy steel)

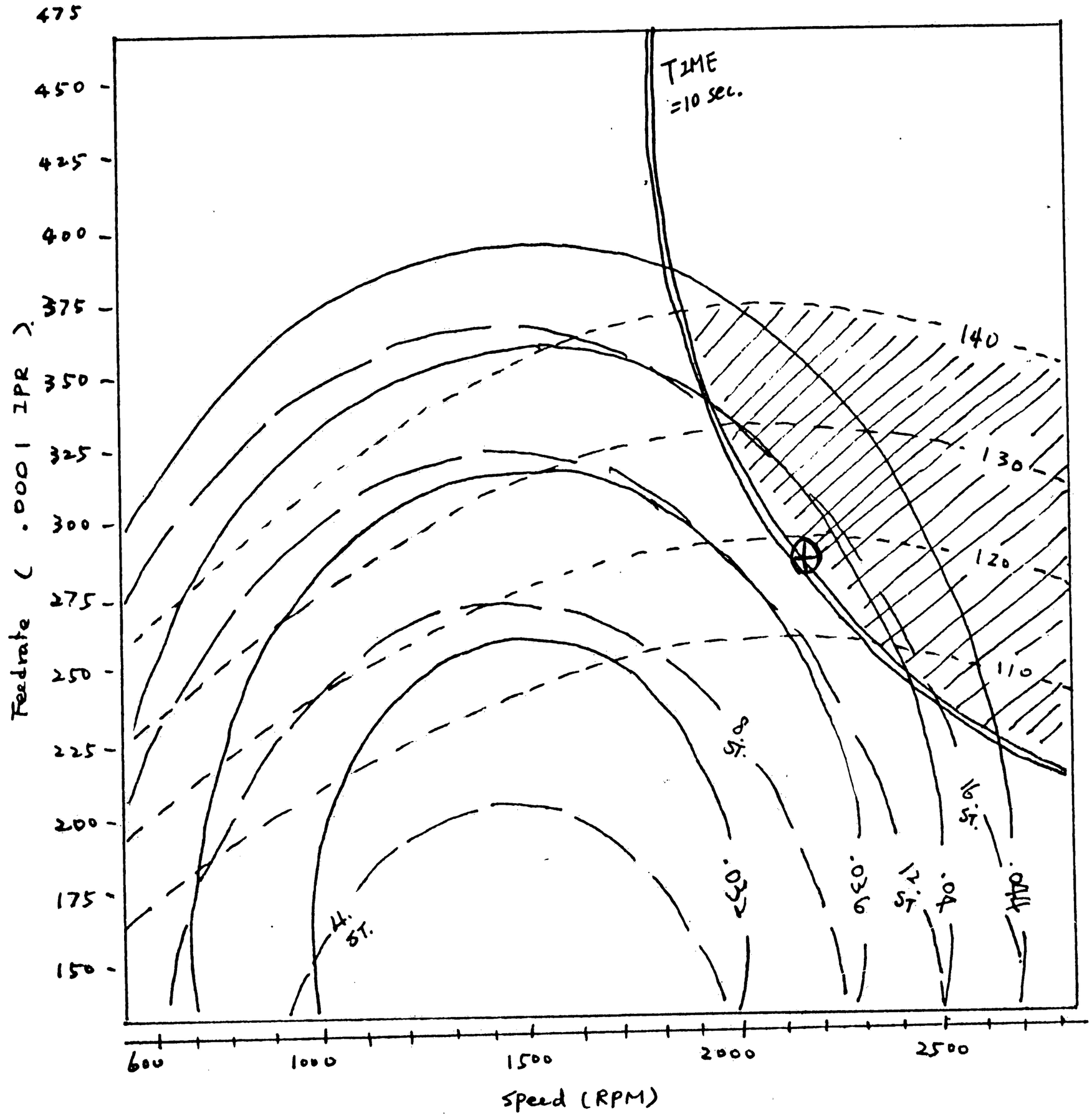

Figure 4.31 Selection of the optimal cutting conditions for 1/8" diameter drill. Working constraints : 1. Cutting time 10sec. 2. critical axial load 140 lbf. Dotted line represents thrust force contours in lbf, broken line represents standard deviation of thrust force contours in lbf,and solid line represents flank wear contours in inches. (work material : AISI 4145 HOT ROLLED alloy steel)

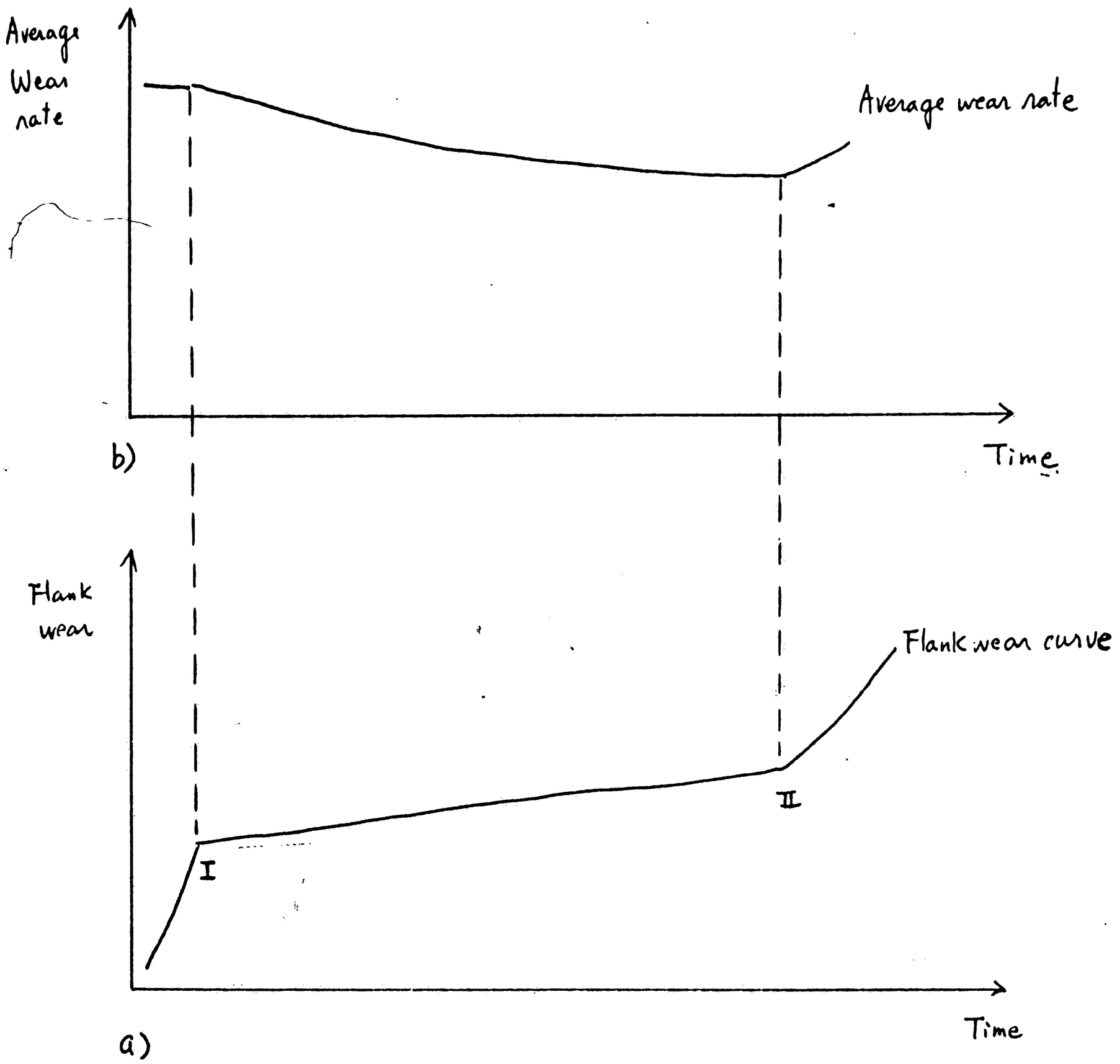

Figure 4.32 Representative pattern of the flank wear curve and the corresponding average wear rate curve.

I : End of break-in region.
II: End of gradual wear regression region.

is always decreasing along the flank wear curve. An increase of the average wear rate indicates the cutting tool has reached the point of thermal instability and rapid wear occurs. As stated in section 4.2.4, the slope of the thrust force was highly correlated with the average wear rate and could be a good indicator of the average wear rate. The slope of the thrust force could be used to monitor the average wear rate.

A plot of the slope of the thrust force versus time is compared with a flank wear curve in Figure 4.33. The thrust force data used to plot Figure 4.33 (a) was obtained from thrust force reading at cutting conditions corresponding to the center point of the experimental design (Speed = 1700 RPM, feedrate = 0.003 IPR and length of cut to diameter ratio = 7). The intent of Figure 4.33 is to present as a basis for flank wear monitoring. Further investigation would need to be done to verify the approach. The thrust force slope has the same pattern as the average wear rate shown in figure 4.32. S_t represents the slope of the thrust force at time t, and S_{t-1} is the slope of the thrust force at time t-1. To determine the critical point of the onset of the thermal instability, one may succesively calculate the ratio of S_t to S_{t-1} to obtain the rate of change of the slope of

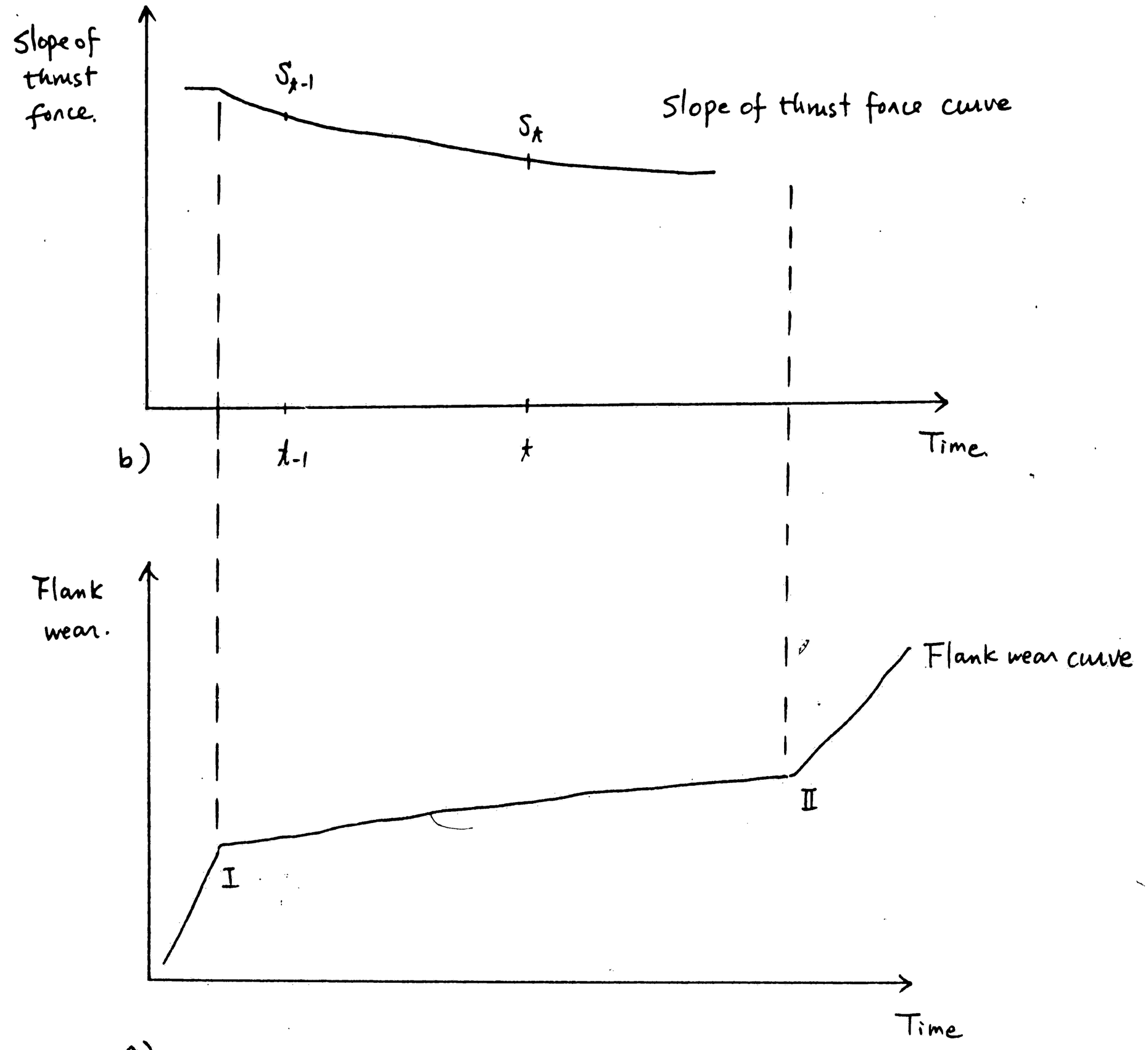

Figure 4.33 Typical plot of the slope of thrust force compared with a representative flank wear curve.

I : End of break-in region.
II: End of gradual wear regression region.
S_t: The slope of thrust force at time t.
S_{t-1}: The slope of thrust force at time t-1.

the thrust force. As the ratio, ($0 < S_t / S_{t-1} < 1$) approaches the value one, the drill tip is approaching the critical point of thermal instability. If the ratio is greater than one, the critical point of the thermal instability is surpassed. The analysis of the data in this thesis supports this approach, but, as mentioned, further work would be necessary to validate this conjecture.

CHAPTER FIVE

CONCLUSIONS AND RECOMMENDATIONS FOR FUTURE RESEARCH.

The following conclusions can be drawn with regard to the deep hole drilling experiments conducted in this research :

1. A reduction in feedrate or cutting speed reduces the thrust force. The effect of feedrate on thrust force reduction is of greater magnitude than the effect of cutting speed.

2. The slope of the thrust force is found to be a good indicator of the average wear rate.

3. There was an indication that the rate of change of the slope of the thrust force may be a possible approach to determine the critical point of thermal instability.

4. Outside wear is highly correlated with the average flank wear. In general, length of cut to diameter ratio and the cutting speed were found to be the dominant factors in generating the average flank wear and the outside flank wear.

5. The standard deviation of the Y component force

and the torque had a similar response pattern within the experiment region.

6. Response Surface Methodology is a viable technique to aid in the selection of the optimal cutting conditions in deep hole drilling.

The following recommendations are made for future research:

1. Forces/torque readings should be ffurther investigated by a technique such as Data Dependent Systems analysis. Such an investigation would be beneficial in improving the underatanding of the physical characteristics of the drilling process.

2. The effect of cutting parameters on the tool path deflection would be a valuable extension to the research investigation on deep hole drilling.

3. Additional research is needed to verify the approach using the rate of change of the thrust force in monitoring the critical point of thermal instability.

4. The interdependency between the response

variables i.e. flank wear, thrust force, torque etc., should be investigated by techniques such as step wise regression. Interdependencies could serve as a basis for a control algorithm for adaptive control in deep hole drilling.

REFERENCES

1. Galloway, D. R., " Some experiments on the influence of various factors on drill performance", ASME Trans., 1957

2. Farris, N. S. & Podder, R. K., " Optimization of drill life: Part 1 : Influence of cutting conditions on tool wear", 10th NAMRC Proceedings, May 1982

3. Burnham, M. W., " The mechanics of drilling small holes", 10th NAMRC Proceedings, May 1982

4. Burnham, M. W., " An analysis of drill deflection for deep miniature holes", 10th NAMRC Proceedings, May 1982

5. Kahng, C. H. & Ostwald, P. F., " Performance analysis of drilling by minicomputer", 10th NAMRC Proceedings, May 1982

6. Bedini, R., Pinotti, P. C. & Prescittini, G., "Adaptive control in drilling", Int. J. Mach. Tool Des. & Res., 1977

7. Mcdunn, T. P., Bray, D. S. & Wu, S. M., " Microcomputer based drill wear on-line monitoring", Proceedings of the 22th Int. Mach. Tool Des. & Res. Conference. 1981

8. Burnham, M. W., " Deep hole drill wear limits", 11th NAMRC Proceedings, 1983

9. Pandit, S. M. & Kashou, S., " A data dependent systems : strategy of on-line tool wear sensing", J. of Eng. for Ind., ASME, Aug. 1982

10. Rakharishnan, T. & Wu, S. M., " On-line hole quality evaluation for drilling composite material using dynamic data", J. of Eng. for Ind., ASME, Feb. 1981

11. Pandit, S. M., Suzuki, H. & Kahng, C. H., " Application of data dependent systems to diagnostic vibration analysis", J. of Mechanical Design, ASME, Apr. 1980

12. Subramanian, K. & Cook, N. H., " Sensing of drill wear and prediction of drill life", J. of Eng. for Ind., ASME, May 1977

13. Pandit, S. M., " Stochastic linearization by data dependent systems", J. of Dynamic system, Measurement and Control, ASME, Dec. 1977

14. Pandit, S. M. & Wu, S. M.," Time series & system analysis with application", Wisely Co., 1982

15. Wu, S. M., "Dynamic data system: A new modeling approach", J. of End. for Ind., ASME, Aug. 1977

16. Shaw, M. C. & Oxford, C. J.,"On the drilling of metals 2 -- the torque and thrust in drilling", ASME trans., 1957

17. Pandit, S. M. & Revach, S., "A data dependent system approach to dynamics of surface generation in turning", J. of Eng. for Ind., ASME, Nov. 1981

18. Pandit, S. M. & Wittig, W. H.,"A data dependent system approach to optimal microprocessor control illustrated by EDM", J. of Eng. for Ind., ASME, May 1984

19. Groover, M. P., "A review of methods for on-line tool wear measurement", 1976

20. SME, "Machining data handbook", 1982

21. Montegometry, D. C.,"Design and analysis of experiments", Wiley and son, 1976

22. Pandit, S. M.,"Analysis of vibration records by data dependent system", The shock & vibration bulletin 47, part 4, Sep. 1977

23. Raymond, H. Myers, "Response surface methodology", Allyn & Bacon, 1971

24. Owen, L. Davie ed.,"The design & analysis of industrial experiment", 1956

25. Box, G. E. P.," The exploration and exploiration of response surface: some general considerations & examples" Biometrics, March 1954

26. Box, G. E. P. & Youle, P. V.,"The exploration and exploiration of response surface: An example of the link between the fitted surface and the basic mechanism of the system", Biometrics, Sep. 1955

27. Box, G. E. P., "Replication of non-center points in the rotatable and non-ratatable central composite design" Biometrics, March 1958

APPENDIX I

WORK MATERIAL HARDNESS TEST

Results of hardness test of work material

1. Material : AISI 4145 Hot Rolled alloy steel

2. Testing machine : Wilson, Rockwell hardness test machine, model 3JR

3. Date ; Sept. 17, 1984.

4. Specimen : The specimen were cut and ground to obtain the best surface finish.

The following figure exhibits the testing points on the specimen :

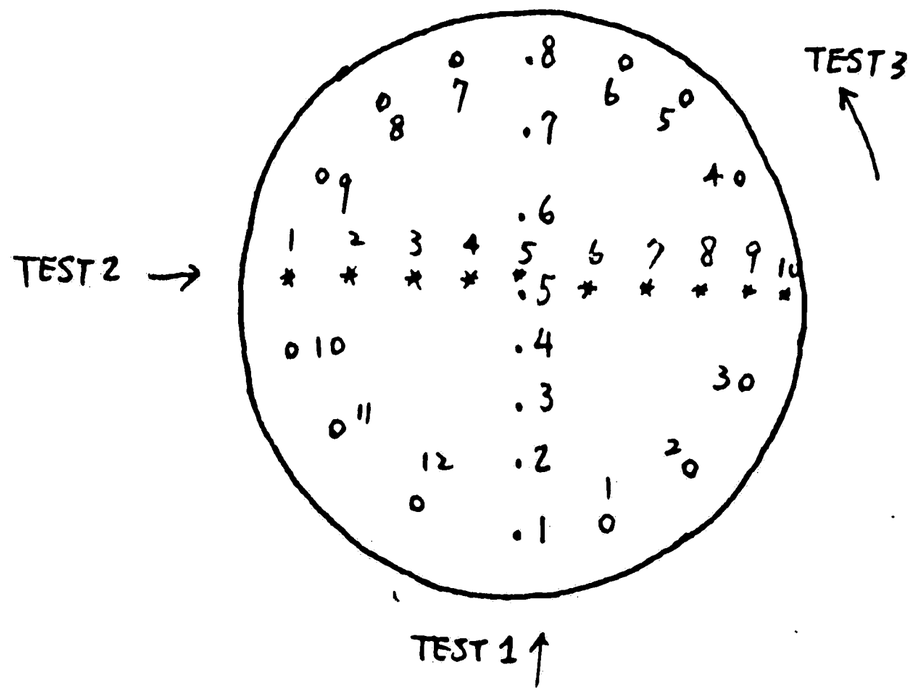

5. Results :

	Test 1		Test 2		Test 3	
	Rock A	BHN	Rock A	BHN	Rock A	BHN
1.	60	228	62.5	257	62	245
2.	63	264	60	228	62.5	257
3.	63	264	61.5	240	62	245
4.	62.5	257	61.5	240	63.5	260
5.	61	235	62.5	257	63.5	260
6.	62	245	60	228	62	245
7.	62.5	257	60.5	230	61	235
8.	61.5	240	62	245	61.5	240
9.			61.5	240	63	264
10.			63.5	260	62.5	257
11.					62	245
12.					62.5	257
13.					63	264
14.					61.5	240

15.					61.5	240
16.					60	228
Ave.	61.9375	248.75	61.55	242.5	62.125	248.875

Total average : 247 BHN
Variance : 11.85 BHN

APPENDIX II

IMPLIMENTATION OF COMPUTER PROGRAM

Computer programs developed for this research were all FORTRAN-based program. Programs included :

1. Data acquisition program.

   Impliments on PDP 11/34 computer system to read the voltage signal from A/D conveter and translate to the corresponding forces/torque.

2. Data analysis program.

   Impliments on PDP 11/34 computer system to read the data files that generated from the acquisition program and calculate the slope of forces/torque, the mean values and their standard deviations.

3. Model fitting and F-test program.

   Impliments on the CYBER 850 system. Three-variable second order equations was employed to use in generating the response model. F-tests on each terms of the model were conducted to identify the contribution of each terms in the model.

4. Response surface plot program.

   Impliments on the CYBER 850 system. Using the TEMPLT graphic package, this fortran-based program use the coefficients of each response model to generate the contour plots for each model.

Computer programs described above are maintained by

Dr. Niclolas G. Odrey
Department of Industrial Engineering
Lehigh University
Bethlehem, PA 18015

APPENDIX III

RESPONSES MEASUREMENT OF BOTH 1/8" AND 19/64" DRILLS

TABLE A3.1 DIRECT RESPONSE MEASUREMENT OF 19/64" DRILL

(REPLICATION 1)

Tool No.	Coded V	F	D	Average Wear	Outside Wear	Inside Wear	Cutting Time
L01	1	1	1	.02825	.0285	.028	632
L02	1	1	-1	.0145	.023	.006	300
L03	1	-1	1	.0395	.029	.050	2220
L04	1	-1	-1	.02625	.026	.0275	1087
L05	-1	1	1	.0555	.0525	.0585	1129
L06	-1	1	-1	.04075	.034	.0475	555
L07	-1	-1	1	.0405	.036	.049	2929
L08	-1	-1	-1	.037	.035	.039	1367
L09	1.6	0	0	.018	.0205	.0155	577
L10	-1.6	0	0	.046	.044	.048	1635
L11	0	0	1.6	.0455	.055	.041	1368
L12	0	0	-1.6	.01975	.0215	.018	382
L13	0	1.6	0	.02975	.040	.0195	514
L14	0	-1.6	0	.02325	.020	.0265	3615
L15	0	0	0	.027	.0285	.0255	856
L16	0	0	0	.032	.0315	.0325	869

(REPLICATION 2)

Tool No.	Coded V	F	D	Average Wear	Outside Wear	Inside Wear	Cutting Time
L01	1	1	1	.0295	.024	.035	599
L02	1	1	-1	.03025	.0385	.022	299
L03	1	-1	1	.06675	.082	.0515	2178
L04	1	-1	-1	.0505	.048	.053	1018
L05	-1	1	1	.0575	.061	.054	1068
L06	-1	1	-1	.03625	.0362	.036	517
L07	-1	-1	1	.040	.0265	.0385	2900
L08	-1	-1	-1	.02075	.0205	.021	1409
L09	1.6	0	0	.013	.0135	.0125	563
L10	-1.6	0	0	.027	.026	.028	1583
L11	0	0	1.6	.04175	.0385	.045	1354
L12	0	0	-1.6	.01975	.0235	.016	364
L13	0	1.6	0	.028	.0335	.0225	488
L14	0	-1.6	0	.0205	.0175	.0235	3553
L15	0	0	0	.0275	.027	.028	869
L16	0	0	0	.038	.0315	.044	881

TABLE A3.2 DIRECT RESPONSE MEASUREMENT OF 19/64" DRILL

(REPLICATION 3)

Tool No.	Coded V	F	D	Average Wear	Outside Wear	Inside Wear	Cutting Time
L01	1	1	1	.01625	.020	.0175	599
L02	1	1	-1	.00925	.0125	.007	299
L03	1	-1	1	.03725	.0175	.052	1625
L04	1	-1	-1	.02525	.0205	.030	774
L05	-1	1	1	.0395	.0345	.0445	1057
L06	-1	1	-1	.02925	.027	.0315	556
L07	-1	-1	1	.0375	.0285	.033	2871
L08	-1	-1	-1	.02775	.0165	.029	1410
L09	1.6	0	0	.036	.0375	.0295	556
L10	-1.6	0	0	.02925	.0235	.035	1556
L11	0	0	1.6	.07875	.0805	.077	1297
L12	0	0	-1.6	.0225	.0235	.0215	359
L13	0	1.6	0	.03575	.028	.0435	465
L14	0	-1.6	0	.05075	.0415	.060	3517
L15	0	0	0	.03125	.0335	.029	795
L16	0	0	0	.03675	.031	.0425	832

(REPLICATION 4)

Tool No.	Coded V	F	D	Average Wear	Outside Wear	Inside Wear	Cutting Time
L01	1	1	1	.02175	.0255	.018	622
L02	1	1	-1	.011	.009	.013	300
L03	1	-1	1	.03225	.024	.0405	1556
L04	1	-1	-1	.0305	.0245	.0365	777
L05	-1	1	1	.030	.0325	.0275	1138
L06	-1	1	-1	.04125	.0545	.028	334
L07	-1	-1	1	.02175	.0265	.017	2906
L08	-1	-1	-1	.025	.026	.024	1406
L09	1.6	0	0	.0235	.026	.021	563
L10	-1.6	0	0	.03375	.027	.0405	1580
L11	0	0	1.6	.03475	.0315	.038	1307
L12	0	0	-1.6	.02725	.027	.0275	359
L13	0	1.6	0	.01425	.018	.0105	471
L14	0	-1.6	0	.032	.020	.044	2430
L15	0	0	0	.03175	.0255	.038	828
L16	0	0	0	.02825	.0225	.034	837

TABLE A3.3 DERIVED RESPONSE MEASUREMENT OF 19/64" DRILL

(REPLICATION 1)

-- Mean of forces/torque --				-- Slope of force/torque --			
Torque	Thrust	X	Y	Torque	Thrust	X	Y
4.46	388.89	-1.08	-1.77	.007	.1804	.001	.0069
3.35	410.46	-0.712	2.399	.0049	.3788	-.0028	.0059
1.22	234.75	-2.965	5.888	-.0001	.0175	.0044	-.0025
1.42	200.72	0.357	5.723	.0003	.0866	-.0001	.0036
4.08	425.90	5.514	5.45	.0026	.0845	-.0025	-.0024
3.28	394.36	4.258	6.041	.0022	.1896	.0022	.0045
2.31	247.54	-5.099	3.114	.0008	.0137	.0005	-.0000
0.21	230.29	-3.635	3.943	.0002	.036	.0014	.0024
2.63	290.07	4.326	6.588	.0021	.2236	.0093	.0055
4.13	377.33	4.355	5.83	.0031	.0465	.0027	.0024
3.97	363.86	3.192	2.632	.0031	.0855	.0065	.0052
2.35	286.21	0.49	1.81	.0025	.176	.0021	.0041
4.10	448.35	0.895	4.539	.0032	.2469	.0055	.0066
1.80	135.08	0.943	5.719	.0006	.017	.0005	.0002
3.25	325.31	4.747	5.556	.0038	.0971	-.0013	-.0042
3.08	320.78	4.967	5.982	.0031	.1047	.0054	-.0004

------- Standard deviation of ------			
torque	thrust	X-force	Y-force
.574	34.724	.85	.931
.278	18.102	.177	.173
.273	12.692	1.341	2.777
.205	22.905	.176	.624
.87	35.262	2.529	2.794
.474	39.774	.526	.682
.609	15.854	1.824	.607
.017	18.017	.393	.324
.358	21.615	.641	.733
.73	26.083	.792	1.458
.555	23.773	1.953	1.589
.39	27.481	.149	.139
.609	45.838	.407	2.942
.215	12.845	.395	1.969
.404	21.861	2.26	2.43
.509	26.47	.649	2.226

TABLE A3.4 DERIVED RESPONSE MEASUREMENT OF 19/64" DRILL

(REPLICATION 2)

-- Mean of forces/torque --				-- Slope of force/torque --			
Torque	Thrust	X	Y	Torque	Thrust	X	Y
3.96	497.36	1.091	-2.21	.0034	.3141	.0034	.0038
3.41	492.508	-.997	1.379	.0029	.5366	.0006	.0018
2.13	223.335	0.63	5.858	.0011	.0519	.0000	-.0005
1.65	223.099	1.228	6.859	.0008	.0669	.0008	.0029
3.96	497.364	1.091	2.21	.0034	.3941	.0034	.0038
3.41	492.508	.997	1.379	.0029	.5366	.0006	.0018
2.13	223.335	.63	5.858	.0011	.0519	.0	-.0005
1.65	223.099	1.228	6.859	.0008	.0669	.0008	.0029
4.32	540.706	6.013	5.399	.0028	.17	-.001	-.0047
3.49	504.297	5.125	5.405	.003	.4115	.0047	-.0125
2.08	265.801	5.064	2.912	.0004	.0235	.0006	.0002
2.24	234.356	2.389	5.6	.001	.0254	.004	.0025
2.78	316.475	5.689	5.28	.0028	.2034	.0014	.0036
3.67	365.038	4.855	4.901	.0021	.0627	.0014	-.0012
3.31	334.596	.612	1.52	.0013	-.0324	.0004	.0033
2.48	381.436	.426	1.594	.0026	.5221	.0025	.0024
4.08	459.535	.966	3.878	.003	.2331	.0031	.0115
1.46	130.867	1.968	5.386	.0004	.0145	.0012	-.0005
2.99	353.355	3.608	5.676	.0024	.1902	.0011	-.0023
2.92	355.634	4.761	5.216	.0013	.0483	.0029	-.002

------- Standard deviation of ------			
torque	thrust	X-force	Y-force
.307	36.629	.819	.459
.609	83.754	.181	.174
.287	23.452	.336	2.745
.183	27.935	.196	1.354
.636	36.469	2.741	2.932
.484	44.609	.614	2.511
1.025	30.438	2.201	.901
.269	15.293	.339	1.575
.512	29.605	2.577	2.431
.676	25.872	1.876	2.379
.35	60.17	.575	1.548
.454	59.344	.273	.355
.592	53.264	.634	2.513
.209	17.179	.494	2.318
.482	30.687	.44	2.643
.491	33.298	.62	2.121

TABLE A3.5 DERIVED RESPONSE MEASUREMENT OF 19/64" DRILL
(REPLICATION 3)

-- Mean of forces/torque --				-- Slope of force/torque --			
Torque	Thrust	X	Y	Torque	Thrust	X	Y
4.52	399.07	.545	1.538	.0065	.0768	.0008	.0025
1.96	339.60	1.017	4.272	-.0105	.1849	.0044	.0124
2.28	201.62	2.228	6.762	.0011	-.0065	.0045	-.0003
1.76	205.02	.502	6.691	.001	.0179	.0014	.0038
4.42	373.40	5.439	5.215	.0036	.1373	.0002	-.0019
3.51	355.97	5.598	4.805	.003	.1868	.0052	.0027
1.51	248.11	-5.022	3.161	.0	.0131	-.0002	.0
1.79	212.54	1.501	4.162	.0006	.0516	-.0003	.0023
3.16	352.04	5.471	4.572	.0029	.1863	-.0015	.0065
3.72	430.86	3.33	5.045	.0021	.0585	.0007	-.0002
4.19	667.58	2.289	3.067	.0034	.3129	.0049	.0048
2.37	254.61	.318	1.068	.0028	.1753	.0017	.0026
4.37	615.78	1.687	4.175	.0005	.3366	.0061	.0072
1.70	138.49	1.431	4.793	.0005	.009	.0008	.0006
3.16	342.45	4.827	4.907	.0033	.1461	.0045	-.005
3.60	360.29	4.176	5.181	.005	.2159	.005	-.0005

------- Standard deviation of ------			
torque	thrust	X-force	Y-force
.544	28.886	.346	.446
.748	38.034	.433	2.428
.644	20.67	.77	2.388
.195	21.551	.219	.516
.744	27.013	2.476	2.866
.427	30.553	.445	.686
.317	17.817	2.49	.801
.184	18.942	.284	.27
.275	14.744	2.206	.566
.54	27.656	.53	2.262
.765	75.238	1.832	1.995
.366	22.974	.129	.15
.791	94.465	.925	2.695
.272	17.976	.401	.844
.49	28.074	.804	2.257
.988	38.465	.792	2.263

TABLE A3.6 DERIVED RESPONSE MEASUREMENT OF 19/64" DRILL

(REPLICATION 4)

-- Mean of forces/torque --				-- Slope of force/torque --			
Torque	Thrust	X	Y	Torque	Thrust	X	Y
3.81	409.36	3.895	2.559	.0031	.1058	.0094	.0002
3.22	417.11	2.971	.259	.0052	.5204	.0149	.0019
2.48	219.03	1.704	4.799	.0014	.0276	.0021	-.0034
1.84	212.65	.229	6.907	.0015	.0503	-.0002	.0016
3.72	736.15	5.054	6.07	.0013	.2401	-.0033	-.0012
3.44	389.47	3.893	6.889	.0027	.2977	.0044	.0056
3.53	402.27	2.988	5.222	.0017	.0561	-.0002	.0012
1.43	230.30	3.145	1.415	.0003	.023	.0009	-.0006
2.68	339.45	5.444	4.535	.0027	.1979	-.0018	.0041
3.59	412.61	5.401	4.393	.0018	.1131	.003	-.0001
4.18	333.67	3.992	.93	.0033	.0586	.0027	.0005
2.53	345.47	.179	1.488	.0027	.1084	.0008	.0032
4.34	367.23	.582	3.251	.006	.1607	.0031	.0086
1.45	152.86	.587	4.492	.0003	.0083	.0005	.0006
3.61	366.09	4.158	5.323	.0047	.2777	-.0037	-.0048
3.23	311.44	3.927	4.755	.0031	.128	.0051	-.0056

Standard deviation of			
torque	thrust	X-force	Y-force
.694	43.715	2.472	.464
.251	23.811	.263	.147
.372	13.163	.307	2.59
.233	19.291	.151	2.044
.557	76.214	2.821	2.805
.465	40.829	.779	1.51
.912	31.96	1.222	1.132
.201	22.631	.504	.509
.482	34.162	2.376	.757
.978	59.169	1.439	1.153
.686	23.733	2.694	.541
.432	35.914	.157	.214
.484	12.374	.34	2.417
.204	18.91	.397	.916
1.133	58.039	1.625	2.813
.431	24.737	.701	2.446

TABLE A3.7 DIRECT RESPONSE MEASUREMENT OF 1/8" DRILL
(REPLICATION 1)

Tool No.	Coded V	F	D	Average Wear	Outside Wear	Inside Wear	Cutting Time
S01	1	1	1	.1045	0.135	.0735	174
S02	1	1	-1	.02025	0.0275	.023	86
S03	1	-1	1	.0475	0.076	.019	356
S04	1	-1	-1	.0545	0.061	.048	180
S05	-1	1	1	.078	0.0875	.0685	434
S06	-1	1	-1	.03975	0.046	.0335	227
S07	-1	-1	1	.0465	0.049	.039	896
S08	-1	-1	-1	.05175	0.052	.0515	476
S09	1.6	0	0	.058	0.092	.024	157
S10	-1.6	0	0	.0559	0.06975	.0422	884
S11	0	0	1.6	.05125	0.0505	.0522	383
S12	0	0	-1.6	.0115	0.0175	.0055	129
S13	0	-1.6	0	.035	0.0265	.0385	613
S14	0	1.6	0	.06725	0.103	.0315	166
S15	0	0	0	.05675	0.0825	.0311	249
S16	0	0	0	.039	0.042	.036	258

(REPLICATION 2)

Tool No.	Coded V	F	D	Average Wear	Outside Wear	Inside Wear	Cutting Time
S01	1	1	1	.09975	0.131	.0645	172
S02	1	1	-1	.02175	0.0345	.009	86
S03	1	-1	1	.0465	0.0705	.0225	343
S04	1	-1	-1	.0205	0.024	.017	175
S05	-1	1	1	.072	0.1035	.0405	420
S06	-1	1	-1	.0145	0.0125	.0165	215
S07	-1	-1	1	.032	0.035	.029	855
S08	-1	-1	-1	.02875	0.0225	.035	471
S09	1.6	0	0	.06825	0.0995	.037	145
S10	-1.6	0	0	.03875	0.045	.0325	864
S11	0	0	1.6	.06375	0.097	.0305	386
S12	0	0	-1.6	.0335	0.034	.033	128
S13	0	-1.6	0	.02575	0.0245	.027	615
S14	0	1.6	0	.04925	0.0785	.02	160
S15	0	0	0	.0365	0.0485	.0245	253
S16	0	0	0	.036	0.0475	.0245	258

TABLE A3.8 DIRECT RESPONSE MEASUREMENT OF 1/8" DRILL
(REPLICATION 3)

Tool No.	Coded V	F	D	Average Wear	Outside Wear	Inside Wear	Cutting Time
S01	1	1	1	.09445	0.1225	.0665	186
S02	1	1	-1	.0095	0.01	.009	90
S03	1	-1	1	.02725	0.028	.0265	353
S04	1	-1	-1	.023	0.022	.024	181
S05	-1	1	1	.04375	0.0635	.024	428
S06	-1	1	-1	.024	0.0205	.0275	226
S07	-1	-1	1	.03725	0.0345	.04	898
S08	-1	-1	-1	.03675	0.0405	.033	482
S09	1.6	0	0	.02825	0.0355	.021	86
S10	-1.6	0	0	.033	0.041	.025	859
S11	0	0	1.6	.04075	0.049	.0325	386
S12	0	0	-1.6	.018	0.0185	.0175	131
S13	0	-1.6	0	.0235	0.0195	.0275	471
S14	0	1.6	0	.054	0.0915	.017	176
S15	0	0	0	.023	0.0225	.0235	258
S16	0	0	0	.0205	0.028	.013	266

(REPLICATION 4)

Tool No.	Coded V	F	D	Average Wear	Outside Wear	Inside Wear	Cutting Time
S01	1	1	1	.07775	0.1005	.055	177
S02	1	1	-1	.0145	0.021	.008	92
S03	1	-1	1	.04425	0.07	.0185	343
S04	1	-1	-1	.0155	0.019	.012	178
S05	-1	1	1	.07925	0.072	.0865	428
S06	-1	1	-1	.02075	0.0205	.016	220
S07	-1	-1	1	.03925	0.0505	.028	869
S08	-1	-1	-1	.01775	0.017	.0185	449
S09	1.6	0	0	.08275	0.123	.0425	157
S10	-1.6	0	0	.03775	0.0405	.035	863
S11	0	0	1.6	.06725	0.027	.0485	386
S12	0	0	-1.6	.01575	0.0205	.011	127
S13	0	-1.6	0	.03775	0.079	.0555	606
S14	0	1.6	0	.053	0.083	.023	172
S15	0	0	0	.03475	0.0485	.021	258
S16	0	0	0	.0335	0.045	.022	258

TABLE A3.9 DERIVED RESPONSE MEASUREMENT OF 1/8" DRILL

(REPLICATION 1)

-- Mean of forces/torque --				-- Slope of force/torque --			
Torque	Thrust	X	Y	Torque	Thrust	X	Y
.64	169.19	-1.23	-1.438	.0045	1.585	.0202	.9243
.48	111.58	.259	.341	.0023	.321	-.0041	.0131
.74	90.40	1.456	4.169	.0034	.138	.0112	.018
.43	93.32	.971	3.044	.002	.149	.0084	.0038
.82	179.92	2.853	3.757	.0025	.329	.008	.0113
.51	137.16	2.448	2.738	.0016	.195	.0083	.0083
.90	115.06	-1.148	4.028	.0017	.044	-.0005	.0089
.38	106.42	-1.783	1.624	.0005	.030	-.0017	.0015
.66	117.86	.57	3.742	.0062	.550	.0016	.0236
.96	152.44	-2.704	3.969	.0016	.174	.0055	.0075
.55	134.28	-2.79	1.093	.0014	.075	.0188	.0043
.37	106.45	1.14	.204	.0008	.112	-.0009	.0018
.34	75.26	1.478	2.78	.0007	.016	.0015	.0036
.57	163.80	1.15	4.274	.003	.633	.0001	.0258
.64	110.82	1.532	1.352	.0043	.120	.0025	-.0048
.53	132.02	1.668	1.36	.0023	.370	.0059	.0108

------- Standard deviation of ------			
torque	thrust	X-force	Y-force
.172	56.292	.415	.779
.021	2.7556	.079	.131
.112	12.055	.489	.536
.032	7.437	.181	.303
.165	33.681	.765	1.62
.053	15.643	.305	.3
.147	13.563	.221	.68
.032	7.262	.259	.134
.178	37.025	.354	1.693
.126	21.347	.5	.594
.112	10.658	1.013	.233
.034	6.932	.147	.068
.047	2.7	.172	.271
.17	39.742	.283	1.919
.154	9.604	.217	.526
.049	22.759	.472	.267

TABLE A3.10 DERIVED RESPONSE MEASUREMENT OF 1/8" DRILL
(REPLICATION 2)

-- Mean of forces/torque --				-- Slope of force/torque --			
Torque	Thrust	X	Y	Torque	Thrust	X	Y
.679	199.89	-.992	2.988	.0051	1.6792	.0168	.0447
.047	120.63	-.711	.095	.0035	.0961	.0139	.003
.453	101.55	-.56	2.672	.000	.1453	.0052	.0024
.476	69.51	.681	3.395	.0035	.0948	.0049	.0131
.783	199.86	2.574	4.278	.0018	.3439	.0054	.0089
.502	117.43	2.645	2.858	.0011	.1319	.0085	.0121
.932	97.62	2.034	2.469	.0017	.0489	.0076	.0028
.396	113.33	-2.0	2.078	.0003	.0431	.0005	.0024
.339	118.81	-3.473	1.252	-.0009	.6128	.0414	.001
.925	150.12	-1.713	2.449	.0016	.184	.0018	.0022
.073	130.72	2.173	-2.543	.0018	.2218	.0155	.0191
.397	117.26	-.422	.226	.0005	.0648	-.0008	-.0003
.461	72.52	.557	4.201	.001	.003	.0014	.0074
.696	144.97	.303	4.291	.0042	.2884	-.0022	.0275
.707	143.42	3.618	2.357	.0054	.199	.0232	-.0002
.435	123.69	.804	2.74	.0016	.1629	-.0035	.013

------- Standard deviation of ------			
torque	thrust	X-force	Y-force
.119	41.753	.431	.597
.047	2.091	.139	.034
.122	7.67	.386	.276
.063	2.421	.095	.139
.209	34.783	.594	2.101
.034	3.623	.175	.188
.096	7.977	1.479	.122
.044	8.139	.22	.187
.168	30.519	.764	.281
.114	15.602	.251	.311
.137	16.249	1.447	1.535
.053	13.412	.088	.212
.044	4.123	.138	.424
.172	21.591	.102	.825
.153	17.03	.74	.402
.091	11.473	.409	.299

TABLE A3.11 DERIVED RESPONSE MEASUREMENT OF 1/8" DRILL
(REPLICATION 3)

-- Mean of forces/torque --				-- Slope of force/torque --			
Torque	Thrust	X	Y	Torque	Thrust	X	Y
.66	187.48	1.7	2.906	.0041	1.0995	.029	.0426
.37	123.58	.403	-.813	.0007	.0396	.0127	.0077
.75	97.40	1.786	1.752	.0036	.0489	.0144	-.0049
.42	80.94	.621	2.696	.003	.1254	.0057	.0032
.46	161.11	1.159	4.021	-.0003	.1836	-.0022	.0091
.63	158.69	3.121	2.715	.0025	.2278	.0046	.0106
.75	103.25	-2.244	4.008	.0016	.0491	.0042	.0094
.53	95.47	-1.292	1.689	.0016	.0348	-.0016	.0032
.25	131.70	-2.008	-1.095	-.0019	.1705	-.0061	.0165
.77	158.33	3.307	3.37	.0012	.108	.0085	.007
.58	124.39	-2.538	.833	.001	.098	.0182	.0002
.36	120.83	-.108	-.945	.0014	.2131	.0018	.0072
.06	75.57	-1.038	2.829	-.0005	.0469	.0048	.0009
.79	162.53	.919	4.393	.0072	.5942	.0145	.0114
.37	130.13	3.435	3.24	.0004	.1255	.0119	.0184
.43	119.24	1.845	4.041	.0016	.1289	.0034	.0253

------- Standard deviation of ------			
torque	thrust	X-force	Y-force
.221	71.027	.502	.747
.052	14.094	.221	0.066
.11	7.149	.667	.538
.102	4.178	.177	.14
.198	9.231	.444	2.256
.11	17.164	.454	.332
.165	14.066	.497	1.202
.117	4.724	.179	.116
.059	8.891	.273	.7
.109	14.422	.952	.687
.19	10.892	1.457	.195
.038	9.872	.058	.142
.053	5.389	.256	.392
.236	29.028	.503	1.726
.036	5.936	.378	.531
.083	9.448	.282	.382

TABLE A3.12 DERIVED RESPONSE MEASUREMENT OF 1/8" DRILL

(REPLICATION 4)

-- Mean of forces/torque --				-- Slope of force/torque --			
Torque	Thrust	X	Y	Torque	Thrust	X	Y
.64	204.26	1.279	-1.135	.0031	1.5671	.0228	.0241
.40	123.13	-.152	-.62	.0025	.0283	.0046	-.0013
.82	110.49	2.342	4.242	.0047	.1002	.0221	.0139
.24	83.87	-.318	2.81	.0004	.1149	.0061	.0028
1.10	192.46	3.467	2.657	.005	.3442	.0138	.0046
.62	152.61	2.926	2.098	.0034	.1113	.0089	-.0028
.85	131.56	-.829	3.738	.0018	.1015	.829	3.738
.44	104.04	-2.513	1.78	.0008	.0341	.0045	.0017
.51	156.12	-2.725	2.398	.003	.992	.0192	.0209
.73	154.68	-2.631	1.774	.0011	.1291	.0053	.0
.76	110.48	2.672	1.779	.0027	.1055	.0236	.0099
.39	119.35	-.129	-.444	.001	.0862	.0	-.0001
.31	71.03	-.264	2.647	.0004	.0175	.001	.0006
.47	160.69	-1.4	4.853	-.0002	.2493	.0235	.021
.61	115.10	3.525	2.31	.0036	.179	.0159	.0061
.67	133.67	3.03	2.567	.0042	.19	.0172	.0093

------- Standard deviation of ------			
torque	thrust	X-force	Y-force
.158	62.192	.517	.891
.057	15.15	.139	.131
.097	10.881	.99	.559
.042	4.934	.147	.224
.244	23.116	1.764	.697
.087	14.514	.43	.24
.136	23.129	.426	.959
.069	5.639	.204	.121
.191	53.402	1.108	.919
.101	12.083	.668	.217
.159	11.503	1.125	.41
.055	13.792	.045	.075
.03	2.963	.059	.17
.085	17.129	1.036	1.355
.075	5.296	.391	.161
.13	5.031	.49	.139

APPENDIX IV

COEFFICIENT MATRIX FOR RESPONSE MODELS

TABLE A4.1 COEFFICIENT MATRIX FOR 19/64" DRILL

	Average Wear	Outside Wear	Inside Wear	Cutting Time	Mean value of Torque
Bo	.314E-01	.288E-01	.328E-01	.855E+03	.327E+01
B1	-.344E-02	-.274E-02	-.115E-01	-.285E+03	-.152E+00
B2	-.182E-02	.818E-03	.407E-02	-.682E+03	.854E+00
B3	.593E-02	.457E-02	-.138E-02	.368E+03	.417E+00
B12	-.710E-02	-.598E-02	-.222E-01	.102E+03	-.386E-01
B13	.305E-03	.756E-03	.147E-01	-.102E+03	-.106E-01
B23	-.211E-03	.463E-03	-.124E-01	-.195E+03	.762E-01
B11	-.784E-03	-.310E-03	.149E-02	.598E+02	-.577E-01
B22	-.441E-03	-.288E-03	.237E-02	.344E+03	-.193E+00
B33	.198E-02	.314E-02	.388E-02	-.209E+02	-.101E+00
B123	-.570E-03	-.162E-02	.126E-01	.287E+02	.134E+00

Mean value of Thrust	Mean value of X-force	Mean value of Y-force	Mean value of Torque	Slope of Thrust	Slope of X-force
.343E+03	.435E+00	.526E+01	.339E-02	.151E+00	.241E-02
-.220E+02	-.799E+00	-.138E+00	.105E-03	.264E-01	.562E-03
.101E+03	.241E+00	-.458E+00	.914E-03	.934E-01	.858E-03
.272E+02	.574E+00	-.203E-01	.338E-03	-.442E-01	-.171E-03
-.466E+00	-.300E+00	-.153E+01	-.250E-04	.185E-01	.488E-03
-.193E+02	-.147E+00	-.443E-01	.538E-03	-.160E-01	.109E-02
.543E+01	-.270E+00	.743E-01	.506E-03	-.361E-01	-.919E-03
.505E+01	.283E+00	.929E-01	-.435E-03	-.922E-02	-.350E-03
-.142E+02	-.103E+01	-.124E+00	-.660E-03	-.719E-02	-.137E-04
.874E+01	-.927E+00	-.110E+01	-.342E-03	.962E-02	.216E-04
-.557E+01	.187E-02	.908E-01	.594E-03	-.963E-02	.194E-03

	Slope of Y-force	Standard deviation of Torque	Thrust	X-force	Y-force
Bo	-.285E-02	.616E+00	.332E+02	.990E+00	.240E+01
B1	.136E-02	-.525E-01	-.178E+01	-.143E+00	-.134E+00
B2	.124E-02	.986E-01	.998E+01	.124E+00	.155E+00
B3	-.739E-03	.978E-01	.113E+01	.559E+00	.370E+00
B12	.150E-02	.153E-01	-.430E+00	-.509E-01	-.640E+00
B13	-.359E-03	-.674E-01	-.256E+01	-.280E+00	-.447E-01
B23	.147E-03	-.551E-01	-.109E-02	.106E+00	-.418E-01
B11	.141E-02	-.468E-01	-.202E+01	.193E+00	-.340E+00
B22	.203E-02	-.697E-01	-.625E+00	-.180E+00	-.124E+00
B33	.165E-02	-.422E-01	.184E+01	-.135E-01	-.570E+00
B123	.478E-03	.221E-01	.123E+00	-.177E-01	-.370E+00

TABLE A6.2 COEFFICIENT MATRIX FOR 1/8" DRILL

	Average Wear	Outside Wear	Inside Wear	Cutting Time	Mean value of Torque
Bo	.351E-01	.461E-01	.241E-01	.261E+03	.545E+00
B1	.326E-02	.886E-02	-.197E-02	-.178E+03	-.926E-01
B2	.758E-02	.125E-01	.117E-02	-.121E+03	.390E-01
B3	.146E-01	.183E-01	.883E-02	.956E+02	.107E+00
B12	.248E-02	.270E-02	.256E-02	.548E+02	-.198E-01
B13	.519E-02	.783E-02	.225E-02	-.446E+02	-.280E-02
B23	.128E-01	.146E-01	.110E-01	-.358E+02	-.205E-01
B11	.516E-02	.684E-02	.352E-02	.782E+02	.514E-01
B22	.264E-02	.504E-02	.269E-02	.325E+02	-.130E-01
B33	.702E-03	-.342E-02	.227E-02	-.833E+01	-.222E-01
B123	.319E-02	.273E-02	.303E-01	.154E+02	.292E-01

---- Mean value of ----			------- Slope of -------	
Thrust	X-force	Y-force	Torque	Thrust	X-force
.126E+03	.232E+01	.247E+01	.285E-02	.179E+00	.707E-02
-.645E+01	-.191E+00	-.518E+00	.386E-03	.146E+00	-.118E-01
.227E+02	.457E+00	-.178E+00	.604E-03	.180E+00	-.129E-01
.112E+02	.123E+00	.369E+00	.380E-03	.111E+00	.192E-01
.251E+01	-.117E+01	-.818E+00	-.100E-03	.126E+00	.258E-01
.497E+01	-.897E-02	-.193E+00	.238E-03	.149E+00	-.232E-01
.109E+02	-.269E+00	.206E-01	.313E-04	.185E+00	-.253E-01
.650E+01	-.109E+01	-.194E-01	-.315E-03	.771E-01	.607E-02
-.294E+01	-.513E+00	.529E+00	-.143E-03	.297E-01	.463E-02
-.129E+01	-.588E+00	-.800E+00	-.373E-03	-.885E-02	.602E-02
.219E+01	.137E+00	.194E+00	.225E-03	.158E+00	.274E-01

	Slope of Y-force	Standard deviation of Torque	Thrust	X-force	Y-force
Bo	-.424E-02	.968E-01	.108E+02	.432E+00	.350E+00
B1	-.484E-01	-.244E-02	.361E+01	-.481E-01	-.396E-01
B2	-.472E-01	.235E-01	.789E+01	.538E-01	.230E+00
B3	.882E-01	.405E-01	.563E+01	.276E+00	.273E+00
B12	.147E+00	-.397E-02	.442E+01	-.667E-01	-.111E+00
B13	-.855E-01	-.372E-02	.416E+01	-.233E-01	-.133E+00
B23	-.856E-01	.169E-01	.610E+01	-.634E-02	.149E+00
B11	.339E-01	.111E-01	.472E+01	.420E-01	.921E-01
B22	.347E-01	.188E-02	.160E+01	-.606E-01	.166E+00
B33	.322E-01	-.731E-03	.302E+00	.645E-01	-.198E-01
B123	.148E+00	.128E-02	.505E+01	-.340E-01	-.519E-01

VITA

Chang-Sheng Liu was born January 19, 1959 in Tainan, Taiwan, Republic of China, son of Sih-Wei and Yu-Hwa (Yang) Liu. Having graduated from the high school of National Taiwan Normal University in 1977, he began his undergraduate study at Tunghai University. In 1980, he was honored as a national outstanding college student. He got his bachelor of Science from Tunghai University in Industrial Engineering in June 1981.

He had served in Chinese army for two years. In August 1983, he began graduate study for the master of science degree in Industrial Engineering at Lehigh University.